BERICHTE
aus dem Fachbereich Geowissenschaften
der Universität Bremen

Nr. 139

Klump, J.

BIOGENIC BARITE AS A PROXY OF PALEOPRODUCTIVITY VARIATIONS IN THE SOUTHERN PERU-CHILE CURRENT

Berichte, Fachbereich Geowissenschaften, Universität Bremen, Nr. 139,
107 Seiten, Bremen 1999

ISSN 0931-0800

Die "Berichte aus dem Fachbereich Geowissenschaften" werden in unregelmäßigen Abständen vom Fachbereich 5, Universität Bremen, herausgegeben.

Sie dienen der Veröffentlichung von Forschungsarbeiten, Doktorarbeiten und wissenschaftlichen Beiträgen, die im Fachbereich angefertigt wurden.

Die Berichte können bei:

Frau Gisela Boelen

Sonderforschungsbereich 261

Universität Bremen

Postfach 330 440

D 28334 BREMEN

Telefon: (49) 421 218-4124

Fax: (49) 421 218-3116

e-mail: eggerich@uni-bremen.de

angefordert werden.

Zitat:

Klump, J.

Biogenic barite as a proxy of paleoproductivity variations in the Southern Peru-Chile Current.

Berichte, Fachbereich Geowissenschaften, Universität Bremen, Nr. 139, 107 Seiten, Bremen, 1999.

ISSN 0931-0800

Biogenic Barite as a Proxy of Paleoproductivity Variations in the Southern Peru-Chile Current

Dissertation zur Erlangung des Doktorgrades am Fachbereich Geowissenschaften der Universität Bremen

vorgelegt von Jens Klump, Bremen 1999

Tag des Kolloquiums: 7. Mai 1999

Gutachter: Prof. Dr. Gerold Wefer
Prof. Dr. Horst D. Schulz

In der Flucht

In der Flucht
welch großer Empfang
unterwegs -

Eingehüllt
in der Winde Tuch
Füße im Gebet des Sandes
der niemals Amen sagen kann
denn er muß
von der Flosse in den Flügel
und weiter -

Der kranke Schmetterling
weiß bald wieder vom Meer -
Dieser Stein
mit der Inschrift der Fliege
hat sich mir in die Hand gegeben -

An Stelle von Heimat
halte ich die Verwandlung der Welt -

Nelly Sachs

Danksagung

Für die Vergabe der Arbeit sowie die Betreuung und vielfältige Unterstützung bei deren Durchführung möchte ich mich ganz herzlich bei Prof. Dr. Gerold Wefer bedanken.
Dr. Dierk Hebbeln stand mir während meiner Arbeit stets betreuend zur Seite. Bei ihm möchte ich mich ausdrücklich für die vielen interessanten Diskussionen und für die gute Zusammenarbeit beim verfassen der gemeinsamen Manuskripte bedanken.
Prof. Dr. Horst-D. Schulz danke ich dafür, dass er sich ohne Zögern für die Übernahme des Zweitgutachtens bereit erklärte.

Mein ganz besonderer Dank gilt Dr. Frank Lamy. Der ständige Gedankenaustausch in zahllosen Diskussionen und die intensive Zusammenarbeit hat wertvolle Daten, Gedanken und Anregungen geliefert. Desgleichen gilt mein Dank auch Dr. Margarita Marchant für die Zusammenarbeit und für die Vermittlung der chilenischen Fluss-Sedimentproben.

Für die wertvollen Diskussionen zu den Manuskripten danke ich Prof. Dr. Wolfgang Berger, Dr. Laurence Vidal, Dr. Ralf Schneider, Dr. Sabine Kasten, Dr. Jelle Bijma, Dr. Abhijit Sanyal, Dr. Henning Kuhnert, Dr. Franz Gingele und Dr. Susanne Neuer. Nicht unerwähnt bleiben sollen die fruchtbaren Diskussionen mit Dr. Helge Arz, Dr. Tobias Wolf, Albert Benthien, Dr. Stefan Mulitza, Dr. Carsten Rühlemann, Dr. Oscar Romero und Dr. Peter Müller. Auch ihnen sei hiermit gedankt.

Bei den Vollaufschlüssen und Elementmessungen mittels ICP-AES wurden ich von Sigrid Hinrichs, Karsten Enneking, Dr. Matthias Zabel und Dr. Martin Kölling unterstützt. Dr. Monika Segl und Birgit Meyer-Schack führten die für diese Arbeit benötigten Isotopenmessungen durch und Dr. Peter Müller stellte die Karbonat- und TOC-Daten zur Verfügung.. Die Aufbereitung der Proben für die Altersbestimmung mittels AMS-C-14 Chronometrie wurde von Dr. Monika Segl durchgeführt. Die Versuche zur Bestimmung von Schwermineralphasen in marinen Sedimenten wurden insbesondere von Dr. Bernhard Diekmann und Helga Rhodes unterstützt. Bei Problemen mit dem Computer, Druckern, oder dem Ausdrucken von Postern standen Götz Ruhland, Dr. Volker Ratmeyer, Dr. Gerrit Meinecke und Thorsten Klein stets hilfreich zur Seite. Ihnen allen möchte ich hiermit danken.

Besonders zu schätzen gelernt habe ich die angenehme Arbeitsatmosphäre und den intensiven wissenschaftlichen Austausch in der Arbeitsgruppe Meeresgeologie. Wichtige fachliche und auch nichtfachliche Gespräche gab es mit den Mitliedern der Arbeitsgruppe Geochemie.

Meine Eltern Prof. Dr. Horst Klump und Lisa Klump, sowie Elsa Verloren van Themaat, Else Klump und Frank Puckhaber haben mich stets in vielfältiger Weise unterstützt, wofür ich ihnen ganz herzlich danken möchte. Mein Dank gilt auch Prof. Dr. John Gurney, Prof. Dr. Maarten de Wit, Prof. Dr. Johann Lutjeharms und Prof. Dr. Geoff Brundrit, die mein Studium an der University of Cape Town begleitet haben.

Finanziell unterstützt wurde diese Arbeit durch das Projekt "CHIPAL" des Bundesministeriums für Bildung und Forschung, durch Mittel der Joint Global Ocean Flux Study (JGOFS) und durch das EU-Projekt "CANIGO". Des weiteren wurde ich unterstützt vom Graduiertenkolleg "Stoff-Flüsse in marinen Geosystemen" und durch Reisemittel des Stifterverbandes für die deutsche Wissenschaft.

Contents

Zusammenfassung

Das Ziel dieser Dissertation war es, die Entwicklung der Paläoproduktivität im südlichen Peru-Chile Strom vor Nord- und Zentralchile im Spätquartär zu rekonstruieren. Dies war möglich durch die Verwendung von organischem Kohlenstoff und biogenem Karbonat als zwei voneinander unabhängigen Proxies im Sediment. Zusätzlich wurde die Eignung von biogenem Baryt als Produktivitätsproxy untersucht. Da der terrigene Eintrag am chilenischen Kontinentalhang sehr hoch ist, konnte der Anteil von biogenem Baryt am Sediment nicht mit direkten Methoden bestimmt werden. Statt dessen musste auf eine normative Berechnung des biogenen Bariums im Sediment zurückgegriffen werden. Die dafür benötigten terrigenen Ba/Al Verhältnisse wurden anhand von Sedimentproben aus Flüssen und Oberflächenproben aus Profilen vom chilenischen Kontinentalhang ermittelt. Die dabei gemessenen Elementverhältnisse weichen zum Teil stark von dem, in der Literatur veröffentlichten, "durchschnittlichen" Wert für die Erdkruste ab. Es konnte gezeigt werden, dass das terrigene Ba/Al Verhältnis in Sedimenten des Kontinentalhangs von der Geochemie des kontinentalen Hinterlandes abhängig ist. Ein geochemisches Modell wurde erstellt um das terrigene Ba/Al Verhältnis aus dem Fe/Al Verhältnis der Gesamtprobe errechnen zu können. Die damit korrigierten Akkumulationsraten für biogenes Barium konnten dann mit den Berechnungen der Paläoproduktivität auf der Basis von organischem Kohlenstoff und von biogenem Karbonat verwendet werden.

Die Paläoproduktivität im Peru-Chile Strom vor Nord- und Zentralchile folgte während des Spätquartärs dem Zyklus der Präzession. Die Paläoproduktivität war am höchsten während der Präzessionsminima, und am geringsten während des letzten glazialen Maximums (LGM) und während des späten Holozäns. Ursache für die sich ändernde Paläoproduktivität waren Veränderungen im regionalen Zirkulationsmuster der Atmosphäre, im wesentlichen bestimmt durch Verschiebungen der südlichen Westwindzone. Die Verschiebung der Westwindzone zum Äquator hin während des LGM und vorangegangener Substadiale führte zu eine äquatorwärtigen Verlagerung der für den Küstenauftrieb günstigen küstenparallelen Winde. Dies führte somit auch zu einer Verlagerung des Gebietes des intensivsten Küstenauftriebs. Während des Holozäns

verlagerte sich das Gebiet des stärksten Küstenauftriebs von seiner nördlichsten Position zu seiner gegenwärtigen südlichsten Position.

Veränderungen der räumlichen Ausdehnung der Auftriebszellen konnten durch die Verwendung von organischem Kohlenstoff und biogenem Karbonat als voneinander unabhängigen Proxies rekonstruiert werden. Während die Akkumulationsrate des organischen Kohlenstoffes die Gesamtproduktivität widerspiegelt, ist die Karbonatakkumulationsrate nur ein Abbild der Produktivität kalkschaliger Organismen. Änderungen des Anteils kalkschaliger Organismen an der Gesamtproduktivität zeigen an, wie die Vergesellschaftung im Oberflächenwasser an der Kernposition zeitweise von Kieselalgen und zeitweise von Kalkalgen dominiert wurde. Da Auftriebszellen stets in ihrem Zentrum von Kieselalgen dominiert sind, während außerhalb davon Kalkalgen vorherrschen, weist ein Ansteigen der Produktivität kalkschaliger Organismen während einer Phase verringerter Gesamtproduktivität auf eine räumliche Verkleinerung der örtlichen Auftriebszelle hin.

In allen drei untersuchten Kernen wurde eine ungewöhnlich hohe Konzentration von Barium in den Abschnitten festgestellt, die seit dem Ende des LGM abgelagert wurden. Aus einem geochemischen Modell ließ sich ableiten, dass diese ungewöhnlich hohen Bariumkonzentrationen im Sediment die Folge eines Anstiegs in der Bariumkonzentration im Wasser des Südostpazifik sein können. Diese zeigt einen graduellen Anstieg vom Ende des LGM bis zum mittleren Holozän und fällt seit dem wieder ab. Der Anstieg ist überlagert von zwei kurzzeitigen Barium-Maxima, die auf das Ende des LGM und nach der Jüngeren Dryas folgen. Das Holozäne Barium-Maximum resultierte wahrscheinlich aus einem Anstieg der Flussrate von vormals in Karbonat gebundenem Barium aus dem Sediment in die tiefen Wassermassen des Pazifik, das durch die holozäne Verflachung der Lysokline im Pazifik freigesetzt wurde. Ergebnisse aus Modellen des marinen Bariumkreislaufs zeigen, dass die kurzzeitigen Barium-Maxima verursacht wurden durch den Einstrom von Wasser mit erhöhter Konzentration an gelöstem Barium, das infolge wiedereinsetzender Produktion von Nordatlantischem Tiefenwasser nach dem Ende des LGM und nach der Jüngeren Dryas in den Pazifik eindrang.

Abstract

The aim of this dissertation was to reconstruct the Late Quaternary paleoproductivity in the Peru-Chile Current off northern and central Chile, using organic carbon and biogenic carbonate as mutually independent proxies of paleoproductivity, and to assess the suitability of biogenic barite as proxy of paleoproductivity. Since the terrigenous input to the Chilean continental slope is very high, the amount of biogenic barite in the sediment could not be determined by direct methods but had to be derived from normative calculations. The required terrigenous Ba/Al ratios were determined from stream sediments and from surface sediment samples from continental slope transects. Most of the measured ratios differ markedly from the 'crustal average' ratio that can be found in the literature. It was shown that the terrigenous Ba/Al ratio in sediments of the continental slope is determined by the geochemistry of the continental hinterland. A geochemical model was devised to calculate the terrigenous Ba/Al ratio from the Fe/Al ratio of the bulk sediment. The corrected biogenic barium accumulation rates were then compared with paleoproductivity reconstructions based upon organic carbon and biogenic carbonate.

During the Late Quaternary the paleoproductivity in the Peru-Chile Current off northern and central Chile followed the precessional cycle. The export productivity was highest during precession minima, and lowest during the Last Glacial Maximum (LGM) and the late Holocene. The variations in productivity are driven by changes in the regional atmospheric circulation pattern which is mainly determined by the position of the Southern Westerlies. The equatorward shift off the Southern Westerlies during the LGM and previous sub-stadials resulted in an equatorward shift of the upwelling favourable wind fields, and thus of the region of most intense coastal upwelling and highest productivity, even though the individual upwelling cells remained in place. During the Holocene the zone of most intense upwelling moved from its northernmost position during the LGM to its present southernmost position.

Changes in the spatial extent of the upwelling cells next to the core positions were reconstructed by using organic carbon and biogenic carbonate as independent proxies of paleoproductivity. While organic carbon accumulation reflects the total productivity at the site, the accumulation rate of biogenic carbonate responds only to changes in the productivity

of carbonate-shell secreting organisms. The varying proportion of carbonate-based productivity to the total productivity shows how the biocoenosis in the surface waters at the core position varied between diatom dominated and coccolithophorid dominated phytoplankton associations. Since the centre of an upwelling cell is dominated by diatoms, while coccolithophorids dominate the zones outside, a shift towards a higher proportion of carbonate-based productivity during times of reduced total productivity indicates a contraction of the upwelling cell, and vice versa.

An anomalous barium peak was found in the all three cores investigated in sediments deposited since Termination I. Geochemical modelling could show that these anomalous peaks may be related to an increase in the concentration of dissolved barium in the waters of the Southeast Pacific. The concentration of dissolved barium increased from the end of the LGM to a maximum the Middle Holocene, and since then declined to modern values. Superimposed on this gradual increase are two short-term peaks, found after the end of the LGM and after the Younger Dryas. The broad Holocene barium maximum is probably the result of an increased flux of previously carbonate-bound barium from the sediment to the deep ocean, caused by shoaling of the Pacific carbonate compensation depth during the Holocene. The increased carbonate dissolution caused the release of great amounts of carbonate-bound barium from the sediment. Models of the oceanic barium cycle show that the superimposed short-term barium peaks are the result of an influx of barium-enriched waters, which entered the Pacific in two pulses, following the resumption North Atlantic Deep Water production after the end of the LGM and after the Younger Dryas (YD).

Preface

Cumulative dissertations are becoming more and more common today, but most of us are still accustomed to reading dissertations in the 'classical' format. The advantage of the 'classical' format is that it is easier to follow a line of argument than in the sectioned format of the cumulative dissertation. In addition, the requirements of a scientific journal are quite different to those of a PhD thesis. The concise format of scientific articles comes with the price of omitting interesting sidelines that may or may not have been successful in the investigative process. In the introductory first chapter of this thesis I will attempt to compensate for some of the shortcomings of the cumulative format by giving an overview of the aims of this project, the regional geological, geochemical, oceanographic and climatic framework, descriptions of the analytical methods, and detailed descriptions of the age models used on the sediment cores. Most of this will be repeated somewhere in the subsequent chapters, though often not in the same detail, or it can be found in the quoted literature. The principal results of this thesis are summarised at the end in Chapter 6. To make the list of references easier to use, the references from the end of each article have been combined into one reference list and moved to the back of this volume.

Chapter 1 - Introduction

1.1. Main objectives

The main objective of this project was to reconstruct Late Quaternary variations of the paleoproductivity in the Peru-Chile Current and to see how productivity responds to climatic change. The high productivity in the Peru-Chile Current is sustained by coastal upwelling. The extreme latitudinal extent of the upwelling system along the western margin of South America makes it the largest coastal upwelling system and places it among the most important regions of high productivity in the world ocean. Despite the importance of this region, little was know about the Late Quaternary history of the Peru-Chile Current, especially about its southern part off Chile.

Investigations on ice cores from Greenland (Dansgaard *et al.*, 1993; Grootes *et al.*, 1993) and from Antarctica (Barnola *et al.*, 1987; Delmas *et al.*, 1980; Genthon *et al.*, 1987) showed that Late Quaternary climatic cycles were coeval with changes in the atmospheric content of CO_2. In the context of the global carbon cycle upwelling areas in the oceans are of particular importance for the exchange of CO_2 between the oceans and the atmosphere. The deep oceans are capable of storing great amounts of dissolved CO_2 , far greater than the amount of CO_2 stored in the atmosphere. The activity of the 'biological pump' (Berger *et al.*, 1989) transfers carbon from the atmosphere to the deep ocean and into the sediment by export of carbon from the food web of the euphotic surface waters to greater depths. At the same time upwelling brings cold CO_2-rich deep water to the surface where it warms up and looses CO_2 to the atmosphere, a process called the 'physical pump' (Berger *et al.*, 1989). It has been postulated that changes of upwelling and productivity in highly productive coastal upwelling areas control the amount of CO_2 in the atmosphere (Berger *et al.*, 1989). It had to be investigated whether upwelling and productivity in the Peru-Chile Current served as a source or as a sink of atmospheric CO_2.

The activity of the 'biological pump' is expressed in the amount of organic carbon exported from the euphotic surface waters of the ocean (Berger *et al.*, 1989). Due to microbial activity in the water column and at the water-sediment interface, only a small amount of organic

carbon is eventually buried in the sediment. In addition, organic carbon may be subject to post-depositional degradation, and there is no agreement yet in the literature on which factors control organic carbon preservation (Müller and Suess, 1979; Sarnthein *et al.*, 1992; Sarnthein *et al.*, 1988). To overcome the problems associated with organic carbon as a paleoproductivity proxy, and since ocean productivity is a key mechanism in the global carbon cycle, a number of alternative paleoproductivity indicators have been devised (see e.g. Berger *et al.*, 1989; Elderfield, 1990). Biogenic barite seemed to be particularly suitable as a paleoproductivity proxy because of its high degree of preservation in the sediment (Dymond *et al.*, 1992). However, a number of problems complicated its application in the past. In most hemi-pelagic sediments biogenic barite cannot be detected quantitatively by X-ray diffraction analysis, so the amount of biogenic barium in the sediment has to be derived from normative calculations. If, however, the proportion of barium-bearing aluminosilicates in the terrigenous fraction of the sediment exceeds 50 wt% then it becomes a crucial issue to determine the barium content of the terrigenous material. Due to the lack of data, Dymond *et al.* (1992) proposed to estimate the amount of barium in terrigenous fraction of the sediment on the basis of an 'average' terrigenous Ba/Al ratio. Our study on stream sediments from Chilean rivers and on surface sediments from the Chilean continental slope showed that this 'average' terrigenous Ba/Al ratio is not applicable to the Chilean margin.

Having derived the regional Ba/Al ratios of the terrigenous material on the Chilean continental slope a geochemical model was devised to correct for changes in sediment provenance on the Chilean continental slope. The corrected sedimentary barium contents could then be used to calculate the flux rate of biogenic barium to the sediment. Comparing these data with paleoproductivity reconstructions on the basis of organic carbon, following the method of Müller and Suess (1979), shows a good agreement between these two paleoproductivity proxies during the last glacial period. However, the cause of anomalous barium peaks found in the Holocene sections in all cores from the Chilean margin had to be investigated. Even though the geometry of these peaks differs between cores, they all share an extraordinary similarity if plotted on a common time scale. The similarity of these barium peaks on a common time scale points to a regional, if not global, process that influenced the deposition of marine barite around Termination I. It had to be investigated whether these peaks were caused by a dramatic increase in export productivity, by changes in sediment provenance, or by changes in the biogeochemical cycle of barium in the ocean. The presence

of such peaks at glacial Terminations I, II, and IV in sediment cores from the Atlantic (Kasten, 1996; Thomson *et al.*, subm. 1998) and the western equatorial Pacific (Schwarz *et al.*, 1996) indicates that this may be a global phenomenon. The constant ratio of barium to alkalinity in the flux from the sediment to the deep waters, as reported by McManus *et al.* (1999) for sediments of the equatorial and north-east Pacific, points to a link between the carbonate system and the biogeochemical cycle of barium in the ocean.

1.2. Study area

The studied area encompasses the Chilean continental slope from 27.5°S to 42°S. Both climate, geology, and geomorphology of the continental hinterland, as well as the bathymetry of the continental margin, change markedly along this latitudinal transect. This exerts a strong control on the terrigenous input to the continental slope (Lamy *et al.*, 1998b). At the same time the regional hydrography and atmospheric circulation remain fairly uniform. Some detail that is relevant to the terrigenous supply of sediment and to coastal upwelling will be given below.

1.2.1. Regional hydrography, atmospheric circulation, and modern climate

The main feature of the regional hydrography is the Peru-Chile Current (PCC), also known as Humboldt Current. It originates from the Antarctic Circumpolar Current (ACC) which, as it approaches the South American Continent at about 45°S, splits into a southern branch (Cape Horn Current, CHC) and a northern branch, the PCC. The PCC flows north along the western South American margin and turns west between 20°S and 5°S to form the South Equatorial Current (SEC) (Pickard and Emery, 1990). An additional northward flowing current, the Chile Coastal Current (CCC) flows between the PCC and the coast. It is partly fed from water originating in the fjord region of southern Chile (Fjord Water, FW) (Strub *et al.*, 1998). Little understood is the behaviour of the Peru-Chile Counter Current (PCCC) which is found between the PCC and the CCC. It is formed from subtropical surface water. The PCCC is sometimes found to the east of the CCC and may be absent at times (Strub *et al.*, 1998) (Fig. 1.1).

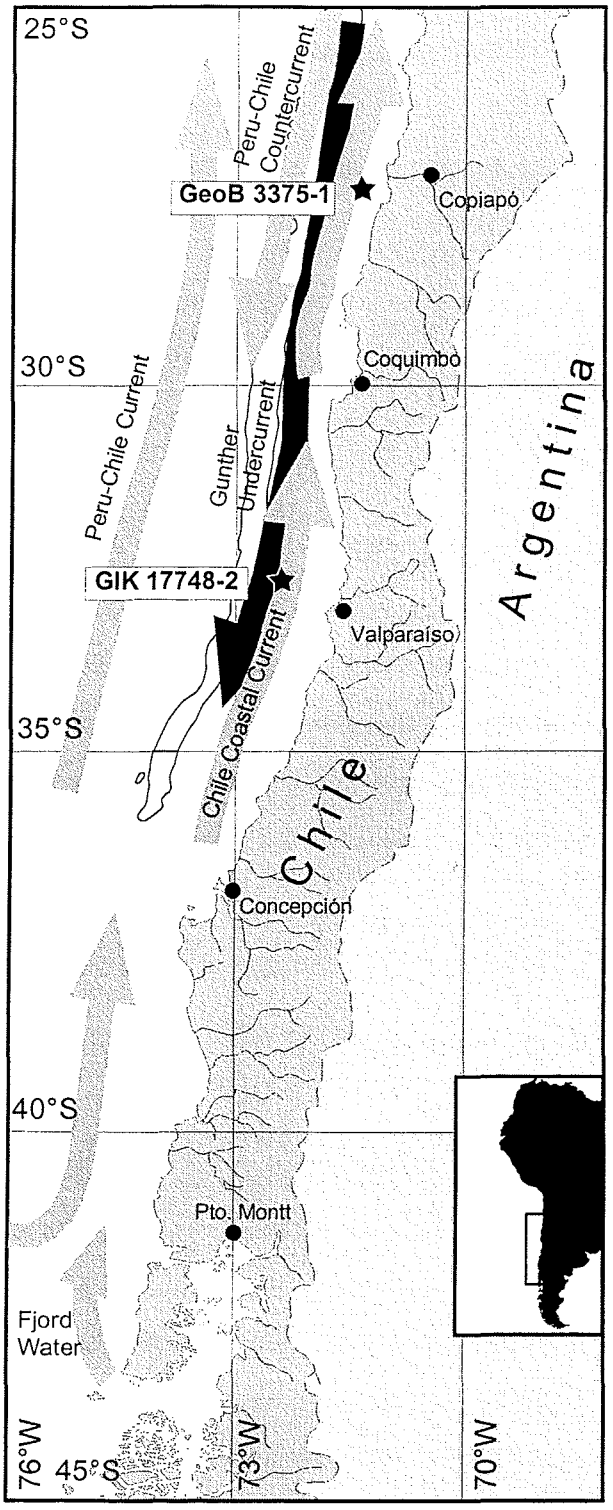

Figure 1.1. Schematic diagram of the surface hydrography in the Southeast Pacific off Chile. The Gunther Undercurrent is shown by a dashed line underneath the Chile Coastal Current.

At a water depth of 100 to 400 m a poleward flowing undercurrent, the Gunther Undercurrent, GUC) is found over the shelf and upper continental slope. Its maximum velocity may be up to 25 cm/s (Johnson *et al.*, 1980; Shaffer *et al.*, 1995). At depths from 400 to 1,200 m Antarctic Intermediate Water (AAIW) flows equatorward. It is underlain by Pacific Deep Water (PDW) (Shaffer *et al.*, 1995; Strub *et al.*, 1998). It should be noted that in this case the name PDW describes the region where the mass is found, rather than where it is formed as is usually the case with water mass names (Pickard and Emery, 1990). Antarctic Bottom Water (AABW) is found only in the deepest parts of the Peru-Chile Trench. During upwelling water from the GUC is brought to the surface. Under very intense upwelling conditions even AAIW can be brought to the surface (Strub *et al.*, 1998) (Fig. 1.2).

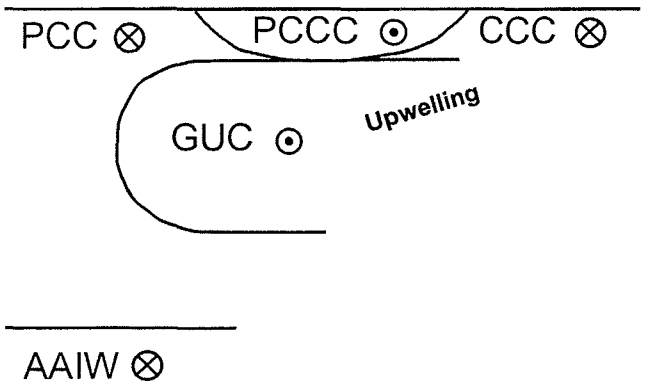

Figure 1.2. Schematic cross-section (not to scale) of the hydrography off northern and central Chile. The flow directions are indicated by arrowheads (poleward) and -tails (equatorward). The currents shown are the Peru-Chile Current (PCC), the Peru-Chile Countercurrent (PCCC), the Chile Coastal Current (CCC), the Gunther Undercurrent (GUC), and Antarctic Intermediate Water (AAIW). The upwelling of water from the GUC is indicated by an arrow.

Remote sensing studies identified several localised upwelling centres adjacent to headlands of northward-facing bays, similar to the setting found off Peru and off south-western Africa (Armstrong *et al.*, 1987; Johnson *et al.*, 1980; Strub *et al.*, 1998). The position of these upwelling cells is determined by the topography, therefore they may change in size in response to upwelling intensity, but they do not move along the coast with changes of the wind field. Wind field and upwelling change on various time-scales, ranging from synoptic scale to Milankovitch-scale orbital forcing. The biotic succession found from the upwelling centre to the filament zone, however, is a feature common to all coastal upwelling cells (Armstrong *et al.*, 1987; Blasco *et al.*, 1980; Richert, 1975). At the centre of an upwelling cell, where nutrient (e.g. silicate) levels are high, the phytoplankton assemblage is dominated by diatoms. With increasing distance from the shore, and thus decreasing nutrient availability, the biomass in the water column decreases and diatoms are replaced by calcareous phytoplankton, mainly

coccolithophorids (Fig. 1.3). This biotic succession is also recorded in the sediment. The sedimentary record can therefore be used to infer changes in the size of the upwelling cell at the position of a gravity core from the ratio of calcareous to total primary paleoproductivity recorded in the sediment. How this is done is discussed in more detail below in Section 1.4 and in Chapter 4.

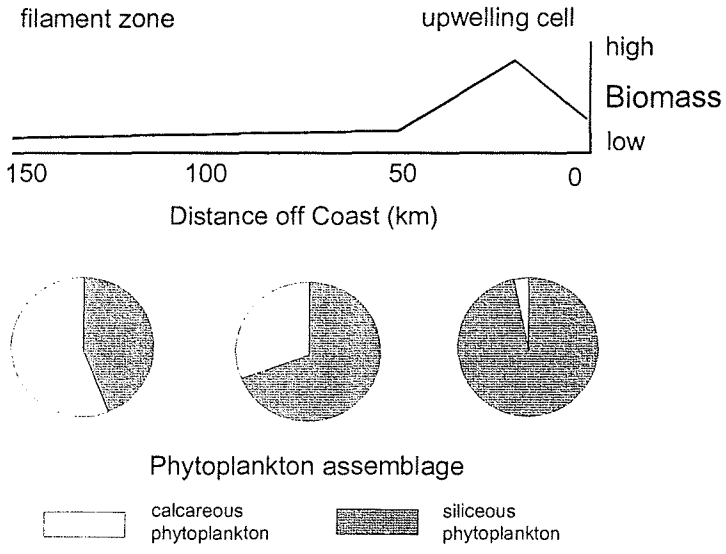

Figure 1.3. With increasing distance from the centre of a coastal upwelling cell, the total biomass supported by this upwelling cell decreases. At the same time the phytoplankton assemblage changes from predominantly siliceous phytoplankton to predominantly calcareous phytoplankton (after Richert, 1975).

The atmospheric circulation pattern over the Southeast Pacific region is driven by two principal features: the Southern Westerlies south of 37°S and the Southeast Pacific anticyclone (Miller, 1976). In central and northern Chile the Southeast Pacific anticyclone produces seasonal upwelling-favourable winds along the coast, while in southern Chile the Southern Westerlies produce downwelling (Strub *et al.*, 1998). Between the hyper-arid north and the humid cool-temperate south the climate of Chile is characterised by a gradient in precipitation between the two extremes which produces a distinct latitudinal climatic zonation (Fig. 1.4).

Off northern Chile cold water, brought to the surface by coastal upwelling, causes fog to precipitate above the coastal waters and thus removes moisture from the air moving from the ocean onto the shore. This regional setting is typical for eastern boundary currents and similar to the situation e.g. off south-west and north-west Africa. It is responsible for the existence of the hyper-arid Atacama Desert north of 27°S (Miller, 1976). In this region the amount of precipitation is generally lower than 50 mm/year. The drainage system remains dry throughout the year, except for rare flash-flood events caused by El Niño events (Grosjean *et*

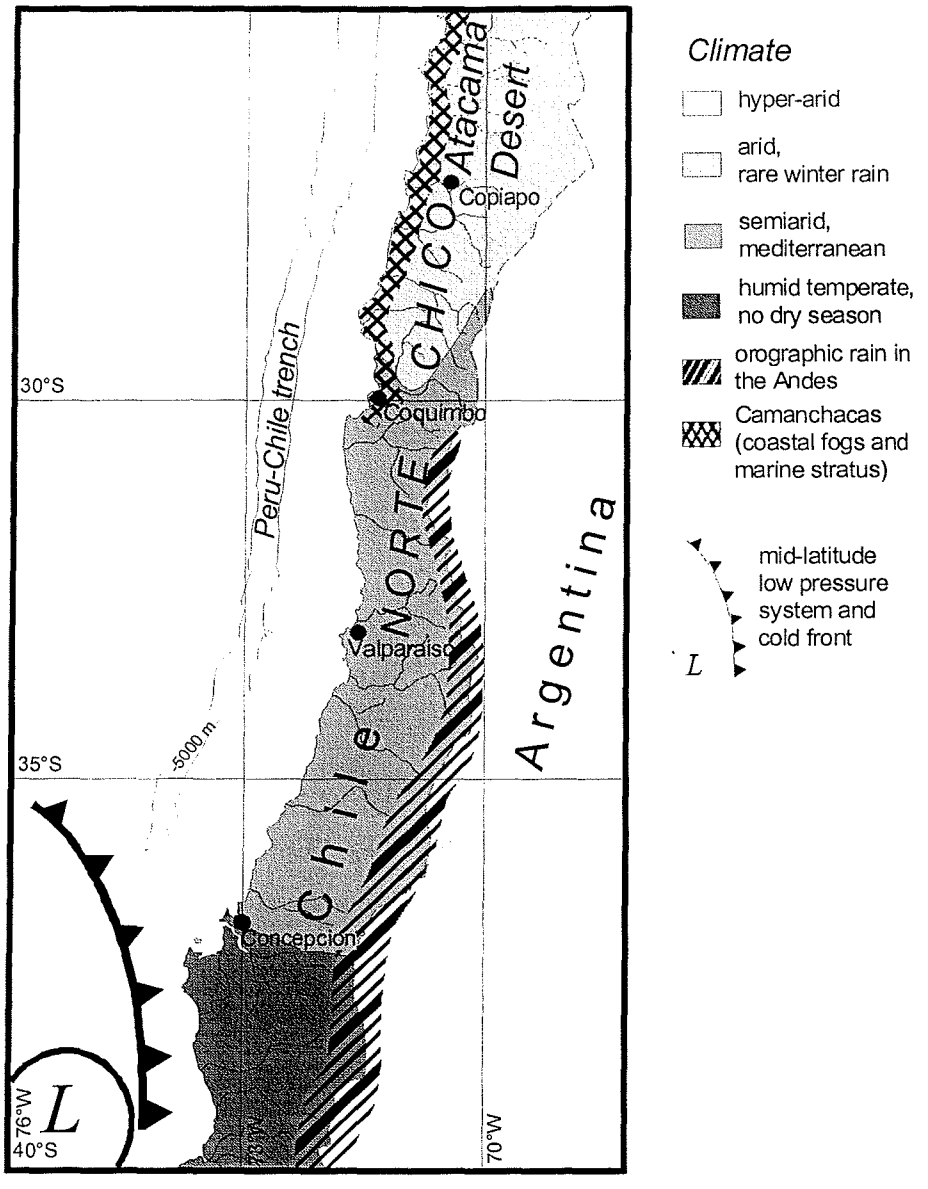

Figure 1.4. Schematic diagram of the present-day climatic zonation of Chile. Also shown are the occurrence of coastal fog ('Camanchacas'), orographic rain in the Andes, and the position of mid-latitude low-pressure systems and associated cold-fronts.

al., 1997). The southern border region between the hyper-arid climate of the Atacama Desert in northern Chile and the semi-arid, Mediterranean climate of mid-latitude Chile is characterised by seasonal winter rain but otherwise arid conditions and dry valleys with only sporadic water runoff. Sediments derived from the Andes are mostly trapped in the alluvial basins east of the Coastal Range and do not reach the ocean. A prominent feature of this region are coastal fogs ('Camanchacas') and marine stratus clouds. They supply moisture to the Coastal Range and reduce insolation and evaporation (Aravena *et al.*, 1989; Miller, 1976).

This local phenomenon promotes vegetation cover and soil development and is able to sustain relict forests (Aravena *et al.*, 1989; Veit, 1996).

The semi-arid Mediterranean climate of central Chile is characterised by regular winter rain brought by cold fronts from the Southern Westerlies. The annual precipitation increases towards the south and, through orographic rain, it is generally higher in the Andes than in the Coastal Range or central valley. Inter-annual variations in precipitation are caused by El Niño events (Rutlland and Fuenzalinda, 1991; Waylen and Caviedes, 1990). South of 37°S the effect of the Southern Westerlies can be felt. Perennial rain causes a humid temperate climate which cools to a humid cool-temperate climate south of 42°S. Ample precipitation allows forests of southern beech (*Nothofagus*) to grow, which grade into evergreen Patagonian parklands vegetation further south (Heusser *et al.*, 1996; Miller, 1976).

1.2.2. Bathymetry and marine geology

The Chilean continental margin has been an active subduction zone since the Early Mesozoic (Zeil, 1986). This tectonic framework separates the continental margin (from west to east) into three sections: the Peru-Chile Trench, a steep continental slope, and a narrow continental shelf. The bathymetry is controlled by the input of terrigenous material and by the age of the subducted oceanic crust, and thus by its density (Thornburg *et al.*, 1990). The bathymetry of the Peru-Chile Trench can be subdivided into three parts. The trench is deepest north of 27.5°S where it reaches its maximum depth of 8000 m. In this section the oldest oceanic crust is subducted while the terrigenous sediment input in this section is lowest. The angle of the lower and upper continental slope can be as steep as 10° to 15°. The mid-slope is characterised by terraces and small sedimentary basins which are suitable targets for gravity coring (e.g. core GeoB 3375-1). Here the continental shelf is extremely narrow, its average width is only 10 km.

Due to increased terrigenous input and reduced density of the subducting oceanic crust the depth of the Peru-Chile Trench decreases to 5500 m from 27.5°S to 33°S. The characteristics of the continental slope and shelf are essentially the same as north of 27.5°S. On the continental slope at 33°S the Valparaiso Basin forms the largest known fore-arc basin (2,500

km^2) south of Peru (von Huene *et al.*, 1995). Gravity core GIK 17748-2 was retrieved from the Valparaiso Basin (Stoffers and Cruise Participants, 1992). South of 33°S the sedimentary infilling of the trench increases rapidly because northward transport of sediments in the trench is blocked by a structural barrier (Schweller *et al.*, 1981). The trench may be filled by up to 2 km of sediments. South of 38°S the trench is no longer present as a bathymetrical feature. At the same time the inclination of the continental slope is less steep. Here the continental shelf may be up to 150 km wide. The sediments transported into the ocean by larger rivers are deposited in submarine fans which extend onto the continental slope.

1.2.3. Regional geology, geomorphology, and geochemistry

The geology and geomorphology of the continental hinterland of Chile can be subdivided in the same manner as the bathymetry of the continental margin because both are set in a common tectonic framework. North of 27.5°S the continental hinterland is characterised by two mountain ranges, the Coastal Range and the Andes, which run parallel to the coast and are separated by a central valley. The Coastal Range rises steep from the sea to altitudes between 2,000 and 2,500 m. The rocks of the Coastal Range are mainly calc-alkaline plutonics and subordinate metamorphic rock together with basaltic and andesitic volcanics. As a result of the predominant acidic plutonic rocks the sediments derived from the Coastal Range have low Fe/Al ratios and high Ba/Al ratios (Le Maitre, 1976). The central valley is filled with clastic and volcanoclastic sediments and may be classified as a fore-arc basin (Thornburg and Kulm, 1987). The base of the Andes consists mainly of rhyolitic and andesitic ignimbrites, capped by active andesitic stratovulcanoes up to 6,000 m high (Zeil, 1986). These volcanic rocks, in contrast to the mainly plutonic rocks of the Coastal Range, have high Fe/Al ratios and low Ba/Al ratios (Le Maitre, 1976). A general outline of the continental hinterland geochemistry is shown in Figure 1.5.

No Quaternary volcanism is found between 27.5°S and 33°S and there is no central depression between the Andes and the Coastal Range. This is attributed to the shallow angle of subduction below this section of the Chilean margin (Jordan *et al.*, 1983). The geology and geochemistry of the Coastal Range are similar to the situation north of 27.5°S. In this section of the Andes parts of the volcanic rocks are replaced by older plutonic and metamorphic rocks

and some localised sedimentary sequences (Zeil, 1986). The peaks of the Andes between 32°S and 33°S may be up to 7,000 m high.

An increased angle of subduction south 33°S of marks a tectonic break (Jordan *et al.*, 1983). Here the situation is similar to that north of 27.5°S where the Coastal Range and the Andes are separated by a central valley. South of Puerto Montt (42°S) the central valley is below the present day sea-level but can be followed as a tectonic feature to 47°S (Zeil, 1986). The elevation of the Andes and of the Coastal Range decreases markedly south of 33°S. Between 33°S and 42°S the average elevation drops to 1,500 m in the Coastal Range and from 5,000 to 2,000 m in the Andes (Scholl *et al.*, 1970). The geology of the Coastal Range in this section is again characterised by plutonic rocks and low-grade metamorphic rocks, mainly north of 38°S (Zeil, 1986). South of 38°S the Coastal Range consists mainly of metasedimentary rocks of Paleozoic age and ends at 47°S. Between 33°S and 41°S the Andes are composed mainly of sedimentary rocks and andesitic to rhyolitic volcanics. Further to the south the Andes are dominated by andesitic to basaltic volcanics of plio-pleistocene age (Zeil, 1986).

1.3. Materials and methods

1.3.1. Sample material

Three gravity cores (GeoB 3302-1 at 33°13.1'S, 72°05.2'W, water depth 1502 m, core length 421 cm; GeoB 3375-1 at 27°28.0'S, 771°15.1'W, water depth 1947 m, core length 489 cm; GIK 17748-2 at 32°45.0'S, 72°02.0'W, water depth 2545 m, core length 383 cm) from the Chilean continental slope were studied. Their sediments provide a record of Late Quaternary climate change and the resulting changes in paleoproductivity. Gravity core GIK 17748-2 was retrieved during cruise SO-90 with the German R/V SONNE (Stoffers and Cruise Participants, 1992) from the Valparaiso Basin. Gravity cores GeoB 3302-1 and GeoB 3375-1 were retrieved from the Chilean continental slope during cruise SO-102, also with the German R/V SONNE (Hebbeln *et al.*, 1995). The gravity cores were sampled at 5 cm intervals, starting 3 cm below the core top. The sections 4 to 162 cm and 165.5 to 250.5 cm below core top of core GeoB 3375-1 were resampled at 2 cm and 2.5 cm intervals, respectively. The surface samples were also collected during cruise SO-102 using a multi-corer. The uppermost

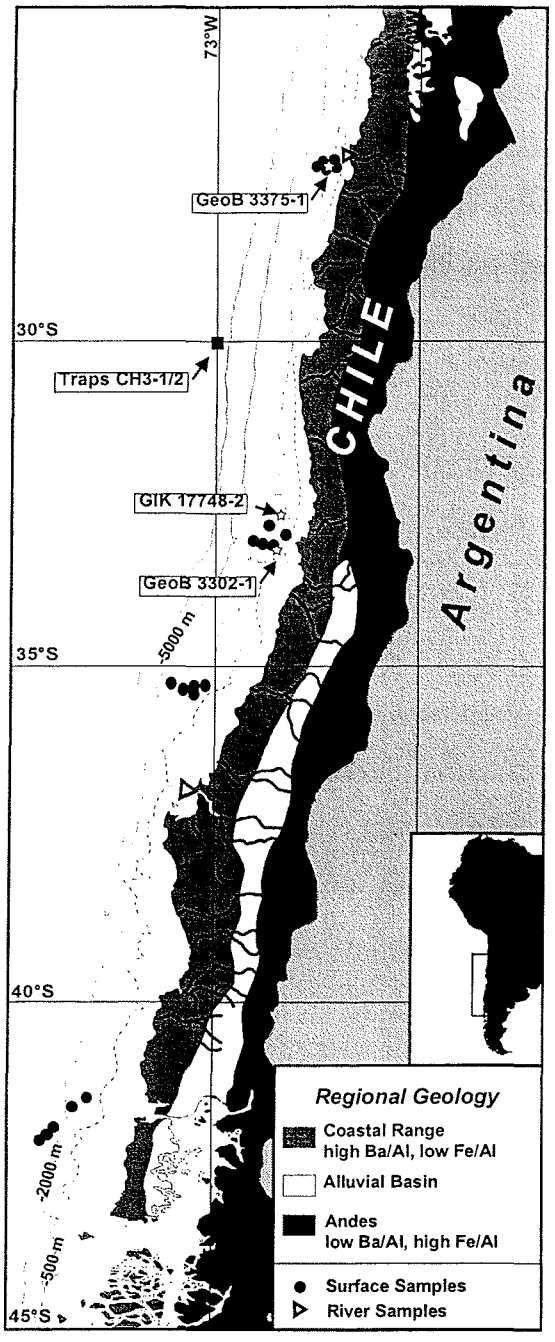

Figure 1.5. Schematic diagram of the principal geological features of Chile and their geochemistry. Symbols show the locations of surface samples, stream samples, gravity cores, and sediment traps used in this study.

centimetre of sediment of these multi-cores was taken as a surface sample. The sediment trap samples were collected in traps CH3-1 and CH3-2 (30°01.1'S, 73°11.0'W, water depth 4350, CH3-1 at 2323 m, CH3-2 at 3676 m) during the period July 1993 to January 1994 in sampling intervals of 9 days (Hebbeln *et al.*, in press 1998). Traps of the type S/MT 230 with twenty sample cups were used. The locations of the cores, surface samples, and of the sediment traps are marked on Figure 1.5.

1.3.2. Total acid digestion and ICP-AES

The freeze-dried and homogenised samples were subjected to total acid digestion using HNO_3, $HClO_4$ and HF in Teflon pressure vessels at 180°C over eight hours. Subsequently, the acid was evaporated close to dryness, and the residue was dissolved in HNO_3 and again digested over eight hours in a PDS-6 pressure system. Finally, the solution was decanted into a pre-cleaned glass flask and filled to 100 ml with deionised water and then filled into pre-cleaned polyethylene bottles for cold storage. The concentrations of Ba, Al, and Fe were measured using a Perkin Elmer ICP atomic emission spectrometer (ICP-AES). The error on the measurements is 4% for Ba, 2.5% for Al, and 2.1% for Fe. The accuracy of the measurements was determined by including a standard sample (USGS Analyzed Marine Mud MAG-1) in every batch of samples processed and repeat measurements (n = 22) on these standard samples.

1.3.3. Carbonate and total organic carbon

The total carbon content of the samples was measured using an elemental analyser (Heraeus CHN-O-Rapid). The carbonate content was calculated by subtracting the total organic carbon (*TOC*) content of decalcified samples from the total carbon (*TC*) content. The carbonate content was calculated using formula (1). More detail on this method can be found in Müller *et al.* (1994).

$$CaCO_3 = TC - TOC \cdot 8.333 \qquad (1)$$

1.3.4. Stratigraphy

Oxygen stable isotope compositions of the samples were measured on a Finnigan MAT 251 mass spectrometer with an automated carbonate preparation device. Twenty individual tests (>212 mm) of the foraminifera *Neogloboquadrina pachyderma* (sin.) were picked for each measurement. The isotopic composition of the sample was measured on the CO_2 gas developed by treating the sample with phosphoric acid at a constant temperature of 75°C. The isotopic ratio of ^{18}O to ^{16}O is given in per mill notation relative to the PDB (Pee Dee Belemnite) standard. A working standard (Burgbrohl CO_2 gas) was used to measure the isotopic ratios of the standards NBS 18, 18, and 20 of the National Bureau of Standards. The analytical standard deviation is about ±0.07‰ PDB (Isotope Laboratory at Bremen University).

The ^{14}C-ages were determined at the Leibniz Laboratory for Age Determinations and Isotope Research (Christian-Albrechts Universität Kiel, Germany) using 10 mg carbonate (only shells of *N. pachyderma* sin.) (Nadeau *et al.*, 1997). All ages were corrected for ^{13}C and for a reservoir age of 400 years (Bard, 1988) and then converted to calendar years using the method of Bard *et al.* (1990).

The age model for core GeoB 3375-1 was constructed on the basis of orbital tuning of the median silt grain size (Lamy *et al.*, 1998a) to the precession of Earth's orbit (Berger, 1978; Martinson *et al.*, 1987) and graphical correlation with the SPECMAP $\delta^{18}O$ stack (Imbrie *et*

al., 1984; Martinson *et al.*, 1987). The phase relation of the grain size parameter to precession was determined by using four AMS-^{14}C dates (Tab. 1.1; Fig. 1.6a) as anchor points in the orbital tuning procedure. The resulting sedimentation rates show an increase in the sedimentation rate from 3.6 to 8.1 cm ka^{-1} from 120 ka BP to the Holocene (Lamy *et al.*, 1998a).

The age model for core GIK 17748-2 is based upon six AMS-^{14}C dates (Tab. 1.1; Fig. 1.6b) and linear interpolation between these age control points (Marchant, 1997). The composite core depth of the modern sediment surface was set to -13 cm because, compared with samples from a box corer at the same site, the upper 13 cm seem to be missing (Stoffers and Cruise Participants, 1992). In addition, three turbidites (9-16 cm, 47-54 cm, and 160-177 cm) were identified in the core. These are considered to be geologically instantaneous events and are therefore excluded from the linear interpolations from which the linear sedimentation rate was determined. AMS-^{14}C dates immediately above and below the older turbiditic layer show that erosion by the turbidite did not occur. The same is assumed for the two younger layers. The maximum age of the core is 15,600 years B.P. Sedimentation rates vary between 7 and 20 cm/ka during the Holocene and were significantly higher during the deglaciation.

The age model for core GeoB 3302-1 is based upon seven AMS-^{14}C dates (Tab. 1.1; Fig. 1.6b) (Lamy *et al.*, 1999). In addition, the δ^{18}O isotope record of the uppermost section of the core was correlated to the isotope record of core GIK 17748-2. The linear sedimentation rate was interpolated where AMS-^{14}C dates were available. For the lowermost section of the core the linear sedimentation rate was extrapolated from the sedimentation rate between the two oldest AMS-^{14}C dates. According to this age model (Lamy *et al.*, 1999), the sedimentary record of core GeoB 3302-1 covers the period 28 ka to 9.8 ka. In contrast to core GIK 17748-2 the sedimentation rates during the early Holocene and glacial termination were rather low (5 to 6 cm/ka). A sharp peak in the sedimentation rate is found around 17.7 ka (>60 cm/ka). The sedimentation rates during the last glacial were fairly high (20 to 40 cm/ka). Both cores are presented together, since they were retrieved from positions in close proximity of each other. Their sedimentary records could be combined because of the good agreement of their isotopic and sedimentological records in the region where the two records overlap.

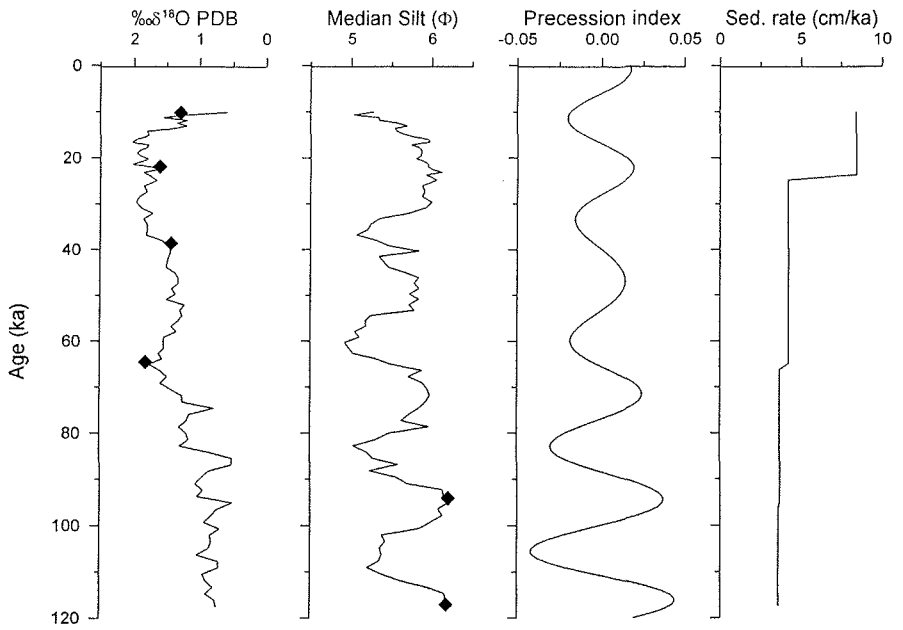

Figure 1.6a. Age model of core GeoB 3375-1. Shown here (from left to right) are the $\delta^{18}O$ curve measured in the planktic foram N. pachyderma (sin.), the median size of sortable silt, the precession index (Berger & Loutre, 1991) and the resulting linear sedimentation rate. The diamond symbols indicate the age control points used for linear interpolation in the age model. All sediment data are from Lamy et al. (1998a).

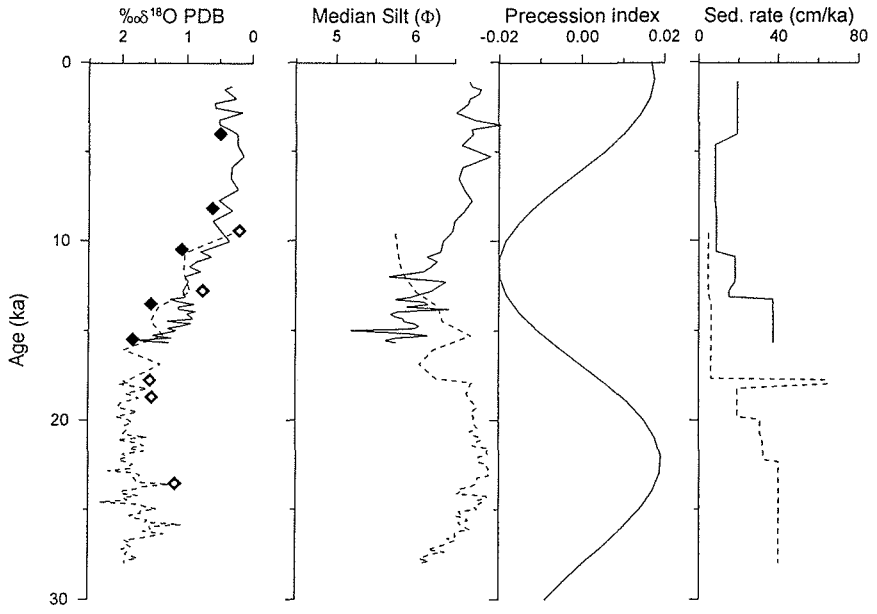

Figure 1.6b. Age models of cores GIK 17748-2 (solid line) and GeoB 3302-1 (stippled line). Parameters used for the age models are (from left to right) the $\delta^{18}O$ curve measured in the planktic foram N. pachyderma (dex.), the median size of sortable silt, the precession index (Berger & Loutre, 1991) and the resulting linear sedimentation rate. The diamond symbols indicate the age control points used for linear interpolation in the age models (solid symbols - GIK 17748; open symbols - GeoB 3302-1). All sediment data can be found in Lamy et al. (1999).

Depth cm	C-14 Age yrs. B.P.	+ Err.	- Err.	Cal. Age yrs. B.P.	Remarks
GeoB 3375-1					
13	9760	100	100	11262	a
118	20060	330	320	23722	a
183	34460	2120	168	39146	a
293				65000	b
403				95000	c
478				116000	c
GIK 17748-2					
63-78	3760	40	40	4030	a
98-103	6890	40	40	7530	a
128	9650	79	79	10620	a
153-158	10520	50	50	12210	a
183-188	11200	50	50	13050	a
333-348	12890	60	60	15140	a
GeoB 3302-1					
3				9790	d
18	11030	160	160	12840	a
48	14950	120	120	17700	a
68	15200	130	130	18010	a
103	16660	150	150	19820	a
133	17450	170	170	20800	a
178	18590	180	180	22210	a
233	18700	210	210	23590	a

Table 1.1. Age control points used to construct the age models of cores GeoB 3375-1, GIK 17748-2, and GeoB 3302-1.
a.) *AMS ^{14}C dates converted after the method of Bard et al. (1993).*
b.) *Marine Isotope Stage 4.2 (Imbrie et al., 1984).*
c.) *Precession maximum (Berger & Loutre, 1991).*
d.) *Correlation of $\delta^{18}O$ isotope record to GIK 17748-2.*

All data used in this manuscripts are archived in the Pangaea database (URL: http://www.pangaea.de/Projects/GeoB/JKlump).

1.4. Reconstructing paleoproductivity from proxy parameters in the sediment

How can the paleoproductivity in the ocean be studied? As a first approach the amount of organic carbon buried in the sediment may be used to estimate the paleoproductivity in the overlying water column. However, a major problem arises from the large variability in the degree of preservation of organic carbon once it has been exported from the euphotic zone. The carbon signal measured in the sediment is therefore a productivity signal overprinted to an unknown extent by a preservation signal. Because paleoproductivity is such an important factor, several proxy indicators of paleoproductivity have been developed (see Elderfield, 1990). Of the many proxies available, biogenic carbonate was used to gain additional information about Late Quaternary productivity variations in the Peru-Chile Current. In addition, the potential of biogenic barite to serve as a proxy of paleoproductivity was tested. Both proxies have the advantage to be far less influenced by preservation effects than organic carbon.

Several methods of reconstructing paleoproductivity from organic carbon accumulation can be found in the literature (Müller and Suess, 1979; Sarnthein *et al.*, 1992; Sarnthein *et al.*, 1988). Of the methods available, the method of Müller and Suess (1979) was used to reconstruct the primary productivity of the total biomass, because it the most suitable formula for hemi-pelagic environments (Rühlemann *et al.*, 1996). Carbonate-based productivity reconstructions (modified after van Kreveld *et al.*, 1996) were used to estimate the proportional contribution of carbonate-shell secreting organisms to the total productivity. More detailed discussions of these methods can be found in Chapter 4. Upwelling cells have been observed to remain in a fixed position, but change in size (Armstrong *et al.*, 1987; Johnson *et al.*, 1980; Strub *et al.*, 1998). A common feature of all upwelling cells is a typical phytoplankton zonation from diatoms in the centre of the upwelling cell to coccolithophorids in the filament zone (Armstrong *et al.*, 1987; Blasco *et al.*, 1980; Richert, 1975). These changes of the phytoplankton assemblage are recorded in the sediment by changes in the ratio of carbonate to total organic carbon (Mortyn and Thunell, 1997). As the local upwelling cell expands due to increased upwelling, the biogenic sedimentation at the core site changes from coccolithophorid-dominated to diatom-dominated, and vice versa as the cell contracts again. Thus, the changes in the relative contribution of carbonate-shell secreting organisms to the total productivity at the core position can be used to infer changes of the spatial extent of the local upwelling cell.

1.5. Biogenic barite in marine sediments

Because of the problems associated with organic carbon as a paleoproductivity proxy we decided to use biogenic barite as an alternative paleoproductivity proxy. (Goldberg and Arrhenius, 1958) were the first to report high concentrations of barium beneath the equatorial upwelling zone of the Pacific Ocean and suggested a link between barium accumulation and productivity. Many years later Dehairs *et al.* (1980) identified particulate barite in the sediment and in the water column as the carrier of this signal. The process of formation of marine barite, especially a possible biotic origin of marine barite crystals, is still unclear. Some authors interpret the Ba enrichment in decaying organic matter to be caused by biotic processes, i.e. organisms enriching Ba in their skeletons, like acantharians (Bernstein *et al.*, 1992; Bernstein *et al.*, 1998), xenophyphores (Gooday and Nott, 1982), and filamentous blue-green algae (Gayral and Fresnel, 1979). The incorporation of the remains of these biota into biogenic aggregates, such as faecal pellets, provides an environment for barium sulphate to precipitate and a transport mechanism to the sea-floor. This model is supported by the similarity of marine barite crystals in surface sediment samples and from oblique net hauls from surface waters (Bertram and Cowen, 1997). Other authors interpret the formation of biogenic barite as an abiotic process. In their model, barium sulphate precipitates from the sulphate of decaying proteins in organic aggregates, such as faecal pellets, and dissolved barium in the ocean (Dehairs *et al.*, 1980; Gingele and Dahmke, 1994; Stroobants *et al.*, 1991), which is supported by a clear correlation between C_{org}/Ba ratios in particulate matter in sediment traps and the concentration of dissolved Ba in sea-water (Dymond *et al.*, 1992).

Studies on the morphology and internal structure of marine barite (Gingele and Dahmke, 1994; Stroobants *et al.*, 1991) support a model in which barium sulphate forms amorphous precipitates in decaying organic aggregates and crystallises on the way through the water column to the sea-floor. A systematic increase of biogenic barium in sinking particulate matter (Dymond *et al.*, 1992) and in sediments (see von Breymann *et al.*, 1992, and Chapter 3) with water depth points to such an abiotic process in the formation of marine barite. However, without organic matter marine barite will not be formed. To clearly indicate the relation between marine barite and biological production the term 'biogenic barium' is commonly used to describe this portion of the total barium content and to distinguish it from terrigenous barium.

A major uncertainty in the application of biogenic barium as a proxy of paleoproductivity in the ocean is the terrigenous input of barium to the sediment. In sediments with a dominant terrigenous component biogenic barite, the carrier phase of biogenic barium in the sediment, cannot be determined directly but has to be determined by normative calculations (Dymond *et al.*, 1992). An accurate knowledge of the terrigenous Ba/Al ratio is crucial for such calculations. This ratio depends on the geochemistry of the sediment source and may show considerable variability between different regions on the continent. The terrigenous input of barium to the Chilean continental slope depends not only on the geochemistry of the hinterland, but also on how much the two major sediment source areas, the Andes and the Coastal Range, contribute to the measured bulk geochemical signal of the continental slope sediment. The amount of material eroded from the Andes or from the Coastal Range depends on the regional precipitation patterns which are known to have changed in response to Late Quaternary climate changes (see Heusser, 1984; Lamy *et al.*, 1998a; Lamy *et al.*, 1998b; Lamy *et al.*, 1999; Veit, 1996; Villagrán, 1993; Villagrán and Varela, 1990; and Chapter 2). However, beyond these descriptive interpretations of Late Quaternary climate change in northern and central Chile a quantitative measure was needed to assess the variations of the geochemistry of the terrigenous material deposited on the Chilean continental margin. As outlined above (Section 1.2.3.), both sediment sources, the Andes and the Coastal Range, are geochemically distinct and a two-end-member model can be used to calculate the proportions to which both sources contribute to the sediments on the continental slope (see Chapter 3).

Having derived the terrigenous Ba/Al ratio from the geochemical model, the biogenic fraction of barium in the sediment can be determined and then, together with the sedimentation rate, be used to calculate the flux rate of biogenic barium to the sediment. The paleoproductivity can then be reconstructed from biogenic barite through the algorithm proposed by (Dymond *et al.*, 1992). However, this algorithm requires the concentration of dissolved barium in intermediate and deep waters of the ocean region studied. Due to the lack of paleo-data (Dymond *et al.*, 1992) used modern day Ba concentrations measured during the GEOSECS Expeditions (GEOSECS, 1987). From Ba/Ca ratios in planktic and benthic foraminifera we know that the concentration of dissolved Ba in sea water has changed even in recent geological times (Lea, 1993). Anomalous biogenic barium peaks found around Termination I in sediments from the Atlantic and Pacific Oceans also hint at global changes in the biogeochemical cycle of barium in the ocean in connection with glacial/interglacial changes of ocean circulation and sea water

chemistry. Recent work by McManus *et al.* (1999) shows that barium and alkalinity flux from the sediment to the deep ocean are coupled. Chapter 5 discusses the possibility whether the anomalous barium accumulation found after Termination I in cores from the Chilean continental margin may be the result of: (1) changes in ocean circulation after the Last Glacial Maximum and the Younger Dryas, and (2) changes in sea water chemistry linked to changes in the oceanic carbonate system.

To assess whether biogenic barium can be used as a paleoproductivity proxy a number of questions had to be answered:

(1) Can biogenic barite be detected quantitatively by direct methods such as XRD analysis?
(2) If biogenic barite cannot be detected directly and quantitatively, but has to be derived from normative calculations, how could the regional terrigenous Ba/Al ratio be determined?
(3) Does the regional terrigenous Ba/Al ratio change with changes of sediment provenance?
(4) What was the scale of Late Quaternary climate change in northern and central Chile?
(5) Does water depth influence the accumulation rate of biogenic barium in the sediment?
(6) How do changes in the concentration of dissolved barium in sea water influence the accumulation rate of biogenic barium in the sediment?
(7) How do the results from biogenic barium compare to the paleoproductivity reconstructions derived from organic carbon and from biogenic carbonate?

The manuscripts, which make up the body of this thesis, will follow all these questions and try to provide answers.

1.6. Submitted manuscripts and manuscripts in preparation

The work conducted in the course of this project is summarised in the following manuscripts:

Chapter 2

J. Klump, F. Lamy, D. Hebbeln, and G. Wefer

Late Quaternary rapid climate change in northern Chile. To be submitted to *Terra Nova*.

Late Quaternary rapid climate change in northern Chile was reconstructed from illite crystallinity and from the Fe/Al ratio of the bulk sediment. Superimposed on cyclical changes, which follow a precessional cycle, are rapid climate changes on sub-Milankovitch time-scales. These rapid climate changes can be correlated to the 'Bond cycles' of the North Atlantic and thus to the climate record of the GISP2 ice-core, Greenland. In northern Chile the recorded climate changes are expressed as changes of the regional precipitation pattern which are caused by latitudinal shifts of the Southern Westerlies.

Chapter 3

J. Klump, D. Hebbeln, and G. Wefer

The impact of sediment provenance on barium-based productivity estimates. Submitted to *Geochimica et Cosmochimica Acta.*

In most hemi-pelagic sediments the concentration of biogenic barite cannot be measured directly, but has to be derived from normative calculations. Working with sediments with a high (>50 %) proportion of terrigenous material an accurate knowledge of the geochemistry of the local terrigenous material becomes essential. Surface samples from the Chilean continental slope and sediments from two major Chilean rivers were used to define a two end-member mixing model of the Chilean continental hinterland geochemistry. The terrigenous background Ba/Al ratios were shown to vary along the Chilean coast, with significant deviations from the average continental Ba/Al ratio quoted in the literature. This method was applied to two gravity cores from the continental slope off northern and central Chile. The results show that changes in sediment provenance significantly affect barium-based productivity estimates.

Chapter 4

J. Klump, D. Hebbeln, and G. Wefer

Late Quaternary paleoproductivity variations in the Peru-Chile Current off northern and central Chile. To be submitted to *Marine Geology.*

The late Quaternary paleoproductivity in the Peru-Chile Current was studied in the sedimentary record of two gravity cores from the continental slope off northern and central Chile. The combined record of the two cores shows that the paleoproductivity was highest during the last glacial period and during the early and middle Holocene. The lowest paleoproductivities were

found during the Last Glacial Maximum and during the late Holocene. Paleoproductivity reconstructions based on biogenic carbonate show that the paleoproductivity of carbonate shell-secreting organisms was highest during times of low total productivity. The change of the phytoplankton assemblage points to a change in size of the respective local upwelling cells at the two core positions.

Chapter 5

J. Klump, D. Hebbeln, and G. Wefer

High concentrations of biogenic barium in marine sediments around Termination I - A signal of changes in productivity, ocean chemistry and deep water circulation. To be submitted to *Marine Geology*.

In two gravity cores from the Chilean continental slope anomalously high concentrations of barium were found in sediments deposited during the early and middle Holocene. These barium peaks cannot be explained by changes in sediment provenance to high-barium source rocks, by a dramatically increased paleoproductivity, or by diagenetic processes. The biogenic barium flux was used in a geochemical model to calculate the concentration of dissolved barium in the intermediate and deep waters of the Southeast Pacific. The modelling results show that the concentration of dissolved barium in the Pacific was increased during the early and middle Holocene. This increase is found on two time-scales: (1) short-term increases caused by influx of water masses with increased barium concentrations from the North Atlantic following the end of the Last Glacial Maximum and the end of the Younger Dryas, and (2) an increased flux of previously carbonate-bound barium from the sediment caused by shoaling of the Pacific carbonate compensation depth after the end of the Last Glacial Maximum.

Chapter 2 - Late Quaternary rapid climate change in northern Chile

by J. Klump, F. Lamy, D. Hebbeln, and G. Wefer

Fachbereich Geowissenschaften, Universität Bremen.

Abstract

Climate variability in a presently arid region like the Atacama desert in northern Chile is mainly expressed by changing precipitation patterns. Thus, more humid conditions in Chile during the Last Glacial Maximum have been explained by an equatorward shift of the Southern Westerlies. Analyses of terrigenous sediments from the Chilean continental slope off the southern border of the Atacama desert (27.5°S), focusing on illite crystallinity and the Fe/Al ratio of the sediments, support such a latitudinal shift of the Southern Westerlies. Besides showing dominantly precession driven variability in precipitation over the Andes, these analyses revealed also rapid changes in weathering intensity along the Chilean Coastal Range during the last 80,000 years. These rapid changes occur at much shorter timescales than the 19 to 100 kyr orbital forcing of the Milankovitch cycles. With periods of only a few thousand years, this pattern of high frequency variability of the position of the Southern Westerlies is very similar to the coeval short-term climatic events known from Greenland ice cores and from North Atlantic sediments.

2.1. Introduction

High resolution paleoclimatic records from southern South America and the adjacent Southeast Pacific are rare. Existing reconstructions are primarily based on terrestrial data (e.g. Clapperton, 1993; Heusser, 1990; Lowell *et al.*, 1995; Veit, 1996) and only few studies of marine sediments exist (e.g. Lamy *et al.*, 1998a; Lamy *et al.*, 1999). The paleoclimatic variability recorded in these data-sets is mainly expressed in terms of changing precipitation patterns induced by latitudinal shifts of the Southern Westerlies. However, the direction of Late Pleistocene shifts of the westerly wind belt in South America - equatorward (e.g. Heusser, 1989) or poleward (Markgraf, 1989) - has long been discussed. More recent results based on paleoclimatic modelling (Hulton *et al.*, 1994), on glacier fluctuations in southern Chile (Clapperton *et al.*, 1995), and on analyses of marine sediments (Lamy *et al.*, 1998a) are mostly in favour of an equatorward shift of the Southern Westerlies during the Last Glacial Maximum.

In this paper we present data of terrigenous sediment analyses from the continental slope off the Chilean Norte Chico (27.5°S). By tracing the input of material from the Andes to the ocean, which depends on medium- to large-scale shifts of the Southern Westerlies, and by tracing the weathering intensity in the Coastal Range, which also varies with small-scale shifts of the Southern Westerlies, the continental paleoclimate in Chile during the last 80 kyr can be reconstructed. Besides giving further support to a precessional driven large-scale shift of the westerly wind belt, e.g. resulting in more humid conditions in Chile during the Last Glacial Maximum, these data also exhibit small-scale but high frequency climate variations. The pattern found is very similar to the well known millennial-scale climate variability found in Greenland ice cores (Dansgaard *et al.*, 1993) and in North Atlantic deep-sea sediments (Bond *et al.*, 1993). Combined with high frequency glacier fluctuations in the Southern Andes (Lowell *et al.*, 1995), these results point to a global extent of such short-term climatic events during the last glaciation.

2.2. Regional climate and geology

The positions of the sediment cores we report on lie off the Norte Chico (27.5°S), the border region between the hyper-arid climate of the Atacama Desert in northern Chile and the semi-arid, Mediterranean climate of mid-latitude Chile, characterised by seasonal winter rain (Fig. 2.1). In the Norte Chico rare winter rain occurs today only in connection with passing frontal systems from the Southern Westerlies (Miller, 1976). The extreme climatic gradient makes the region very sensitive to latitudinal shifts of the climate zones along the South American Pacific margin. Thus, small shifts of the present atmospheric circulation systems could cause significant climatic changes and modifications of the terrestrial sedimentary environment, presumably also affecting the input of terrigenous sediments to the core site. Such a latitudinal shift, mainly a northward displacement of the Southern Westerlies, has been proposed to be the major reason for a more humid and colder climate in northern Chile during the Last Glacial Maximum (Heusser, 1984; Heusser, 1989). Shifts of the Southern Westerlies to the north follow the precessional cycle throughout the last 120 kyr resulting in more humid periods roughly every 20 kyr (Lamy *et al.*, 1998a).

The continental hinterland of the core sites is characterised by an abrupt rise from the coast to the Coastal Range with elevations of 2000 m to 2500 m. The Coastal Range consists primarily of plutonic rocks and is separated from the Andes by a longitudinal depression zone marked by several alluvial basins, especially north of 27.5°S, and the Chilean Central Valley south of 33°S. The geology of the Andes is characterised by abundant volcanics which can be divided into Pre-Pliocene rhyolitic to andesitic ignimbrites and Pliocene-Quaternary andesitic rocks and tephra forming up to 6000 m high stratovolcanoes with modern activity north of 27.5°S and south of 33°S (Thornburg and Kulm, 1987; Zeil, 1986).

The southern border region of the Atacama Desert is characterised by prevailing arid conditions and dry valleys with only sporadic water runoff. Sediments derived from the Andes are mostly trapped in the alluvial basins east of the Coastal Range and do not reach the ocean. A prominent feature of the Norte Chico are coastal fogs ('Camanchacas') and marine stratus clouds (Figures 2.1 and 2.2). They supply moisture to the Coastal Range and reduce insolation and evaporation (Aravena *et al.*, 1989; Miller, 1976). This local phenomenon promotes

vegetation cover and soil development (Aravena *et al.*, 1989; Veit, 1996), and therefore also controls chemical weathering.

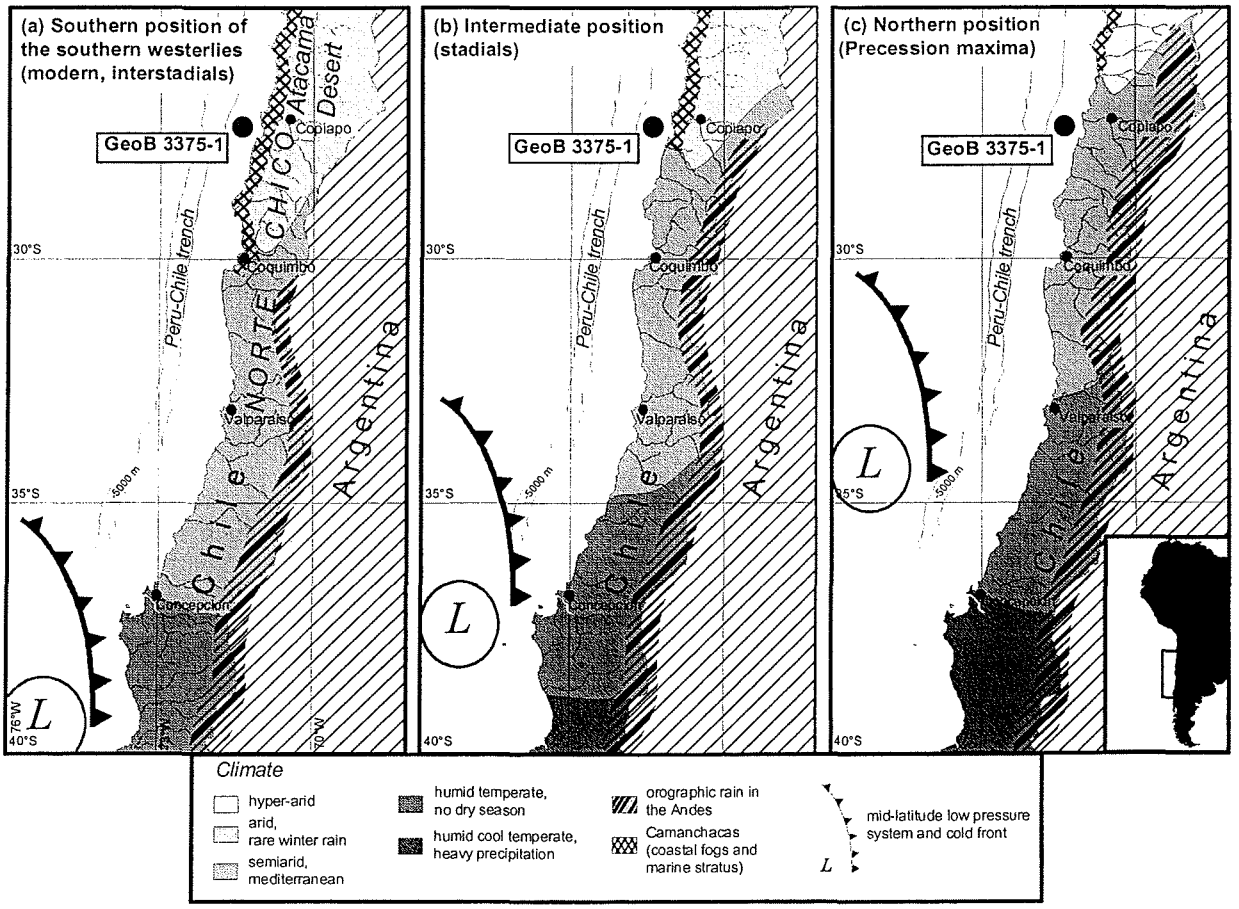

Figure 2.1. Climatic zonation in Chile for various positions of the Southern Westerlies. Superimposed are the positions of the Camanchacas (coastal fogs), areas of orographic rain, a schematic representation of a mid-latitude cyclone with its associated cold-front, and the location of marine sediment core GeoB 3375-1 (27°28'S, 71°15'W; 1947 m water depth). A northward displacement of the Southern Westerlies leads to a northward shift of the climatic zones resulting in a northward extension of orographic rain in the Andes and a equatorward shift of the Camanchacas: (a) southern position of the Southern Westerlies reflecting modern conditions (Miller, 1976) and assumed position during interstadials, (b) intermediate position of the Southern Westerlies assumed for stadials, and (c) northern position of the Southern Westerlies reached during precession maxima.

2.3. Methods

The age model of core GeoB 3375-1 is based on three ^{14}C AMS dates and the $\delta^{18}O$ isotope record of *Neogloboquadrina pachyderma* (sin) (Lamy *et al.*, 1998a). Cyclic variations of

grain-size parameters fit well to the orbital precession index supporting the age model (Lamy *et al.*, 1998a). The core comprises a record from 9 to 120 kyr; here we focus on the interval from 9 kyr to 80 kyr, where high resolution sampling provided a temporal resolution between 300 and 600 years for the section younger than 60 kyr, and up to 1200 years beyond that point.

Illite crystallinity was measured by X-ray diffraction methods (Petschick *et al.*, 1996), using the $CaCO_3$ and C_{org}-free clay fraction (<2 mm) which was separated by Atterberg procedures (Müller, 1967). The half height width (HHW) of the 10 Å illite peak was taken as a measure of crystallinity. The mean relative error of this procedure is about 5.2%. To measure the elemental ratios, bulk samples were subjected to total acid digestion. The elemental concentrations were then obtained by ICP-OES spectroscopy. The mean relative error of this procedure is 4.0% for Al and 2.2% for Fe measurements.

2.4. Results and discussion

Marine sediments from the continental slope off the Norte Chico consist mainly of terrigenous material with $CaCO_3$ contents between 9 and 21 wt-%. Variations in the composition of the terrigenous fraction of the sediment are mostly due to changing environmental conditions on the continent. Given the strong modern gradient in humidity, climate change in this area probably would result in changing precipitation patterns. Such changes can be traced in continental slope sediments by proxies e.g. for the intensity of chemical weathering or for changing sediment source areas. In core GeoB 3375-1 illite crystallinity and the Fe/Al ratio of the bulk sediment have been used as such proxies.

Fe-contents of the bulk sediment vary between 2.5 and 3.4 wt-% and are thus several orders of magnitude higher than possible variations induced by changes in paleoproductivity (organic carbon content 0.6 - 1.1 wt-%). Therefore, we interpret changes in the Fe/Al ratio of the bulk sediment as a terrigenous signal, which is determined primarily by the geochemistry of the source rocks. In general, the Fe/Al ratio of acidic-plutonic rocks, as found in the Coastal Range, is lower than the Fe/Al ratio of basaltic-andesitic rocks (Le Maitre, 1976), as found in

the Andes. Thus, changes in the Fe/Al ratio in the bulk sediment of the two cores are interpreted to reflect variations in the relative contributions of these two source areas to the continental slope sediments.

In the Norte Chico, an increase in the Fe/Al ratio points to increased precipitation, which results in higher river run-off and thus transport of material with high Fe/Al ratios from the Andes into the ocean. During periods of decreased precipitation the run-off is not high enough to pass the longitudinal depression separating the two mountain ranges, leaving only a Coastal Range signal (i.e. low Fe/Al ratios) in the sediments.

In the Norte Chico the Fe/Al ratio follows mainly the precessional cycle, with higher Fe/Al ratios, indicating increased precipitation, occurring during times of maximum austral summer insolation (i.e. precession maxima) (Fig. 2.2c). The distinct cyclicity shown by the Fe/Al record clearly points to precessional forced shifts of the Southern Westerlies, which reach their northernmost position during precession maxima (Fig. 2.1). This interpretation is consistent with palynological studies from mid-latitude Chile (Heusser, 1984). Superimposed on these Milankovitch-scale cycles are shorter fluctuations. These are marked by increased Fe/Al ratios during precession minima at approx. 10 to 13 kyr, 40 kyr, and 65 kyr (Fig. 2.3). During these events, which occurred in a generally dry climate, a northward shift of the Westerlies increased the precipitation in northern Chile, resulting in a considerable input of material from the Andes into the ocean. If further short-term northward shifts occurred during humid periods, a further increase in precipitation does not increase the Fe/Al ratio because the Andean source was active anyway.

The illite in the continental slope sediments off the Norte Chico is mainly derived from acidic-plutonic source rocks of the Coastal Range. Its crystallinity is an indicator of the chemical weathering intensity in the sediment source area (Chamley, 1989; Singer, 1984). Stronger chemical weathering leads to an opening of the illite structure (i.e. lower crystallinity) due to leaching of Fe/Mg from the illite crystal lattice. The intensity of chemical weathering is determined by temperature and available moisture. Due to the extreme diurnal temperature range in the arid to semi-arid Norte Chico, a change in the mean annual temperature will not cause changes in the intensity of chemical weathering. Therefore

variations in the supply of moisture will play a crucial role and appears to be the factor controlling chemical weathering and, thus, illite crystallinity.

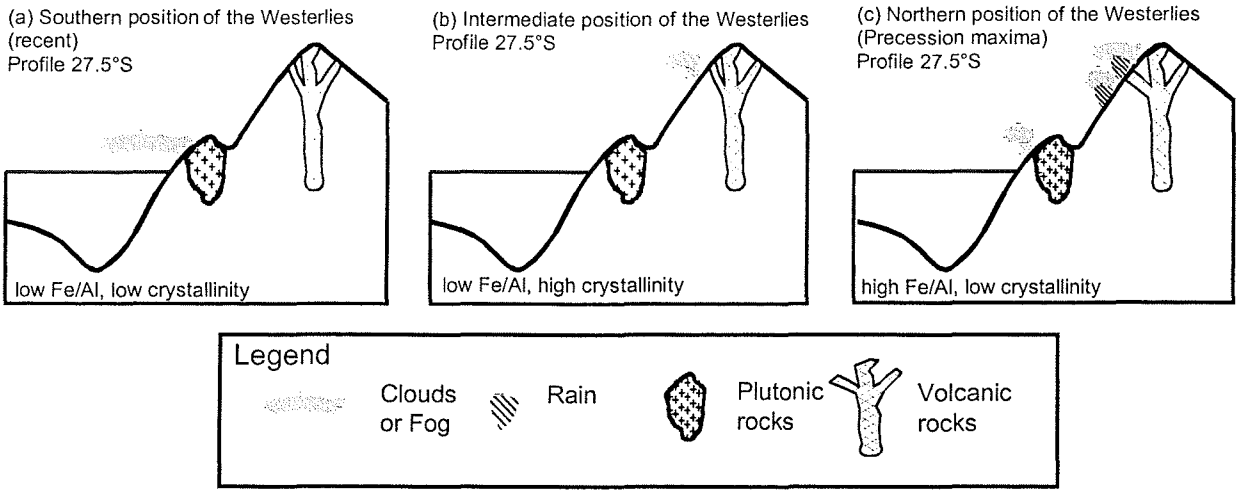

Figure 2.2. Cross-sections through Chile at 27.5°S, showing the precipitation patterns resulting from latitudinal shifts of the Southern Westerlies, and simplified hinterland geology. (a) Southern position of the Southern Westerlies reflecting modern conditions (Miller, 1976) and assumed position during interstadials, (b) intermediate position of the Southern Westerlies assumed for stadials, and (c) northern position of the Southern Westerlies reached during precession maxima

Besides the precession-driven variability in precipitation recorded by the Fe/Al ratios, the illite crystallinity displays a high-frequency, sub-Milankovitch variability during the last glacial (Fig. 2.3). Variations in illite crystallinity are interpreted to reflect the varying strength and frequency of the Camanchacas which supply moisture to the Coastal Range in the Norte Chico. Although these coastal fogs do not result in a considerable run-off, they supply enough moisture to promote soil development and, thus, chemical weathering (Veit, 1996). Once the illite has been altered it can be transported to the ocean by occasional rain events or by eolian transport, which has been proven to be important in this region (Lamy *et al.*, 1998a).

The strength and frequency of the Camanchacas is controlled by the position of the Southern Westerlies. Today the Camanchacas decrease in frequency and intensity towards the south of the study area and only rarely occur south of about 31°S (Miller, 1976) (Fig. 2.1). Thus, a small equatorward shift of the Westerlies would reduce the occurrence of Camanchacas and thus decrease the available moisture in the Coastal Range without markedly increasing rainfall in the Andes (Fig. 2.2b).

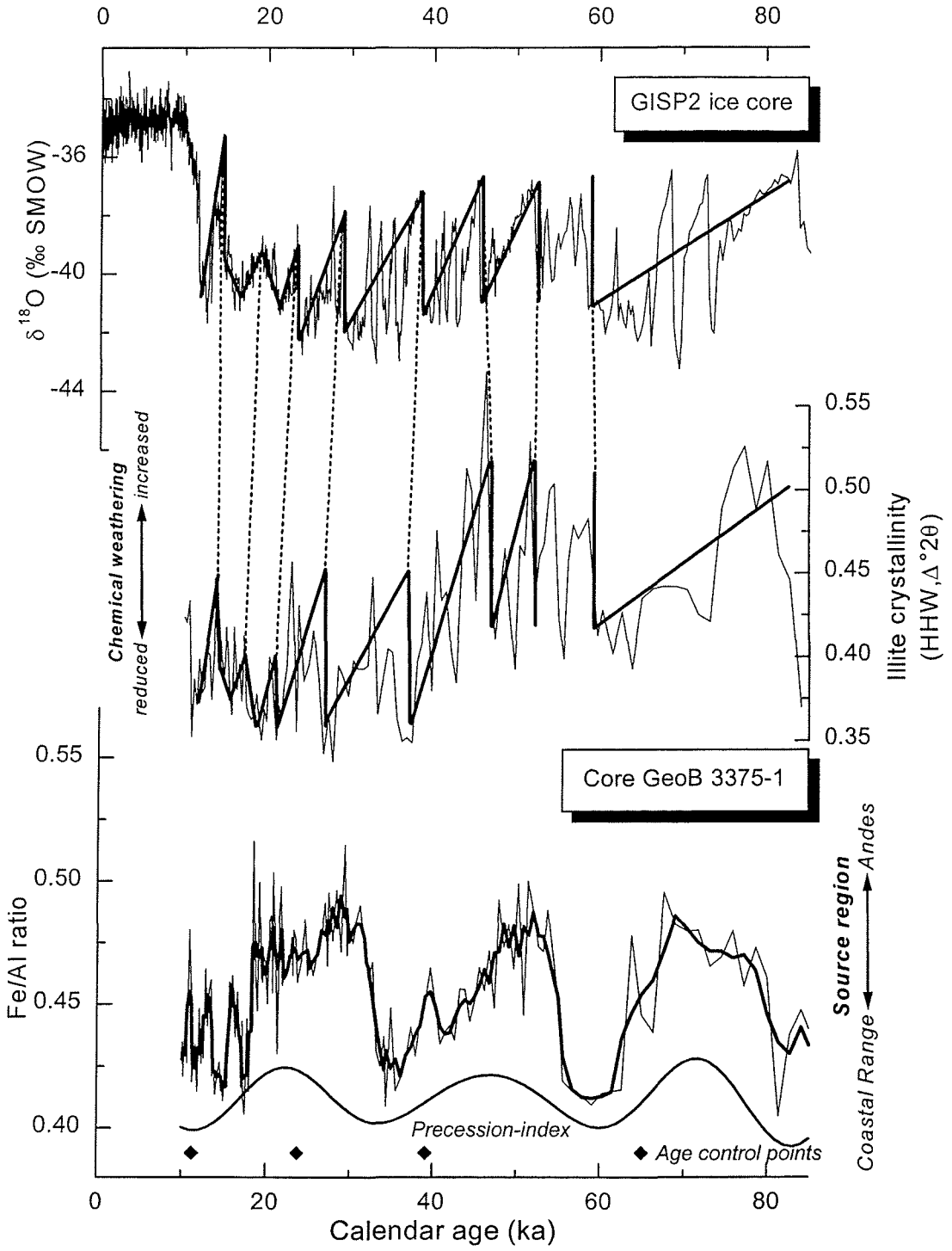

Figure 2.3. Climate proxy data from marine sediment core GeoB 3375-1 compared to the GISP2 ice-core data. The illite crystallinity record of core GeoB 3375-1 can be correlated with the $\delta^{18}O$ isotope record of the GISP2 ice-core (Grootes et al., 1993) for the last approximately 80 kyr. North Atlantic cooling cycles (adapted from Bond et al., 1993) and tentative correlation lines are superimposed on both records.

The short-term variability of the illite crystallinity, reflecting variations in the availability of moisture in the Coastal Range, is not shown by the Fe/Al ratio as a proxy for rainfall in the Andes (Fig. 2.3). Both records are mainly controlled by the position of the Southern Westerlies and shifts in the position of the Westerlies should also affect the rainfall in the Andes. However, for the rivers in the Norte Chico to be able to carry sediments from the Andes to our sampling site a certain threshold in the amount of rainfall has to be passed to activate the rivers cutting through the Coastal Range. If this threshold is not passed, the sediments are deposited in the morphological depression between the Andes and the Coastal Range and thus the signal of higher rainfall in the Andes (i.e. high Fe/Al ratio) does not enter the marine sedimentary record. This leaves the illite crystallinity as the most sensitive proxy of small latitudinal shifts of the Southern Westerlies on millennial time-scales.

2.5. Conclusions

Illite crystallinity and the Fe/Al ratio of sediments from the continental slope off the Chilean Norte Chico have proven to be sensitive indicators of climate change. The combination of these two parameters can be used to reconstruct the precipitation patterns in the Coastal Range and in the Andes of northern Chile. Especially the illite crystallinity in the Coastal Range has shown to record even subtle changes in the regional atmospheric circulation patterns and the resulting precipitation changes.

The changes in the precipitation patterns in northern Chile result from changes in the regional atmospheric circulation, mainly from equatorward shifts of the Southern Westerlies resulting in wetter periods (e.g. precession maxima). The cyclic behaviour of the measured parameters between 10 kyr and 80 kyr (core GeoB 3375-1) can be grouped into cycles of different order. The Fe/Al ratio follows the first order 20 kyr precessional cycle induced by major shifts of the Southern Westerlies. Superimposed are second order excursions of the Fe/Al ratio and rapid third-order fluctuations of the illite crystallinity also reflecting latitudinal shifts of the Southern Westerlies. In the ongoing debate on Late Quaternary climate change in Chile (Heusser, 1989; Markgraf, 1989), our data supports the view of an equatorward shift of the Southern Westerlies during stadials (Heusser, 1989).

A comparison of the short-term variability of the illite crystallinity record and the oxygen isotope record of the GISP2 ice core indicates a very similar pattern in both records (Fig. 2.3). This pattern becomes even more evident if the longer term cooling cycles, known as 'Bond cycles' from the North Atlantic (Broecker, 1994), are superimposed on both the crystallinity and the ice core record (Fig. 2.3). The coincidence of the Chilean moisture conditions record with temperature variations over the North Atlantic region (age deviations up to 2 kyr are due to stratigraphic uncertainties) points to global interhemispheric teleconnections, as suggested by previous glaciological studies from Southern Chile (Lowell *et al.*, 1995).

Acknowledgements — The authors would like to thank W.H. Berger, R. Schneider, and L. Vidal for their constructive discussion and comments on the manuscript. We thank B. Diekmann, G. Kuhn, R. Fröhlking, S. Janisch, and H. Rhodes at the Alfred Wegener Institut für Polar- und Meeresforschung in Bremerhaven for providing analytical assistance. Financial support was provided by the German Bundesministerium für Bildung and Forschung through funding the project *CHIPAL* (03G0102A).

Chapter 3 - The impact of sediment provenance on barium-based productivity estimates

by J. Klump, D. Hebbeln, and G. Wefer

Fachbereich Geowissenschaften, Universität Bremen.

Abstract

Biogenic barium in marine sediments has been suggested to be a reliable proxy of surface ocean paleoproductivity and algorithms have been developed to link these properties. However, problems arise when the proposed algorithms are applied to predominantly terrigenous sediments. A major source of error are incorrect estimates of the terrigenous Ba/Al ratio in normative calculations of the amount of biogenic barium in the sediment. Better results can be obtained by estimating the terrigenous Ba/Al ratio from exponential regression of the Ba/Al ratios of continental slope profiles. The terrigenous Ba/Al ratio varies not only in space, but also in time. A two component mixing model is used to quantify the relative contributions of the two source areas for sediments on the Chilean continental slope. From this, the variations of the Ba/Al ratio through time can be modelled. Applying this correction improves normative calculations of biogenic barium significantly. The calculated accumulation of biogenic barium show that the paleoproductivity in the Peru-Chile Current during the last glacial was higher than during the Last Glacial Maximum (LGM). The paleoproductivity increased again after the LGM.

3.1. Introduction

Proxies for paleoproductivity are needed to assess the ocean's role in changing CO_2 concentrations in the atmosphere through the Late Quaternary climatic cycles. These cycles are believed to be largely driven by productivity variations in the ocean (Broecker and Henderson, 1998). Most paleoproductivity proxy calculations are based upon the organic carbon content in the sediment. However, only between 0.1 and 1% of the organic carbon produced in the surface waters is finally preserved in the sediments (Berger *et al.*, 1989). Thus, every paleoproductivity estimate based on organic carbon is fraught with large uncertainties. To get closer to what the paleoproductivity might have been, a proxy measure independent of organic carbon is needed.

It had been suggested that barium from biogenic barite ($BaSO_4$) in marine sediments could be used as a proxy of surface ocean productivity in the overlying water column (Goldberg and Arrhenius, 1958; Schmitz, 1987) and algorithms have been developed to link these properties (Dymond *et al.*, 1992; François *et al.*, 1995). This method has been applied both in hemipelagic (Gingele and Dahmke, 1994; Schmitz *et al.*, 1997) and pelagic sedimentary environments (Bonn *et al.*, 1998; Nürnberg *et al.*, 1997; Paytan *et al.*, 1996; Schmitz, 1987; Thompson and Schmitz, 1997). Most studies using biogenic barium as a proxy of paleoproductivity have done so in a qualitative fashion (Paytan *et al.*, 1996; Schmitz, 1987; Schmitz *et al.*, 1997; Thompson and Schmitz, 1997). Two algorithms have been proposed to quantify paleoproductivity from the accumulation rate of biogenic barium in marine sediments (Dymond *et al.*, 1992; François *et al.*, 1995). Applying these algorithms has produced promising results (Bonn *et al.*, 1998; Gingele and Dahmke, 1994; Nürnberg *et al.*, 1997). However, as the amount of biogenic barium in the sediment is calculated from the difference between the measured total barium and the terrigenous barium fraction, a major problem is the remaining uncertainty about the terrigenous contribution towards the measured barium signal (Dymond *et al.*, 1992; Nürnberg *et al.*, 1997).

A suitable region to assess this problem is the Chilean continental slope. The coastal upwelling area off Chile is among the most important areas of high biological productivity in the modern ocean. However, the evolution of the paleoproductivity along the Chilean coast is

only poorly understood. The proportion of terrigenous material in sediments on the Chilean continental slope is very high (80 - 90%) (Hebbeln *et al.*, in prep. 1998). In predominantly terrigenous sediments the terrigenous barium input is calculated from the terrigenous Ba/Al ratio and the total Al content. Errors in the estimate of the terrigenous Ba/Al ratio result in large errors in the calculated fraction of terrigenous barium in the sediment (Dymond *et al.*, 1992).

The approach presented here tries to identify regional terrigenous Ba/Al ratios based on the analysis of stream samples from coastal Chile and marine surface sediments from the Chilean continental slope to improve estimates of the biogenic barium content in marine sediments. Such regional data can improve the calculation of the amount of biogenic barite in marine sediments significantly. A way to assess the impact of temporal changes of the sediment provenance on the terrigenous Ba/Al ratios will be given and applied to two sediment cores to calculate the amount of biogenic barium in the sediment. This will be used to provide estimates of the paleo-flux of biogenic barite also and then to estimate Late Quaternary paleoproductivity variations in the Peru-Chile Current.

3.2. Regional geology and climate

The continental hinterland of the core sites is characterised by an abrupt rise from the coast to the Coastal Range with elevations of 2000 m to 2500 m (Fig. 2.1). The Coastal Range consists primarily of plutonic rocks and is separated from the Andes by a longitudinal depression zone marked by several alluvial basins, especially north of 27.5°S, and the Chilean Central Valley south of 33°S. The geology of the Andes is characterised by abundant volcanics which can be divided into Pre-Pliocene rhyolitic to andesitic ignimbrites and Pliocene-Quaternary andesitic rocks and tephra forming up to 6000 m high stratovolcanoes with modern activity north of 27.5°S and south of 33°S (Thornburg and Kulm, 1987; Zeil, 1986). The two types of source rock have different chemical compositions. In general, the Fe/Al ratio of acidic-plutonic rocks, as found in the Coastal Range, is lower than the Fe/Al ratio of basaltic-andesitic rocks (Le Maitre, 1976), as found in the Andes.

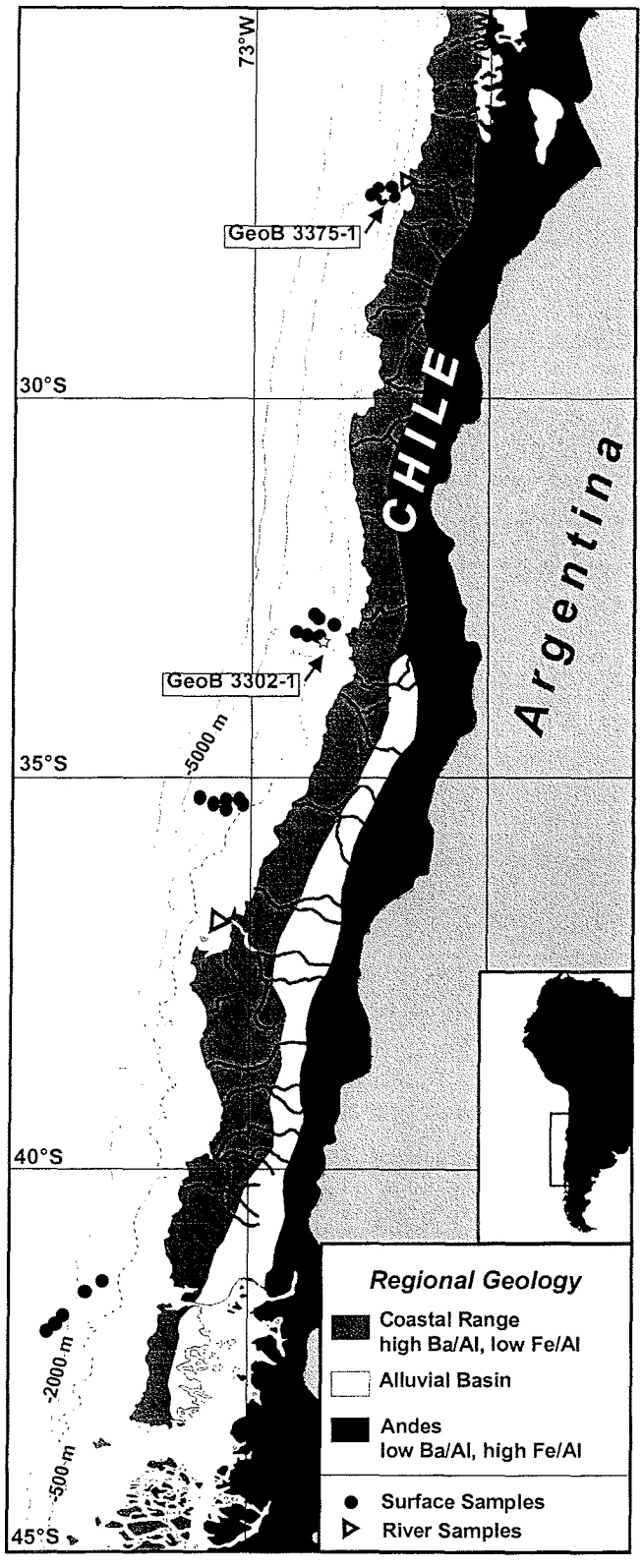

Figure 3.1: Location of sampling sites. Stream sediments are marked by open triangles, surface samples are noted as dots, and the sites of gravity cores GeoB 3375-1 and GeoB 3302-1 are marked with stars.

Marine sediments from the Chilean continental slope consist mainly of terrigenous material with $CaCO_3$ contents between 0 and 20 wt-% (Hebbeln *et al.*, in prep. 1998). The chemical composition of the terrigenous fraction depends on the geochemistry of the source rocks. The climatic gradient along the Chilean coast, from the hot, arid climate of northern Chile to the cold humid climate of southern Chile, has a pronounced effect on the precipitation patterns (Scholl *et al.*, 1970). Today in northern Chile the eroded material is transported mainly by aeolian transport and occasional flash-floods from the Coastal Range to the continental slope (Lamy *et al.*, 1998a). Due to insufficient precipitation in the Andes, the ephemeral rivers originating in the Andes deposit the eroded material in the central depression between the Andes and the Coastal Range. In central and southern Chile seasonal to year-round precipitation allows perennial rivers to flow, which transport large amounts of material from the Andes onto the continental slope with some admixture of material from the Coastal Range (Lamy *et al.*, 1999). As a result, the surface sediments on the continental slope in northern Chile are dominated by terrigenous material from the Coastal Range while the surface sediments on the continental slope off central and southern

Chile are dominated by terrigenous material from the Andes (Lamy *et al.*, 1998b).

Variations in the composition of the terrigenous fraction of the sediment through time are mostly due to changing environmental conditions on the continent. Given the strong modern gradient in humidity, climate change in this area probably would result in changing precipitation patterns (Heusser *et al.*, 1996; Lamy *et al.*, 1998a). Such changes can be traced in continental slope sediments by proxies e.g. for changing sediment source areas (Klump *et al.*, in prep. 1999b; Lamy *et al.*, 1999).

3.3. Materials and methods

The surface sediment samples for this study were retrieved by multi-corer (Dept. Of Geosciences, Bremen; GeoB) (Hebbeln *et al.*, 1995). The multi-cores and the gravity cores GeoB 3302-1 and GeoB 3375-1 were retrieved on cruise SO-102 with the German R/V SONNE (Hebbeln *et al.*, 1995). Stream sediments from the Rio Copiapo (27°S) and the Rio Bio-Bio (37°S) were collected by A. Marchant (Geological Survey of Chile) and V.H. Ruiz (University of Conceptión, Chile). The sampling sites and the location of the gravity cores GeoB 3375-1 and GeoB 3302-1 are marked on Fig.3.1.

For chemical analysis, the freeze-dried and homogenised samples were subjected to total acid digestion. The sample material (100 mg) was weighed directly into Teflon pressure vessels. The digestion was performed using HNO_3 , $HClO_4$, and HF in a PDS-6 pressure system at 180°C over eight hours. Subsequently, the acid was evaporated close to dryness, and the residue was dissolved in HNO_3 and again digested over eight hours in a PDS-6 pressure system. Finally, the solution was decanted into a pre-cleaned glass flask and filled to 100 ml with deionised water and then filled into pre-cleaned polyethylene bottles for cold storage. The concentrations of Ba, Al, and Fe were measured by inductively coupled plasma atomic emission spectrometry (ICP-AES). The error on repeat measurements is 4% for Ba, 2.5% for Al, and 2.1% for Fe. The accuracy was determined by repeated analysis (n = 22) of control standards (USGS Analyzed Marine Mud MAG-1).

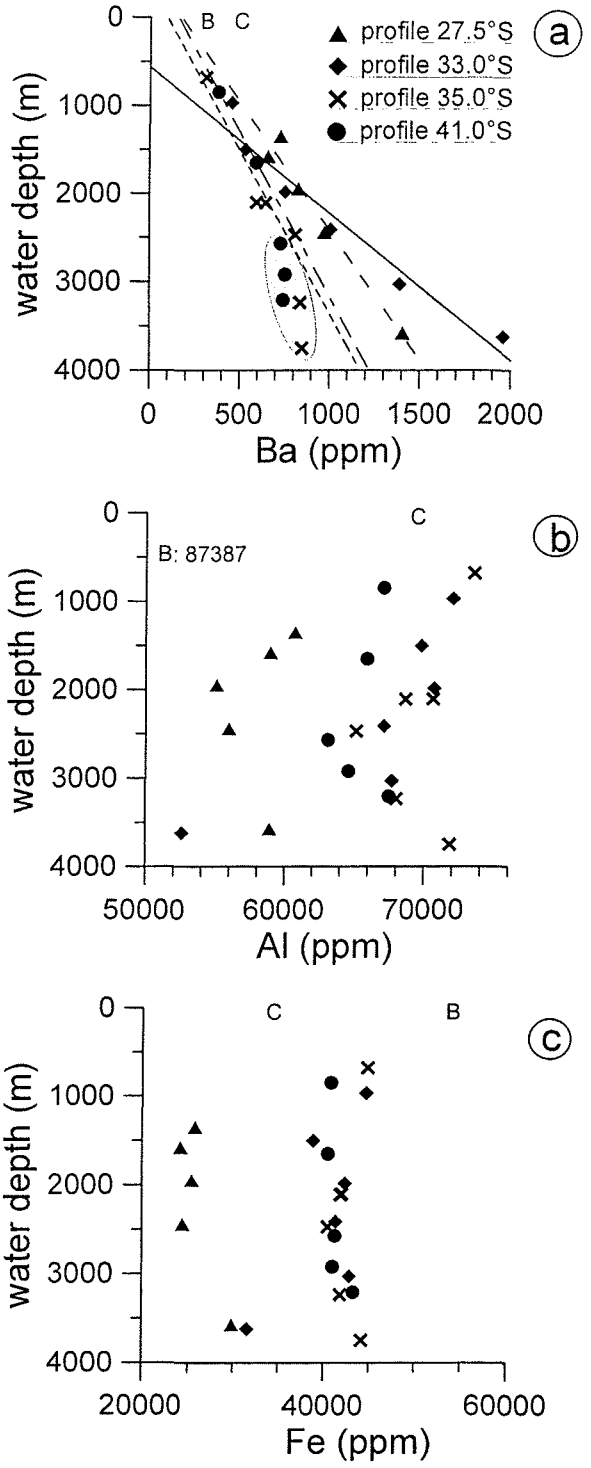

Figure 3.2: Concentration of barium (a), aluminium (b), and iron (c) in the surface sediments versus water depth. Note the linear increase of barium contents with increasing water depth. Those samples in the shaded field do not display this relationship and are excluded from the plotted linear regressions. The letters B and C mark the concentrations of these elements in the stream samples (B: Rio Bio-Bio, C: Rio Copiapo).

3.4. Results

The Ba contents in the surface sediment samples and stream sediments range from 137 to 1959 ppm (Fig. 3.2a), the Al contents range from 34000 to 95000 ppm (Fig. 3.2b), and the Fe contents range from 21000 to 45000 ppm (Fig. 3.2c). The Ba contents are characterised by a significant increase with water depth, which is not found in the Fe contents which are fairly constant along the various profiles (compare Figures 3.2a and 3.2c). However, on the two southernmost profiles the samples from deeper than 2500 m show no more increase in Ba (shaded area in Figure 3.2a). The Al contents show a broad scatter unrelated to water depth (Fig. 3.2b). The Ba/Al ratios in the surface samples range between 0.002 and 0.013 and increase with water depth (Fig. 3.3a). The stream sediment samples show lower Ba/Al ratios than the marine samples at the same latitude (Fig. 3.3a). Their Ba/Al ratios are 0.0073 for Rio Copiapó (27°S) and 0.0035 for Rio Bio-Bio (37°S).

The Fe/Al ratios in the surface samples and stream sediments show a bimodal latitudinal distribution (Fig. 3.4). The

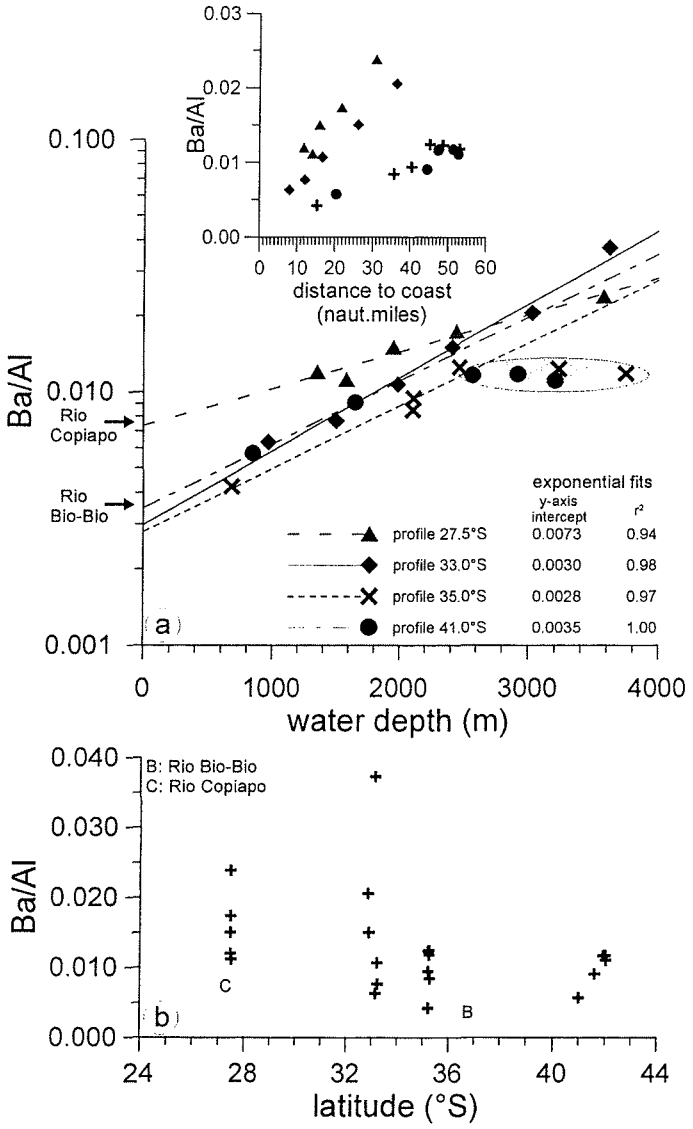

Figure 3.3: (a) Ba/Al ratio of surface sediment samples from the Chilean continental slope vs. water depth. The exponential regression lines intercept the y-axis close to the Ba/Al ratios of the stream sediment samples from the same latitude (see text). Again, the shaded field marks those samples, which do not show the depth dependence and which are excluded from the shown regression. The r^2 of 1 for the 41°S profile results from the fact that only two samples have been used. Also the Ba/Al ratios of the stream sediments are shown. (inset) Relationship between Ba/Al ratio in the surface sediments and distance to coast. Those samples showing no more relationship to water depth are furthest off the coast. (b) Ba/Al ratio in the surface sediments versus latitude along the Chilean continental slope. B and C mark the values for the Rio Bio-Bio and the Rio Copiapo, respectively.

average Fe/Al ratio off northern Chile (27.5°S) is 0.45, off Central Chile (33 - 35°S) it is 0.60, and off south central Chile (41°S) it is 0.63. The higher Fe/Al ratios in the south indicate a dominant contribution from basaltic-andesitic source rocks (Le Maitre, 1976) in the Andes, while the lower ratios in the north point to the acidic-plutonic rocks (Le Maitre, 1976) in the Coastal Range as the main source. Thus, this pattern reflects the varying proportions to which Andean and Coastal Range materials have been mixed into the continental slope sediments (Klump *et al.*, in prep. 1999b). The higher Fe/Al ratios in the south and lower Fe/Al ratio in the northern profile show that there is no lateral transport of material on this scale. The stream sediments fall close to the regional averages.

In gravity core GeoB 3375-1 the Al content of the sediment ranges from 55700 to 77000 ppm, the range of Ba is 490 to 1010 ppm, and the range of Fe is 21000 to 36100 ppm. The Fe/Al ratios range from 0.40 to 0.52 (Fig. 3.5a) and Ba/Al ratios range from 0.0074 to 0.0168 (Fig. 3.5b). The Fe/Al ratio, the Ba/Al ratio, and the

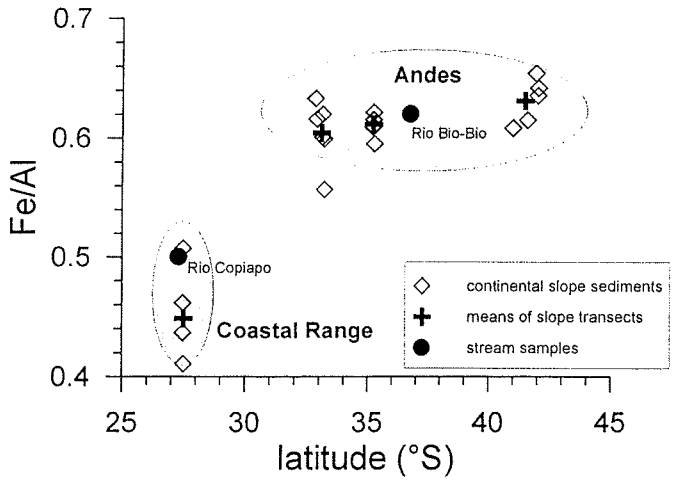

Figure 3.4: Fe/Al ratio of surface sediment samples from the Chilean continental slope (diamonds) versus latitude. The average Fe/Al ratios of the continental slope profiles are marked as crosses. The Fe/Al ratios are significantly higher south of 30°S, where rivers carry more material from the Andes (high Fe/Al) to the continental slope, than in northern Chile, where today sediments are derived mainly from the Coastal Range (low Fe/Al) as it is also seen in the stream sediment data (dots).

Ba content show precessional cyclicity. The age model for gravity core GeoB 3375-1 was described in a previous study (Lamy *et al.*, 1998a).

The Al content of core GeoB 3302-1 ranges from 68200 to 82300 ppm, Ba ranges from 409 to 766 ppm, and Fe ranges from 40500 to 47700 ppm. The Fe/Al ratios range from 0.52 to 0.62 (Fig. 3.5e) and the Ba/Al ratios range from 0.0053 to 0.0110 (Fig. 3.5f). Both the Fe/Al ratio and the Ba/Al ratio increase markedly in the period from 15,000 to 9,600 years B.P. The Age model for gravity core GeoB 3302-1 can be found in (Lamy *et al.*, 1999).

For the complete data set please refer to the 'Pangaea' database (http://www.pangaea.de/Projects/GeoB/JKlump).

3.5. Discussion

3.5.1. Formation of marine biogenic barite

The process of formation of marine barite, especially a possible biotic origin of marine barite crystals, is still unclear. Some authors interpret the Ba enrichment in decaying organic matter to be caused by biotic processes, i.e. organisms enriching Ba in their skeletons, like acantharians (Bernstein *et al.*, 1992; Bernstein *et al.*, 1998), xenophyphores (Gooday and Nott, 1982), and filamentous blue-green algae (Gayral and Fresnel, 1979). The incorporation of the remains of these biota into biogenic aggregates, such as faecal pellets,

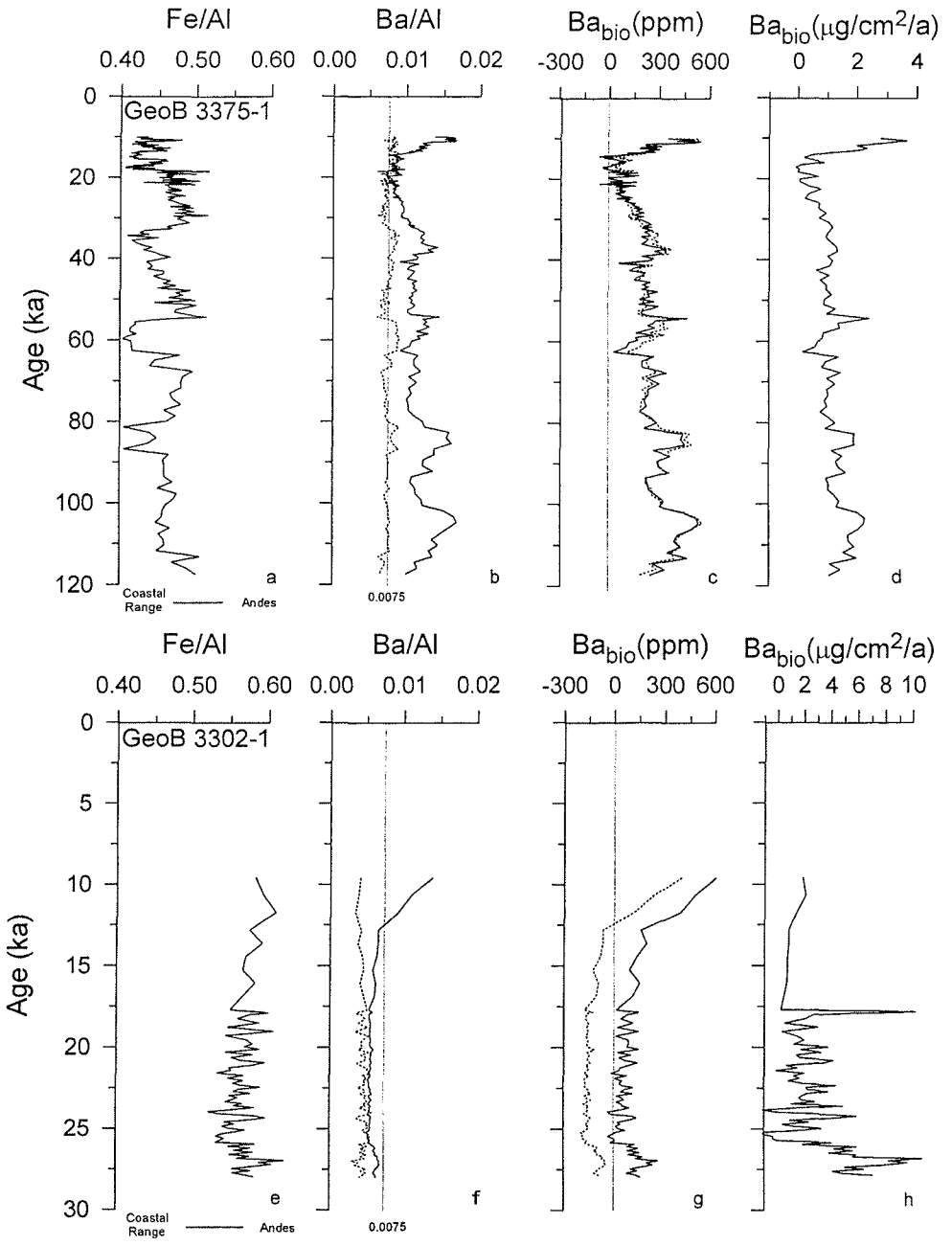

Figure 3.5: Fe/Al ratio (a, e), Ba/Al ratio (b, f), and biogenic barium data (c, d, g, h) of cores GeoB 3375-1 and GeoB 3302-1 from the Chilean continental slope vs. age. The Fe/Al ratio reflects the mixing of material from the coastal range (low Fe/Al, high Ba/Al) with material from the Andes (high Fe/Al, low Ba/Al). The Bulk Ba/Al ratio (solid line in b, f) is plotted together with the regional terrigenous Ba/Al ratio (stippled line in b, f) of the sediments deposited at the time, calculated from the Fe/Al ratios. The straight line reflects the "crustal average" of 0.0075 (b, f). The biogenic barium content (c, g) was corrected for changes in sediment provenance (see text) by using the regional terrigenous Ba/Al ratio (solid line b, f), and biogenic barium content calculated with the "crustal average" Ba/Al ratio of 0.0075 (stippled line b, f). The biogenic barium fluxes (d, h) have been corrected for a preservation effect after Dymond et al. (1992).

provides an environment for barium sulphate to precipitate and a transport mechanism to the sea-floor. This model is supported by the similarity of marine barite crystals in surface sediment samples and from oblique net hauls from surface waters (Bertram and Cowen, 1997). Other authors interpret the formation of biogenic barite as an abiotic process. In their model, barium sulphate precipitates from the sulphate of decaying proteins in organic aggregates, such as faecal pellets, and dissolved barium in the ocean (Dehairs *et al.*, 1980; Gingele and Dahmke, 1994; Stroobants *et al.*, 1991), which is supported by a clear correlation between C_{org}/Ba ratios and the concentration of dissolved Ba in sea-water (Dymond *et al.*, 1992). Studies on the morphology and internal structure of marine barite (Gingele and Dahmke, 1994; Stroobants *et al.*, 1991) support a model in which barium sulphate forms amorphous precipitates in decaying organic aggregates and crystallises on the way through the water column to the sea-floor. A systematic increase of biogenic barium in sinking particulate matter (Dymond *et al.*, 1992) and in sediments (von Breymann *et al.*, 1992) with water depth points to such an abiotic process in the formation of marine barite. However, without organic matter marine barite will not be formed. To clearly indicate the relation between marine barite and biological production the term 'biogenic barium' is commonly used to describe this portion of the total barium content and to distinguish it from terrigenous barium.

The barium contents of the surface sediments from the Chilean continental slope, which show a distinct linear increase with water depth (Fig. 3.2a) support an abiotic model of marine barite formation. Together with scattering aluminium contents (Fig. 3.2b) these data result in increasing Ba/Al ratios towards greater water depths (Fig. 3.3a). There, the Ba/Al ratios reach values which are considerably higher than the terrigenous background values obtained from the stream sediments. Thus, the increasing barium contents are most likely due to increasing portions of biogenic barium.

3.5.2. Differentiation of the barium signal: biogenic vs. terrigenous

Unfortunately, in most cases, there is too much dilution of the marine component in continental slope sediments by terrigenous components to allow a direct and quantitative determination of biogenic barite in the sediment by X-ray diffraction (Dehairs *et al.*, 1980). An alternative approach to differentiate between biogenic and terrigenous barium could be a

normative analysis of bulk sediment compositions (Dehairs *et al.*, 1980; Dymond, 1981; Dymond *et al.*, 1984; Leinen and Pisias, 1984) to allow an estimate of the aluminosilicate contribution. The normative contribution of Ba by aluminosilicates towards the total Ba content of the sediment can be calculated from the terrigenous Ba/Al ratio and the total Al in the sample using equation 3.1.

$$Ba_{terr} = Al \cdot \left(\frac{Ba}{Al}\right)_{terr} \qquad (3.1)$$

The biogenic barium content can be calculated by subtracting the calculated terrigenous Ba from the total Ba in the sediment (equation 3.2).

$$Ba_{bio} = Ba_{tot} - Ba_{terr} \qquad (3.2)$$

where Ba_{terr} is the terrigenous, or background, barium, Al is the total aluminium in the sediment, Ba/Al_{terr} is the terrigenous Ba/Al ratio, Ba_{bio} is the biogenic barium, and Ba_{tot} is the total barium in the sediment. While the total Ba and the total Al contents in the sediment can be measured, an accurate estimate of Ba/Al_{terr} is needed.

In sediments with a terrigenous fraction of more than 50%, as is the case here and along most of the continental margins, errors in the terrigenous Ba/Al ratios introduce large errors in the estimates of biogenic barium in the sediment (Dymond *et al.*, 1992). Since material to determine the Ba/Al ratio of the sediment source is hard to come by, some authors suggest to use an 'average' crustal Ba/Al ratio of 0.0075 (Dymond *et al.*, 1992; Gingele and Dahmke, 1994; Schmitz *et al.*, 1997; Thunell *et al.*, 1994). Only few studies reports a regional estimate from marine sediments (Dean *et al.*, 1997; Nürnberg *et al.*, 1997). However, the stream data shown in Fig. 3.3a indicate that the terrigenous Ba/Al ratio can display significant regional variations. Thus, using a 'crustal average' would introduce large errors in the determination of this ratio in areas where the regional Ba/Al ratio differs significantly from the 'average' crustal ratio. Besides regional differences, temporal variations in terms of shifting sediment provenance might also affect the terrigenous Ba/Al ratio in marine sediments.

A direct way to estimate the Ba/Al_{terr} ratio is to analyse purely terrigenous material unaffected by any marine biogenic contribution, as e.g. stream samples. The stream data analysed here give Ba/Al ratios of 0.0073 for the north (27°S) and 0.0035 (37°S) for the southern part of the study area (Fig. 3.3). This shift is accompanied by a comparable shift of the Fe/Al ratios (0.5 in Rio Copiapo, 27°S, to 0.63 in Rio Bio-Bio, 37°S; Fig. 3.4). Lower Ba/Al ratios and higher Fe/Al ratios in the south are interpreted to indicate a dominant contribution from basaltic-andesitic source rocks in the Andes, while the inverse ratios in the north point to the acidic-plutonic rocks in the Coastal Range as the main source. Thus, based on the stream data, for the area north of 30°S a Ba/Al_{terr} ratio of ~0.0073 and for the area south of 30°S of ~0.0035 can be assumed.

An alternative approach to assess the Ba/Al_{terr} ratio, that can be used when no purely terrigenous material is available, is based on the analyses of marine surface sediments. Plotting the Ba/Al ratio of the surface samples versus water depth shows that the ratio increases exponentially with water depth (Fig. 3.3a). As pointed out above, this increase is assumed to reflect the water depth-related increase in the biogenic barium content of the sediments. In this case the y-axis intercept of the least squares fit of the profiles in Fig. 3.3a should indicate a Ba/Al ratio not affected by any biogenic contribution, i.e. the terrigenous signal. Problematic are the deepest samples from the 35°S and the 42°S profiles, which show no further Ba-increase (and subsequently no further increase in Ba/Al ratio, Fig. 3.3a) below 2500 m water depth (Fig. 3.2a). Due to the wide shelf in the southern part of the study area these samples are so distant from the near coastal upwelling centres (Fig. 3.3) that they are affected by the seaward decreasing production and consequently by a stagnating Ba flux at the respective depths. Thus, from the two southern profiles only the samples from <2500 m have been used to for the regression to estimate the Ba/Al_{terr} ratio. Due to high correlation coefficients (r^2: >0.94) all the y-intercepts give quite robust estimates of the actual Ba/Al_{terr} ratio (Fig. 3.3a). With y-intercepts of 0.0073 north of 30°S and of 0.0028 to 0.0035 south of 30°S there is an almost perfect fit to the results from the stream sediments from Rio Copiapo and Rio Bio-Bio. This points to a dominant terrigenous input from the Coastal Range at 27.5°S and from the Andes south of 30°S, respectively.

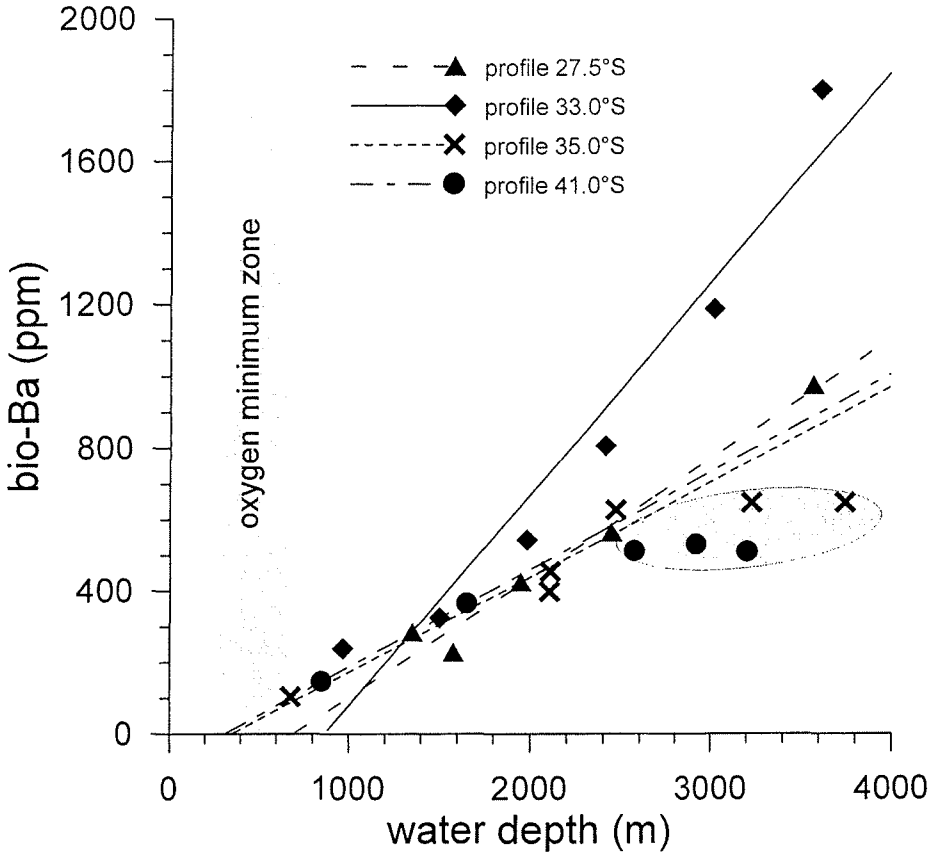

Figure 3.6: Biogenic barium content of the surface samples from the Chilean continental slope versus water depth. The linear increase of biogenic barium with water depth indicates an abiotic process in the formation of marine barite (see text) starting below the oxygen minimum zone. The samples from >2500 m water depth from the two southern profiles (shaded field) have been excluded from the regression.

3.5.3. Biogenic barium contents in the surface sediments

Once the regional terrigenous Ba/Al ratio has been determined it can be used to calculate the amount of biogenic barium in the sediment, as outlined above. Here the Ba/Al_{terr} ratios derived from the surface sediments (Fig. 3.3a) have been used to consider the local composition of the sediments. Plotting biogenic barium versus water depth (Fig. 3.6) shows that the amount of biogenic barium increases linearly with depth (with the exception of the samples from >2500 m in the south). The linear regression lines of the respective profiles mostly have x-axis intercept values of 750 m water depth and less. This corresponds to the base of the oxygen minimum zone off Chile (Shaffer *et al.*, 1995; Silva, 1996) and agrees with observations from the Namibian continental margin (von Breymann *et al.*, 1992), where

biogenic barite seems to form only at depths greater than 1000 m. The onset of a steady increase of biogenic barium below the oxygen minimum zone indicates partial dissolution of biogenic barite within this zone. For marine barite it is required that the sediments remain in an oxic, or at least sub-oxic, environment, otherwise barite will not remain as a stable phase and the resulting chemical data cannot be interpreted in the sense of using biogenic barium as a proxy of paleoproductivity (Dymond *et al.*, 1992).

A comparison of Ba_{bio} contents calculated with (1) the 'crustal average' (Ba/Al = 0.0075) and (2) the regional Ba/Al_{terr} ratios points out the importance to consider such regional values (Fig. 3.7). While deviations between the two calculations are very small in the north of the study area, where the regional Ba/Al_{terr} ratio is very close to the 'crustal average', the difference between the two calculations can reach values of up to 330ppm at 35°S, where the regional Ba/Al_{terr} ratios are lowest. These deviations can result in an underestimation of the Ba_{bio} content by up to of 50% (41°S), depending on the total amount of Ba in the sediment. Using the 'crustal average' may even sometimes result in negative Ba_{bio} contents, which clearly shows that applying a crustal average ratio is not appropriate in these regions.

To assess the regional pattern of productivity from the Ba_{bio} contents these data have to be converted to Ba_{bio} accumulation rates. Accumulation rates along the Chilean continental slope display a wide range with low values in the north (core GeoB 3375-1 from 27.5°S: 4g cm^{-2} kyr^{-1} based on Marine Isotope Stage 5 sediments; (Lamy *et al.*, 1998a)) to intermediate values in the central part of the study area (core 17748-2 from 33°S: 10g cm^{-2} kyr^{-1}; Lamy *et al.*, 1999) and finally to very high rates in the south (core GeoB 3313-1 from 41°S: 80g cm^{-2} kyr^{-1}; Hebbeln, unpubl. data). Based on the strong latitudinal climatic zonation of Chile, with results in a steep precipitation gradient from south to north, this pattern of increasing southward accumulation rates along the Chilean continental slope is persistent throughout the Late Cenozoic (Scholl *et al.*, 1970).

The sampling stations are closely spaced within a slope transect. The down slope changes in sedimentation rate within a transect are expected to be negligible in comparison to the strong differences between transects at different latitudes along the Chilean continental margin. Therefore, the accumulation rate determined for one position of each transect has been used

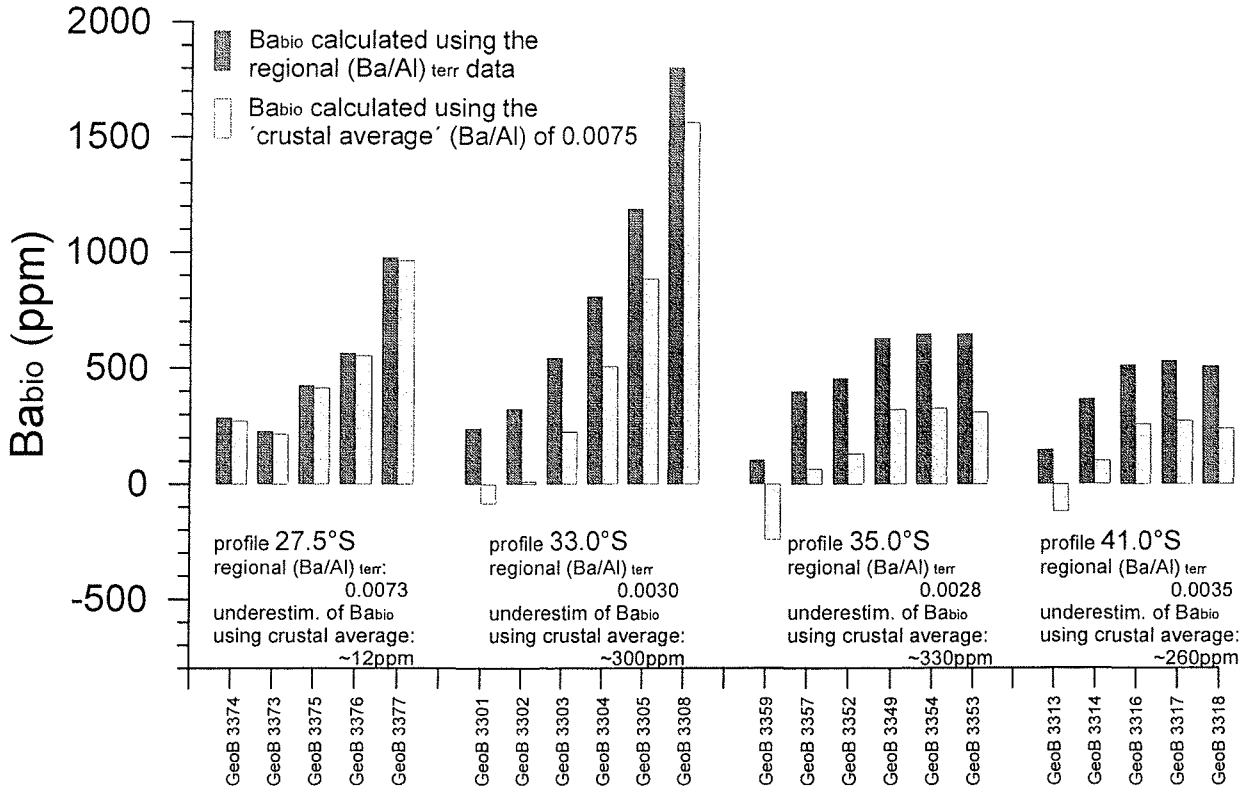

Figure 3.7: Comparison of biogenic barium contents in surface sediments from the Chilean continental slope using regional Ba/Al ratios and the 'crustal average' ratio from the literature (Dymond et al., 1992). The biogenic barium contents are calculated on the basis of the 'crustal average' Ba/Al ratio are consistently lower, especially in the south, and sometimes negative due to the low regional terrigenous Ba/Al ratios.

for all samples from the respective continental slope profile to estimate biogenic barium accumulation rates from the biogenic barium contents of the surface sediments. Although this is a very crude approach it provides a robust pattern of the latitudinal distribution of biogenic barium accumulation rates (Fig. 3.8a). Still, the accumulation of biogenic barium increases with water depth in accordance with the model of biogenic barite formation described above. The non-parallel regression lines indicate a non-linear relationship between organic carbon flux and biogenic barite formation. However, the by far highest Ba_{bio} accumulation, and thus highest productivity, is indicated for the southernmost profile, while considerably lower accumulation rates point to lower productivity at 33°S, which decreases even more further to the north (Fig. 3.8a). Comparing the data from ~1600 m water depth the Ba_{bio} accumulation rates increase from ~1 μg cm^{-2} kyr^{-1} at 27.5°S to ~3 mg cm^{-2} kyr^{-1} at 33°S and finally to ~20μg cm^{-2} kyr^{-1} at 41°S. This pattern of biogenic barium accumulation is comparable to the annual average of pigment concentrations in surface waters derived from measurements by the

Coastal Zone Color Scanner (Thomas *et al.*, 1994). The good agreement between biogenic barium accumulation and chlorophyll concentrations in the surface waters indicate that Ba_{bio} accumulation rates are linked to (paleo)productivity. This has been confirmed in studies on the California Current (McManus *et al.*, 1999).

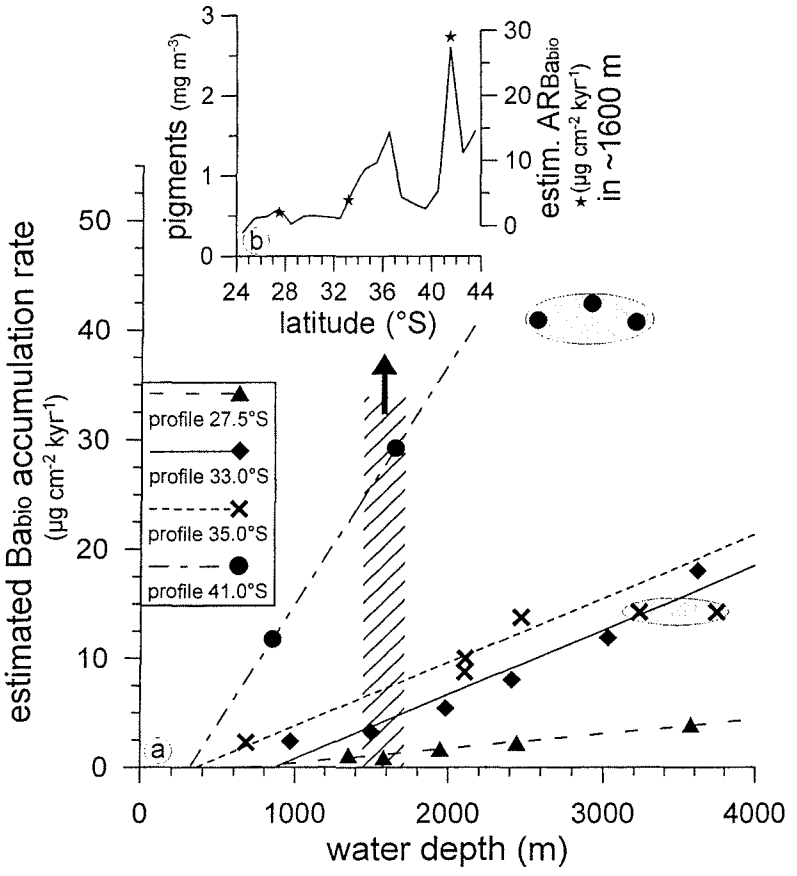

Figure 3.8: (a) Estimated accumulation rate of biogenic barium versus water depth along the Chilean continental slope. The shading marks the samples excluded from the regressions (see text). (b) Comparison of the accumulation rate of biogenic barium (stars) from approximately 1600 m water depth (hatched area in a) versus latitude shows a good agreement with the surface water pigment concentration (solid line) derived from Coastal Zone Color Scanner (CZCS) data. (http://daac.gsfc.nasa.gov)

3.5.4. Modelling the Ba/Al $_{terr}$ ratio through time

Sediment provenance, and with it the Ba/Al_{terr} ratio, changes not only regionally, it may also show changes in time, as is the case along the Chilean margin. Latitudinal shifts of precipitation patterns in western South America through the Late Quaternary (Heusser *et al.*, 1996; Lamy *et al.*, 1998a) resulted in changing relative contributions of the two main terrigenous sediment sources, the Andes and the Coastal Range, to the material on the continental slope (Klump *et al.*, in prep. 1999b; Lamy *et al.*, 1999). Thus, for the use of barium as a paleoproductivity proxy such changes in the Ba/Al_{terr} ratio through time have to be considered.

How can such changes in sediment provenance be assessed? Our approach is based on the assumption that material from the basaltic-andesitic source rocks in the Andes is characterised by high Fe/Al and low Ba/Al ratios, while material from the acidic-plutonic source rocks in the Coastal Range has low Fe/Al and high Ba/Al ratios (Le Maitre, 1976). These ratios do not change with climatic variations in a semi-arid environment (Ben Othman *et al.*, 1997). Because of the large terrigenous component in the continental slope samples any biogenic contribution of Al or Fe to the sediment is considered to be negligible. Both Al and Fe are present in the sediment in amounts which are several orders of magnitude higher than they are present in organic matter, which by itself constitutes only a minor proportion of the sediment (Orians and Bruland, 1986). Thus, we interpret changes in the Fe/Al ratio of the marine sediments to reflect changes in the relative contributions of the two main sediment source areas. Based on a two end-member model with the Andes (high Fe/Al and low Ba/Al ratios) at one end and the Coastal Range (low Fe/Al and high Ba/Al ratios) at the other end, the Fe/Al ratio of the marine sediments can indicate the relative proportions to which material from the two source areas has been mixed (Klump *et al.*, in prep. 1999b). This model is the basis from which an estimate for the Ba/Al_{terr} ratio of the sediments can be calculated. The required relationship between Fe/Al ratio and Ba/Al ratio can be determined from two independent data sets.

For a Ba/Al vs. Fe/Al plot of the marine surface sediments (Fig. 3.9) the regional Fe/Al ratios are averaged from all the data from the various profiles (Fig. 3.4), while the regional Ba/Al_{terr} ratios are deduced from the y-axis intercepts in Fig. 3.3a. Interestingly, the resulting relation is very similar to that resulting from the independent data of the two stream samples (Fig. 3.9). The similarity of the two regressions (Fig. 3.9) indicates the robustness of our two end-member model. To put this relation on a broader statistical base we combined both data sets to derive equation 3.3 to calculate the Ba/Al_{terr} ratio:

$$\left(\frac{Ba}{Al}\right)_{terr} = -0.0266 \cdot \left(\frac{Fe}{Al}\right)_{terr} + 0.0197 \qquad (3.3)$$

where Ba/Al_{terr} is the calculated paleo-Ba/Al ratio of the terrigenous fraction and $(Fe/Al)_{terr}$ is the measured Fe/Al ratio of the sediment (Fig. 3.9). Any positive deviation of

the measured Ba/Al ratio from the respective continental background value (Ba/Al_{terr}) is considered to be of biogenic origin, allowing to calculate the Ba_{bio} content of the sample.

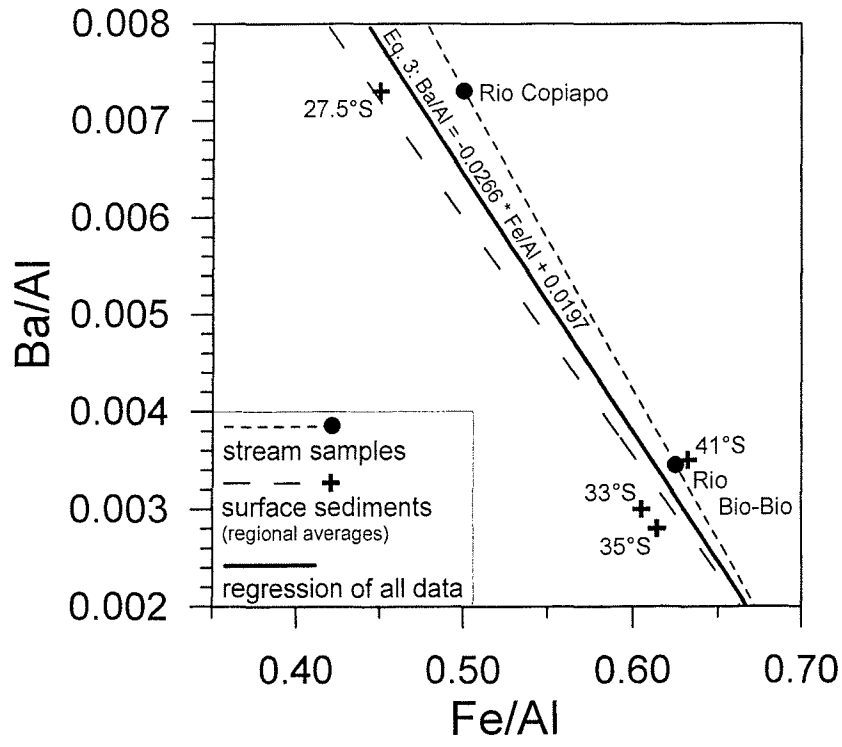

Figure 3.9: Relationship between the Ba/Al and the Fe/Al ratios in the terrigenous sediments along the Chilean continental slope. The regional Ba/Al ratios for the surface sediments are taken from Fig. 3.3a, while the respective data for the Fe/Al ratio are derived from Fig. 3.4. The data from the surface sediments agree well with the stream samples. Based on the two end-member model both data sets are combined to derive equation 3.3 (see text) to estimate the terrigenous Ba/Al ratios in the sediments from the Fe/Al ratio.

3.5.5. Sediment provenance and Ba $_{bio}$ contents through time

The two cores GeoB 3375 and GeoB 3302 have been selected to demonstrate the effect of varying regional background *Ba/Al $_{terr}$* ratios. Based on equation 3.3 the Fe/Al ratio can be used to calculate the Ba/Al_{terr} ratio of the sediments. Core GeoB 3375 from the 27°S profile has a regional present-day background of 0.0073, which is very close to the 'crustal average' of 0.0075 (Fig. 3.5b). In contrast, core GeoB 3302 has a considerable lower regional *Ba/Al $_{terr}$* ratio of 0.0030 (Fig. 3.5f). Thus, compared with data derived using the 'crustal

average' both data sets derived from GeoB 3375 should be very similar, while the data sets derived from GeoB 3302 are expected to have a considerable offset.

For the analysis of sediment cores it has to be kept in mind that marine barite is unstable in the sulphate reduction zone. Then Ba becomes dissolved in the pore water and some of it diffuses upwards. Once it reaches the upper limit of the sulphate reduction zone, where sulphate becomes available again, it re-precipitates as diagenetic barite. The resulting diagenetic barium peaks cannot be interpreted as signs of increased productivity. Porewater analyses are not available for the cores discussed here, but the extremely close co-variation of Fe and Mn (Klump, unpubl. data) and low total organic carbon contents ($\leq$ 1.4 wt.%) point to stable oxic porewater conditions. This co-variation also rules out the presence of Fe-Mn crusts, which would scavenge barium (Dymond *et al.*, 1984).

The Fe/Al ratio in the two investigated sediment cores reflects the varying contributions of the two main source areas, the Andes and the Coastal Range, to the respective sites through time. In core GeoB 3375, which reaches back to 120,000 years B.P., the Fe/Al ratio shows a clear precessional cyclicity (Fig. 3.5a) with an increased relative contribution from the Andes during the more humid precession maxima (Lamy *et al.*, 1998a). Core GeoB 3302 only covers the period from 8,000 to 28,000 years B.P. Besides having much higher Fe/Al ratios reflecting a dominance of Andean material it also shows a slightly increasing Andean contribution in the sediments younger than 18,000 years B.P. (Fig. 3.5e). Contrasting evolutionary patterns in the two cores, especially during the Last Glacial Maximum, are due to different effects of shifting climate zones on the distribution of precipitation at 27.5°S and at 33°S (Lamy *et al.*, 1999).

With the reconstructed Ba/Al_{terr} ratio the amount of Ba_{Bio} in the sediments can be calculated. In both cores the Ba_{Bio} content varies between 0 and 600 ppm with a comparable range (0 - 200) for the time of the stratigraphic overlap of the two cores (Fig. 3.5c and 3.5g). In core GeoB 3375 it also shows a precessional cyclicity (Fig. 3.5c), while the most prominent feature in Core GeoB 3302 is a considerable increase after 15,000 years B.P. (Fig. 3.5g). Comparing the resulting Ba_{Bio} contents with data based on the 'crustal average' Ba/Al ratio (dashed lines in Figs. 3.5c and 3.5g) shows only a small difference for core GeoB 3375. In contrast, for core GeoB 3302 the offset between the two calculations is remarkable. While the Ba_{Bio} contents determined by the approach presented here are low but (almost) consistently above zero. The

Ba_{Bio} contents calculated by using the 'crustal average' Ba/Al ratio display (almost) continuously negative values. This means that the measured Ba values cannot even account for the terrigenous Ba input relative to the measured Al contents, not to mention any biogenic contribution of Ba at all. This comparison makes clear to what extent Ba_{Bio} estimates based on a fixed 'crustal average' Ba/Al ratio may be biased, when regional Ba/Al_{terr} ratios are considerably different from this average value. Considering the importance of such regional variations of elemental ratios highlights advantages of a dynamic model of the terrigenous sediment input which allows to calculate changes of the Ba/Al_{terr} ratio through times.

3.6. Late Quaternary Paleoproductivity Estimated from Biogenic Barium

A qualitative description of the paleoproductivity off northern and central Chile can be made after following the procedures outlined above by calculating the accumulation rates of biogenic barium. The Ba_{Bio} accumulation rate in core GeoB 3375-1 shows that the paleoproductivity off northern Chile during the last glacial period followed a precessional cycle with maximum flux rates during precession minima (Fig. 3.5d). The lowest flux rates are found during the Last Glacial Maximum, indicating a period of reduced paleoproductivity. The biogenic barium flux increases sharply during the early Holocene. Core GeoB 3302-1 shows only a small segment of the record covered by GeoB 3375-1 (Fig. 3.5h). The much higher temporal resolution shows the high variability of the paleoproductivity. The average biogenic barium flux during the period 29,000 to 15,000 years B.P. is comparable to GeoB 3375-1. In contrast to GeoB 3375-1, the Ba_{Bio} flux rate in GeoB 3302-1 does not increase after the Last Glacial Maximum. This points to differences in the development of the paleoproductivity off northern and off central Chile. We interpret these observations to reflect differing responses of individual upwelling cells to changing environmental conditions. To assess the large-scale paleoproductivity of the southern Peru-Chile Current requires higher spatial resolution to cover most of the upwelling cells along the Chilean coast. Nevertheless, a qualitative statement can be made about the paleoproductivity during the last Glacial Maximum. Similar low biogenic barium flux rates in both cores may indicate generally lower productivity during this period. This means, that the Chilean upwelling system probably was a less active during that time.

To quantify this statement biogenic barium flux rates have to be converted to export productivity. Algorithms to do so have been developed by Dymond *et al.* (1992) and by François *et al.* (1995). However, both papers point to the importance of the concentration of dissolved barium in sea-water, which is not very well known for the past, and how it affects the formation of biogenic barite in the water column and at the sea-floor. Therefore it would be beyond the scope of this paper to convert the biogenic barium flux into a quantitative estimate of paleo-export productivity.

3.7. Conclusions

Normative calculations of the biogenic barium content to calculate paleoproductivity are mostly based on the assumption of an 'average' crustal Ba/Al ratio. Here we assessed regional variations of the terrigenous Ba/Al ratio by analysing (1) stream sediments and (2) continental slope sediments. Due to the water-depth dependent formation of biogenic barite the terrigenous Ba/Al ratio can be extrapolated from continental slope sediments by exponential regression of the increasing Ba/Al ratio with water depth. The results show that regional terrigenous Ba/Al ratios range between 0.0028 and 0.0073, depending on the sediment provenance. Compared to the 'crustal average' of 0.0075, ratios as low as 0.0028 will significantly affect the normative calculations of the biogenic barium content. For the Chilean continental slope it could be shown that barium accumulation rates increase from north to south similar to the pigment concentration in surface waters, as measured by the Coastal Zone Color Scanner (CZCS). This shows that biogenic barium is a suitable indicator of productivity.

Late Quaternary climate change caused changes of the continental precipitation patterns, which in turn resulted in changes of sediment provenance. In the case of sediments on the Chilean continental margin the correlation between the terrigenous Ba/Al and Fe/Al ratios can be used to devise a two-end-member geochemical mixing model to calculate the terrigenous Ba/Al ratio from the measured Fe/Al ratio. This approach replaces not only the often used 'average' crustal Ba/Al ratio by a regional Ba/Al ratio, it also allows to correct for changes of the regional Ba/Al ratio with time.

The resulting biogenic barium accumulation can be used as a proxy of paleoproductivity. Off northern Chile the paleoproductivity follows a precessional cycle with maximum biogenic barium content during precession minima. The lowest values of biogenic barium, which indicate a minimum in productivity, are found in sediments from the Last Glacial Maximum. The sedimentary record off central Chile follows the same pattern, except for the early Holocene. However, since both sampling positions are affected by local upwelling cells they might record local changes, rather than changes in the productivity of the entire Chilean upwelling system. More paleoproductivity records from the Chilean margin are needed to be able to reconstruct the large-scale paleoproductivity in the southern Peru-Chile Current.

Acknowledgements — The authors would like to thank L. Vidal, S Kasten and H. Kuhnert for their constructive discussion and comments on the manuscript. We are grateful towards A. Marchant at the Chilean Geological Survey and V.H. Ruiz at the University of Conceptión for collecting the stream sediment samples. We thank S. Kasten and S. Hinrichs at the Universität Bremen, and B. Diekmann at the Alfred Wegener Institut für Polar- und Meeresforschung in Bremerhaven for providing analytical assistance. Financial support was provided by the German Bundesministerium für Bildung und Forschung through funding the project *CHIPAL* (03G0102A).

The complete data set can be found in the 'Pangaea' database (http://www.pangaea.de/Projects/GeoB/JKlump).

Correspondence should be addressed to J.K. (jklump@uni-bremen.de)

Chapter 4 - Late Quaternary paleoproductivity variations in the Peru-Chile Current off northern and central Chile

by J. Klump, D. Hebbeln, and G. Wefer

Fachbereich Geowissenschaften, Universität Bremen.

Abstract

The upwelling system along the Chilean margin is among the most productive in the modern ocean. Thus, it plays an important part in the global carbon cycle through forcing the biological and physical transfer of CO_2 between the ocean and the atmosphere. Despite its importance in the global carbon cycle, variations in Late Quaternary paleoproductivity off Chile are only poorly understood. The paleoproductivity along the Chilean margin was reconstructed using organic carbon and biogenic carbonate in two marine sediment cores, which together cover the last 117,000 years. The paleoproductivity in this region generally follows a precessional cycle and was highest during the precession minima of the last glacial and during the early to Middle Holocene. The lowest productivity was found during the Last Glacial Maximum and the Late Holocene. By using two independent paleoproductivity proxies the productivity of calcareous planktonic organisms can be differentiated from the total productivity. The relative contribution of calcareous organisms to the total paleoproductivity was highest during periods of reduced productivity. The characteristic pattern of floral succession from the diatom-dominated upwelling cells to the coccolithophorid-dominated filament zone can be applied to the geological record of the sediment cores to reconstruct changes in the spatial extent of the local upwelling cells.

4.1. Introduction

Upwelling induced injection of nutrient-rich subsurface waters into the photic zone stimulates the high biological productivity typically found in upwelling areas, placing them among the most productive regions in the world ocean. These regions play important roles in the global carbon cycle due to an intense ocean-atmosphere exchange of carbon dioxide (CO_2), driven by the upwelling of CO_2-rich subsurface waters (physical pump) and by the photosynthetic fixation of CO_2 in organic matter and subsequent export to the deep ocean and partly into the sediment (biological pump) (Berger *et al.*, 1989). The coastal upwelling area along the western margin of South American is one of the most productive among the upwelling systems in the world ocean (Berger *et al.*, 1989). However, the evolution of productivity and, thus, the functioning of the global carbon cycle during the climatic cycles of the Late Quaternary, especially in the south along the Chilean coast, is only poorly understood. The aim of this paper is to reconstruct the Late Quaternary paleoproductivity variations in this region.

Since biological productivity in the oceans is a key mechanism within the global carbon cycle, various paleoproductivity indicators have been devised in order to assess changes of the ocean productivity in the geological past (see e.g. Berger *et al.*, 1989; Elderfield, 1990). Among these the most commonly used is the accumulation of organic carbon recorded in sea-floor deposits. Although only a very small fraction of the organic carbon produced in the surface waters is finally preserved in the sediments, various algorithms have been developed to link organic carbon accumulation at the sea floor to surface ocean productivity (see e.g. Müller and Suess, 1979; Sarnthein *et al.*, 1992). In a further step (Lyle, 1988) showed that the accumulation rates of organic carbon and those of carbonate are very highly correlated. They also concluded that carbonate accumulation rates can be used to predict organic carbon accumulation rates, and that both are governed by (paleo)productivity. Still, carbonate accumulation in marine sediments is not commonly used as a quantitative proxy of paleoproductivity. (Brummer and van Eijden, 1992) were the first to suggest an algorithm to reconstruct the paleo-flux of organic carbon from the euphotic zone by using empirical formulae that link carbonate flux and organic carbon flux in the water column. This method was improved by van Kreveld *et al.* (1996) and then further refined by Rühlemann *et al.* (1996) for pelagic, oligotrophic environments.

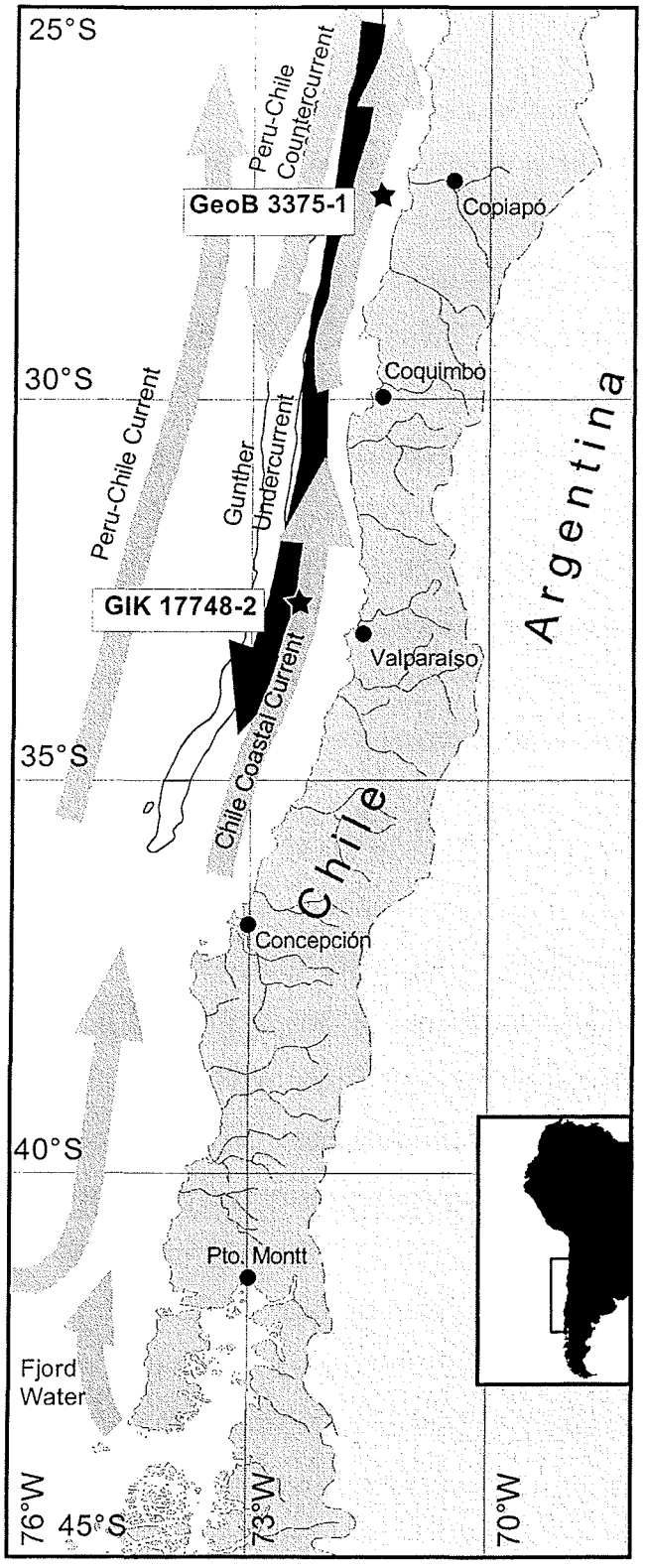

Figure 4.1 Regional hydrography along the Chilean margin and locations of gravity cores GIK 17748-2 and GeoB 3375-1.

Comparing the records produced by these two proxies it has to be noted that both proxies record different things: organic carbon accumulation reflects the total productivity of the water column above the core location, while biogenic carbonate accumulation reflects only the production of calcareous organisms. The use of these two independent proxies of paleoproductivity allows us to infer past changes of upwelling induced productivity in the Peru-Chile Current and of the ecology at the core sites. The study of two gravity cores (GeoB 3375-1, 27.5°S; GIK 17748-2, 33°S, see Fig. 4.1) from the Chilean continental slope showed that changes in paleoproductivity at the core positions followed a precessional cycle. Paleoproductivity was highest during the last glacial, but dropped down to lowest values in the Last Glacial Maximum and recovered to higher than present values during the Middle Holocene. These variations in paleoproductivity resulted from latitudinal shifts of the Southern Westerlies, which caused changes in the activity and extent of the local upwelling cells along the Chilean margin.

4.2. Study Area and Oceanographic Setting

The oceanographic setting off northern Chile has been summarised by Strub *et al.* (1998) (Figures 4.1 and 4.2). The water column above the core positions can be subdivided into four levels (Shaffer *et al.*, 1995; Strub *et al.*, 1998). The surface layer (0-50 m) is formed by the equatorward flowing Chile Coastal Current (CCC). Its water is a mixture of Subantarctic Water (SAAW), Equatorial Sub-Surface Water (ESSW) upwelled from the Gunther Undercurrent (GUC), and a fresh water component from the Chilean fjord region south of 42°S (Fjord Water). Approximately 40 km offshore the Peru-Chile Counter Current (PCCC), formed from Subtropical Surface Water (STSW), flows poleward. It limits the lateral extent of the CCC. The equatorward flowing Peru-Chile Current (PCC) or Humboldt Current is found 150 km offshore and has no effect on the coastal upwelling. Below the thermocline the GUC, the main source of the upwelled water, flows poleward. It is formed from ESSW. Between 400 m and 1500 m Antarctic Intermediate Water (AAIW) flows slowly towards the equator (Shaffer *et al.*, 1995). The southward flow below 1500 m may be associated with Pacific Deep Water (PDW) (Pickard and Emery, 1990).

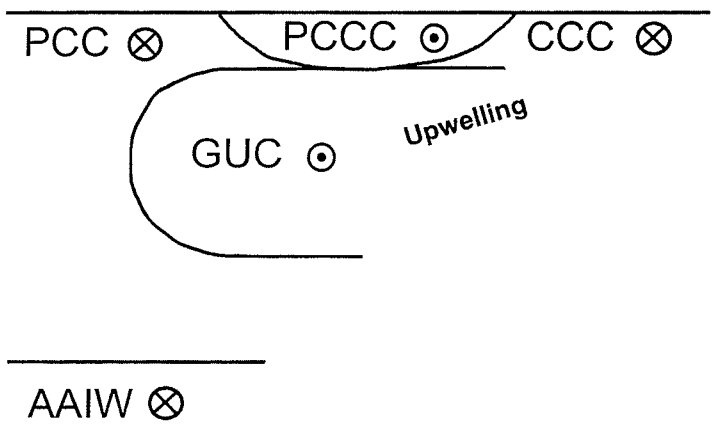

Figure 4.2 Section view of the Chilean upwelling system at 28°S. Water masses are the Peru-Chile Current (PCC), the Peru-Chile Countercurrent (PCCC), the Chile Coastal Current (CCC), the Gunther Undercurrent (GUC), and Antarctic Intermediate Water (AAIW). Equatorward flow is shown by arrow-tails, poleward flow by arrow-points.

Remote sensing studies of the Chilean coast identified localised upwelling centres, including several capes and adjacent northward-facing bays, as off Peru (Shaffer *et al.*, 1995; Strub *et al.*, 1998; Thomas *et al.*, 1994). The region of most intense upwelling today lies between 35°S and 40°S (Strub *et al.*, 1998). The upwelled water is sourced from 150 - 250 m depth (Johnson *et al.*, 1980), mainly from the GUC. Under very intense upwelling conditions even AAIW can be brought to the surface (Strub *et al.*, 1998).

4.3. Materials and Methods

Two sediment cores from the Chilean continental slope were studied: Core GIK 17748-2 (32°45.0'S, 72°02.0'W, water depth 2545 m, length 383 cm; Geological Institute, University of Kiel) was retrieved from the Valparaiso Basin during cruise SONNE-80 (Stoffers and Cruise Participants, 1992), core GeoB 3375-1 (27°28.0' S, 71°15.1' W, water depth 1947 m, length 489 cm; Dept. of Geosciences, University of Bremen) was retrieved from the Chilean continental slope during cruise SONNE-102 (Hebbeln *et al.*, 1995) (Fig. 4.1).

The age models for the cores GIK 17748-2 and GeoB 3375-1 are based on AMS-14C dates, oxygen isotope stratigraphy and orbital tuning of sedimentological parameters (Fig. 4.3). Only the record of the last 12,900 years of Core GIK 17748-2 have been used, as the older sections are strongly affected by resedimentation processes (Lamy *et al.*, 1999; Marchant, 1997). All ages are given in calendar years. The details on the age model of GIK 17748-2 can be found in Lamy *et al.* (1999), the age model of core GeoB 3375-1 is described in Lamy *et al.* (1998a).

The cores were sampled at 5 cm intervals. The total carbon content of the samples was measured using an elemental analyser (Heraeus CHN-O-Rapid). The carbonate content ($CaCO_3$) was calculated by subtracting the total organic carbon (TOC) content measured on decalcified samples from the total carbon (TC) content. The carbonate content was calculated using Equation 4.1. A detailed description of this method can be found in Müller *et al.* (1994).

$$CaCO_3 = TC - TOC \cdot 8.333 \qquad (4.1)$$

4.4. Results

The TOC content ranges from 0.48 to 1.11 wt.% in core GeoB 3375-1, and from 0.76 to 1.44 wt.% in core GIK 17748-2 (Fig. 4.3). The $CaCO_3$ content ranges from 7.9 to 22.5 wt.% in core GeoB 3375-1, and from 6.2 to 17.7 wt.% in core GIK 17748-2 (Fig. 4.3). For all records there are no extreme values, but rather a systematic variation between the maximum and minimum values. There is no obvious relationship between these two parameters in the

investigated cores. The rain ratio of organic carbon over carbonate carbon (C_{org}/C_{carb}) in core GeoB 3375-1 ranges between 0.23 and 0.87 (Fig. 4.3). In core GIK 17748-2 the C_{corg}/C_{carb} ratio is between 0.52 and 1.62. Rain ratios exceeding 1 were measured only during the last ~2,800 cal. yrs. B.P..

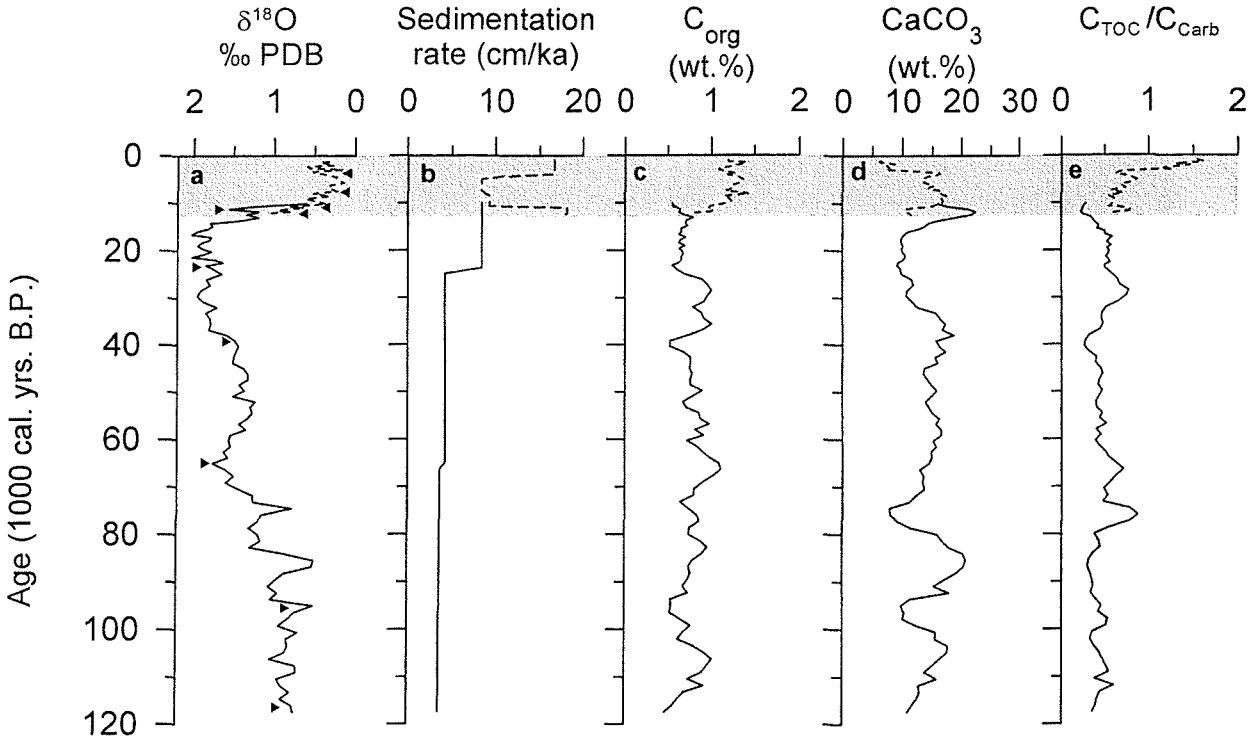

Figure 4.3 Time-series records in gravity cores GIK 17748-2 and GeoB 3375-1(the shaded fields mark the stratigraphic range of the record of Core GIK 17748-2): (a) stable oxygen isotope data measured on N. pachyderma (dex.) (GIK 17748-2) and N. pachderma (sin.) (GeoB 3375-1), the triangles indicate the age control points (younger than 40,000 cal. yrs. B.P: ^{14}C-AMS ages, older than 40,000 cal. yrs. B.P: tuning data (see Lamy et al., 1998a, and Lamy et al., 1999 for details), (b) sedimentation rates, (c) total organic carbon contents, (d) carbonate contents, and (e) the ratio of C_{corg}/C_{carb}.

The linear sedimentation rates have been derived from the published age models for core GeoB 3375-1 (Lamy *et al.*, 1998a) and for core GIK 17748-2 (Lamy *et al.*, 1999). The sedimentary record of core GeoB 3375-1 at the northern position spans the period 117,000 to 10,000 cal. yrs. B.P.. The sedimentation rate was 3.6 cm/ka from 117,000 cal. yrs. B.P. and increased slightly to 4.3 cm/ka at about 65,000 cal. yrs. B.P. (Fig. 4.3). After 23,700 cal.yrs. B.P. the sedimentation rate increased to 8.4 cm/ka. The period 10,000 cal. yrs. B.P. to present is missing in the core. The sedimentary record of core GIK 17748-2 used here covers the period from 12,900 cal. yrs. B.P. to the present. The sedimentation rate was highest (~18

cm/ka) from 12,900 to 10,700 cal. yrs. B.P. and then dropped in two steps to 8.3 cm/ka during the period 10,700 to 4,700 cal. yrs. B.P. (Fig. 4.3). In the youngest part of the core the sedimentation rate increased again to 16.7 cm/ka.

The complete data-set can be found in the Pangaea database at URL: http://www.pangaea.de/Projects/GeoB/JKlump.

4.5. Discussion

4.5.1. Reconstructing paleoproductivity

Two different approaches can be found in the literature to reconstruct paleoproductivity (Müller and Suess, 1979; Sarnthein *et al.*, 1992). Both are based on the accumulation of organic carbon and on the preservation effect of total sediment accumulation. However, the two formulae are sometimes not concordant in their results and may result in opposing patterns of paleoproductivity through time. This is due to the different ways in which organic carbon accumulation and preservation is thought to be influenced by the sedimentation rate. In this study, the formula of Müller and Suess (1979) (equation 4.2) was used to reconstruct paleoproductivity on the basis of organic carbon in the sediment because it is more suitable for hemipelagic environments than other available formulae (Rühlemann *et al.*, 1996):

$$P = \frac{C_{org} \cdot \rho}{0.0030 \cdot SR^{0.3}} \qquad (4.2)$$

where P is primary productivity (gC m^{-2} a^{-1}), C_{org} is the organic carbon in the sediment (wt.%), r is the dry bulk density of the sediment (g cm^{-3}), and SR is the linear sedimentation rate (cm ka^{-1}). The primary productivity calculated here on the basis of organic carbon accumulation is equivalent of the primary productivity of the total biomass.

An alternative, though uncommon, approach to reconstruct paleoproductivity is to use marine carbonate in the sediment as a proxy. Brummer and van Eijden (1992) showed from deep-moored sediment traps that a strong positive correlation exists between modern carbonate and

organic carbon fluxes. Using data on sediment traps from the literature, they developed an algorithm to reconstruct paleoproductivity from carbonate accumulation and tested it on pelagic carbonate sequences drilled during ODP Leg 121 (Peirce *et al.*, 1989). This approach assumes a fixed ratio between carbonate and organic carbon in carbonate shell-secreting organisms. It has to be noted that this method was developed to quantify productivity in oligotrophic 'blue-ocean' environments, where carbonate shell-secreting organisms dominate the biocoenosis. In these oligotrophic areas the primary productivity of carbonate-shell secreting organisms is the predominant component of the total primary productivity (Rühlemann *et al.*, 1996). This method was further tested and refined by van Kreveld *et al.* (1996) who extended the data set of Brummer and van Eijden (1992). From this extended data set they derived a new equation to correlate the flux of organic carbon to the carbonate flux. The formula of van Kreveld *et al.* (1996) (equation 4.3) can be used to estimate the organic carbon flux at a depth of 3200 m (PF_{3200} in mg m^{-2} d^{-1}) from the carbonate accumulation rate (AR_{Carb}) in the sediment.

$$PF_{3200} = AR_{Carb} \cdot 0.043 + 0.353 \qquad (4.3)$$

The non-zero intercept $b = 0.353$ indicates that in oligotrophic regions of the ocean a minimal organic carbon flux remains even when the carbonate flux is zero, due to the production of opaline shell-secreting and non-skeletal organisms. We will use this method to quantify the carbonate-based productivity, not total productivity, so a modified version of equation 4.3 with a zero intercept will be used instead (equation 4.4).

$$PF_{3200} = AR_{Carb} \cdot 0.043 \qquad (4.4)$$

The organic carbon flux at 3200 m was then converted to the carbon flux at 100 m (PF_{100} in gC m^{-2} a^{-1}), which is equivalent to export paleoproductivity, by applying the equation of Suess (1980) (equation 4.5), which relates export production to organic carbon flux (PF_{3200}) at depth ($z = 3200$ m).

$$PF_{100} = PF_{3200} \cdot 0.365 \cdot (0.0238 \cdot z + 0.212) \qquad (4.5)$$

The term 0.365 is a conversion factor from (mg m^{-2} d^{-1}) to (g m^{-2} a^{-1}). This procedure provides us with an estimate of the export productivity (PF_{100} in gC m^{-2} a^{-1}) of carbonate shell-secreting organisms. This export productivity can then be converted to primary productivity of carbonate-shell secreting organisms (PP_{Carb} in gC m^{-2} a^{-1}) by applying the formula of Eppley and Peterson (1979) (equation 4.6).

$$PP_{Carb} = 20 \cdot \sqrt{PF_{100}} \qquad (4.6)$$

4.5.2. Paleoproductivity off Chile

Following the method of Müller and Suess (1979), the primary paleoproductivity in the Peru-Chile Current ranged from 94 to 280 gC m^{-2} a^{-1} during the last 117,000 years (Fig. 4.4). This total paleoproductivity follows a precessional cycle with maximum productivity during precession minima (Fig. 4.4). It was higher on average during the late Pleistocene (200 gC m-2 a-1) than during the Early and Middle Holocene (170 gC m^{-2} a^{-1}). The lowest productivity was found during the Last Glacial Maximum and the latest Holocene (130 gC m^{-2} a^{-1}, equivalent to Pnew = 42 gC m^{-2} a^{-1}, Eppley and Peterson, 1979). This value is comparable to the modern-day situation determined from sediment traps in the region. For the period July 1993 to July 1994 export productivity was measured to be 42 gC m^{-2} a^{-1} in traps moored at 30°S in the Peru-Chile Current (Hebbeln *et al.*, in press 1998).

The paleoproductivities (primary productivity) based on carbonate accumulation range from 65 to 165 gC m^{-2} a^{-1} (Fig. 4.4). This carbonate-based paleoproductivity shows quite a different pattern compared to the total paleoproductivity, resulting from the fact that the organic carbon-based estimate reflects the productivity of the total biomass, while the carbonate-based estimate primarily represents the paleoproductivity of calcareous organisms only. The carbonate-based paleoproductivity was fairly uniform around 90 gC m^{-2} a^{-1} throughout the last

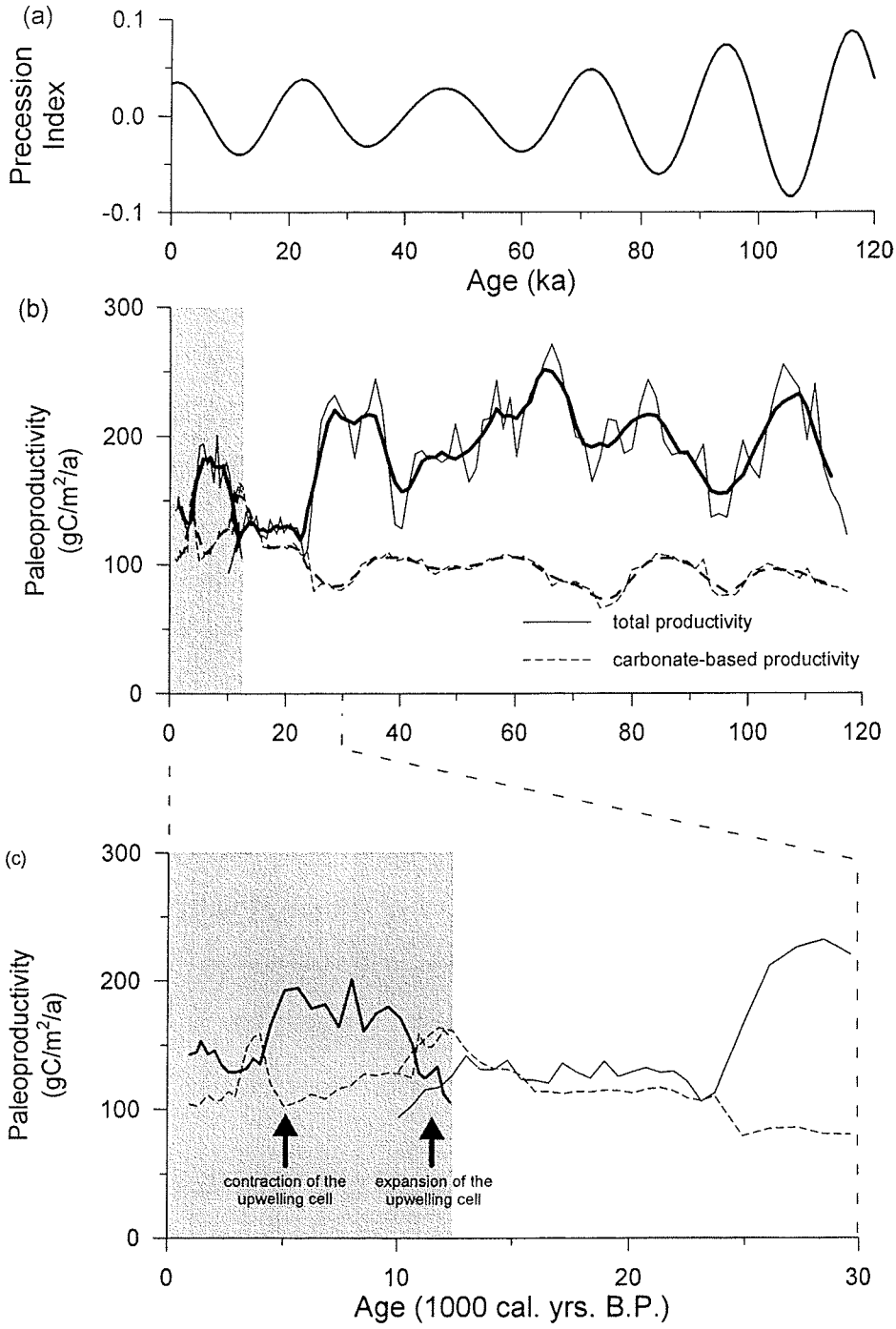

Figure 4.4 (a) Precession index after Berger (1978). (b) Paleoproductivities calculated from organic carbon and from biogenic carbonate accumulation in cores GIK 17748-2 and GeoB 3375-1 for the last 120,000 years. The paleoproductivity curves are overlain with a 5-point moving average. (c) Detailed diagram of the paleoproductivities shown in (b) for the Last Glacial Maximum and the Holocene. The expansion/contraction cycle of the upwelling cell at 32°S, as discussed in the text, is indicated by arrows. The shaded fields in (b) and (c) mark the stratigraphic range of the record of Core GIK 17748-2

glacial. There is an increase in carbonate-based productivity in two steps to about 110 gC m^{-2} a^{-1} from 25,000 to 24,000 cal. yrs. B.P., and another increase to 160 gC m^{-2} a^{-1} from 16,000 to 12,000 cal. yrs. B.P. During the Early and Middle Holocene the carbonate-based paleoproductivity declined back to glacial levels, followed by another peak around 3,700 cal. yrs. B.P. and a sharp drop to modern productivity levels of approximately 110 gC m^{-2} a^{-1} (Fig. 4.4).

The two records presented are assumed to be unaffected by any changes in the degree of preservation of organic carbon and biogenic carbonate in the sediment. Since the sedimentation rates were always higher than 2 cm ka-1 removal of organic carbon by post-depositional oxidation ('burn-down') is unlikely (Jung *et al.*, 1997). Changes in the accumulation rate of biogenic carbonate are unlikely to be caused by dissolution because the core positions are well above the regional lysocline (Archer, 1991a; Hebbeln *et al.*, in prep. 1998). Since the ratio of C_{corg}/C_{carb} is always <1 (Fig. 4.3), carbonate dissolution by metabolic CO_2 from organic carbonate degradation can also be discounted as the cause of the observed variations of the carbonate accumulation rate in core GeoB 3375-1 (Archer, 1991b). In core GIK 17748-2 this ratio is always <1 in sediments older than 2,800 yrs. despite high organic carbon accumulation rates. However, in the top part of the core the C_{corg}/C_{carb} ratio is >1 (Fig. 4.3), but detailed studies on the foraminifera in this core show no signs of carbonate dissolution (Marchant, 1997).

Sometimes the values of carbonate-based productivity estimates exceed the total productivity (Fig. 4.4). This, of course, is impossible and is an artefact resulting from the inaccuracy of the respective algorithms for estimating paleoproductivity. For the same reasons it is of limited use to quantify the percentage contribution of calcareous organisms towards the total productivity. However, the general pattern deduced from these records appears to be a good reflection of the history of productivity along the Chilean slope. Comparing the two productivity indicators and how they vary through time, it is noticeable that the respective calculated paleoproductivities sometimes show changes in opposite directions (Fig. 4.4). Especially during times of decreased total productivity the proportion of calcareous organisms as part of the total biomass increases. This change in the proportion of the carbonate-based paleoproductivity relative to the total paleoproductivity points to a change in the ecology at the sampling sites.

All major upwelling areas in the oceans show a typical floral succession from the central upwelling cells through the filament zone to the open ocean (Armstrong *et al.*, 1987; Blasco *et al.*, 1980; Richert, 1975). Normally, the biocoenosis of the centre of an upwelling cell is dominated by diatoms. As the availability of nutrients decreases in the transition to the filament zone, diatoms are replaced by coccolithophorids. As nutrient levels in the filament zone decline even further with increasing distance from the centre of the upwelling cell, the total biomass decreases as well. In the sediment this general pattern is reflected by the predominance of siliceous diatom frustules under the central upwelling cell, which are gradually replaced by coccoliths towards the filament zone, reflecting the floral change in the water column above (Mortyn and Thunell, 1997; Richert, 1975). Thus, changes in the floral assemblage and in bulk biogenic accumulation rates at a given core site in an upwelling area can be used to infer changes in the spatial extent of upwelling cells.

Position and extent of coastal upwelling cells are governed by the dynamics of land-ocean-atmosphere interaction. Off Chile upwelling is most intense in local upwelling cells concentrated behind headlands of northward facing bays (Armstrong *et al.*, 1987; Johnson *et al.*, 1980; Strub *et al.*, 1998) (Fig. 4.5). Nutrient-rich intermediate waters are mixed into the euphotic zone by Ekman pumping where the direction of the trade winds is parallel to the coast (Berger *et al.*, 1989). Even though the broad zone of coastal upwelling might shift with changes of the regional wind field following seasonal or climatic change, the individual upwelling cells will remain in place. However, variations in the intensity of forcing will cause the upwelling cells to expand or to contract.

A typical expansion/contraction cycle of an upwelling cell is reflected in the record of core GIK 17748-2. Relatively high carbonate-based paleoproductivity and relatively low total productivity between 12,500 and 10,300 cal. yrs. B.P. (Fig. 4.4) indicate that the core site was beneath the filament zone dominated by calcareous organisms (Fig. 4.5b,d) during that period. A much higher total productivity combined with a lower carbonate-based productivity between 10,300 and 4,000 cal. yrs. B.P. reflects the expansion of the central upwelling cell dominated by diatoms to the core site (Fig 4.5a,c). Its subsequent contraction is marked by the shift back to similar conditions as between 12,500 and 10,300 cal. yrs. B.P. indicating the return of the filament zone to the core site, which lasted there for another 1,000 years.

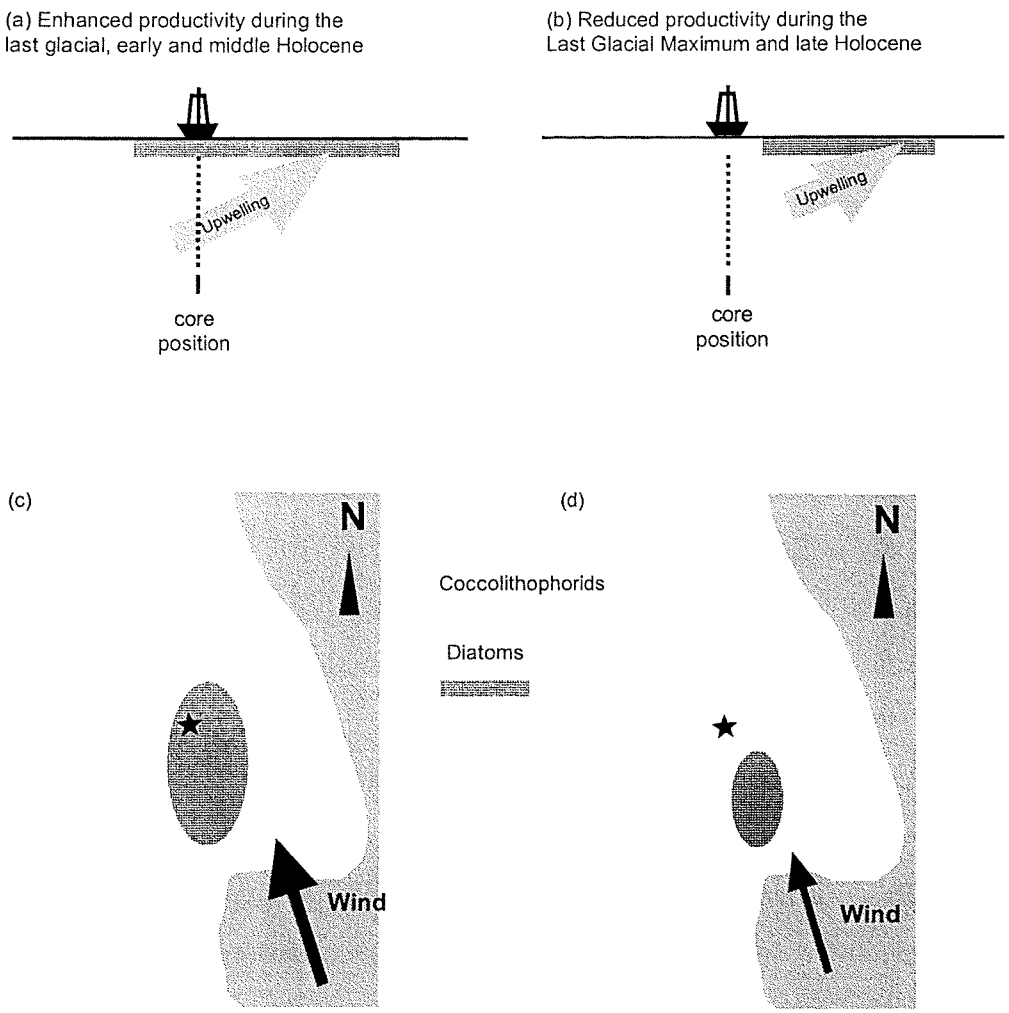

Figure 4.5 Schematic diagram of the floral and faunal succession in an upwelling cell off northern or central Chile (a: section, c: plan view) during periods of intense upwelling (precession minima), and (b: section, d: plan view) during periods of reduced upwelling (precession maxima).

Even though cores GIK 17748-2 and GeoB 3375-1 come from different locations and cover different periods of the geological past, there is a good agreement between the two sedimentary records where they overlap. This indicates a parallel development of the Late Quaternary paleoproductivity both off northern and central Chile, driven by the same forcing mechanisms. Core GeoB 3375-1 taken off northern Chile shows that total productivity was very high between 110,000 and 24,500 cal. yrs. B.P., a period when also the trade winds blew strong (see e.g. (Berger *et al.*, 1989; Sarnthein, 1978)). In Chile the intensity of the trade winds is closely tied to the position of the Southern Westerlies. During the last glacial the Southern Westerlies shifted latitudinal in pace with a precessional forcing, reaching northern positions during precession maxima and southern positions during precession minima

(Heusser, 1989; Lamy *et al.*, 1998a; Veit, 1996). Thus, by driving the atmospheric circulation, precession affected the position and intensity of the trade winds and finally the wind forcing of upwelling. Consequently, the record of total productivity is modulated by a precessional signal with highest total productivity during precession minima. The strong dominance of the total productivity over the carbonate-based productivity throughout the last glacial (except the Last Glacial Maximum) (Fig. 4.4b) indicates a large extent of the central upwelling cell at 27.5°S resulting in a continuous coverage of site GeoB 3375-1. Interestingly, also during precession maxima, when total productivity was relatively lowest, the central upwelling cell was large enough to cover the core site.

Decreasing total productivity and increasing carbonate-based productivity mark the contraction of the upwelling cell at the northern site (27.5°S) at the beginning of the Last Glacial Maximum (Fig. 4.4c). During this period the Southern Westerlies reached an almost similar position compared to the previous precession maxima (Lamy *et al.*, 1998a; Lamy *et al.*, 1999). From this setting one would expect productivity to be on a similar high level as observed during the preceding precession maxima, which was only slightly lower than during the respective precession minima. However, the Last Glacial Maximum is characterised by a much lower total productivity. As the atmospheric forcing of the upwelling is assumed to have been similar to the period before, something special to the Last Glacial Maximum must have caused the drastic decrease in productivity.

From a coastal upwelling point of view the most significant difference between the Last Glacial Maximum and the period before (110,000 to 24,500 cal. yrs. B.P.) is the height of sea-level. Thus, the decrease in productivity at the beginning of the Last Glacial Maximum is probably related to a contemporaneous drop in global sea-level in the order of 25 m, which is the final step towards the -120 m level associated with the last large continental glaciations. This drop in sea-level possibly passed a threshold, which changed the coastal zone morphology around 27.5°S in a way that it lost part of its upwelling favourable features.

An increase in the carbonate-based productivity at 16,000 cal. yrs. B.P. in core GeoB 3375-1, when sea-level already started to rise again, fits perfectly to a similar pattern in core GIK 17748-2 (Fig. 4.4b,c), supporting the comparability of the two records and thus of the two settings. In core GIK 17748-2 this increased carbonate-based productivity marks the onset of

the Early Holocene expansion/contraction cycle of the related local upwelling cell described above. It is also reflected in the faunal analysis of planktic foraminifera in core GIK 17748-2. Maxima in the abundance and flux rates of *Globigerina bulloides* and *Neogloboquadrina pachyderma* (sin.) during the same period have been interpreted as a sign of intensified upwelling (Marchant, 1997). The increased upwelling intensity, especially between 10,300 and 4,000 cal. yrs. B.P., was most likely forced by the Early Holocene precession minimum. The general lower productivity at site GIK 17748-2, in relation to the more northern site (Fig. 4.4), might be due to the local setting (distance of the site from the main upwelling centre) or due to a more southerly position of the Southern Westerlies at this time (Lamy *et al.*, 1999), which might have resulted in a relative decrease of the atmospheric forcing of upwelling compared to the previous precession minima.

The data for the Late Holocene are not fully conclusive. A slight increase in total productivity at ~3,000 cal. yrs. B.P. accompanied by a decrease in carbonate-based productivity point to an expansion of the upwelling cell. It coincides with an increase in the accumulation rates of benthic foraminifera and of the planktic foraminifera species *Neogloboquadrina dutertrei* and a higher relative abundance of *Neogloboquadrina pachyderma* (sin.). (Marchant, 1997) interprets this as a competing influence of subtropical (indicated by *N. dutertrei*) and subpolar (indicated by *N pachyderma* (sin.)) water masses, intermittently supporting high productivity, as indicated by the increased accumulation of benthic foraminifera (Herguera and Berger, 1991). However, throughout the last 3,000 years total productivity remains on a rather low level. Paleoclimatic (Lamy *et al.*, 1999; McGlone *et al.*, 1992) as well as paleoceanographic (Marchant, 1997) studies from the region characterised this period to be very variable, which has been related to increasing frequencies and intensities of Southern Oscillation/El Niño (ENSO) events.

4.6. Conclusions

The study of gravity cores GIK 17748-2 and GeoB 3375-1 shows that the total paleoproductivity along the Chilean margin generally followed a precessional cycle with maximum biological productivity in the water column during precession minima. The driving

factor of productivity variations is most likely the position of the Southern Westerlies, which are known to move north and south in a precessional rhythm. As the Southern Westerlies are responsible for the wind forcing of upwelling along the Chilean margin productivity is directly linked to their position.

Total paleoproductivity was much higher during the last glacial (110,000 to 24,500 cal. yrs. B.P.) than it is today. However, the lowest productivity was found during the Last Glacial Maximum and for the Late Holocene, with slightly enhanced values in the Middle Holocene. The much lower paleoproductivity during the Last Glacial Maximum, which occurred despite a wind forcing comparable to previous precession maxima, is most likely due to the late glacial drop in sea level, which changed the coastal morphology in a way that previously upwelling favourable features were lost. Although the two records investigated are from different areas (off northern and central Chile), the reconstructed absolute paleoproductivities match very well in their general patterns and in the period where the two records overlap. This observation indicates that the pattern found in these two cores is typical for large parts of the Chilean margin.

The evolution through time of the paleoproductivity of carbonate-shell secreting organisms shows a pattern partly opposite to the paleoproductivity of the total biomass. The proportion of carbonate-based productivity of the total paleoproductivity was highest during periods of reduced productivity. This pattern was produced by the biotic zonation typical to upwelling cells. As the local upwelling cells expanded and contracted, in response to changes in the regional wind field caused by Late Quaternary climatic changes, the biotic succession zones, characterised by the proportion of diatoms to coccolithophorids, moved across the core positions and, thus, changed the relation between total and carbonate-based paleoproductivity.

Acknowledgements — The authors would like to thank J. Bijma, S. Neuer and C. Rühlemann for the constructive discussions. Financial support was provided by the German Bundesministerium für Bildung und Forschung through funding the project CHIPAL (03G0102A).

The complete data-set can be found in the Pangaea database at URL http://www.pangaea.de/Projects/GeoB/JKlump.

Correspondence should be addressed to J.K. (jklump@uni-bremen.de)

Chapter 5 - High concentrations of biogenic barium in marine sediments around Termination I - A signal of changes in productivity, ocean chemistry and deep water circulation

by J. Klump, D. Hebbeln, and G. Wefer

Fachbereich Geowissenschaften, Universität Bremen.

Abstract

High concentrations of barium have been found in sediments deposited on the Chilean continental slope shortly after glacial Termination I. These barium peaks coincide with periods of increased productivity, as indicated by independent proxies of paleoproductivity. However, the increase of the barium accumulation rate is too high to be explained by increased productivity or changes in the terrigenous supply of barium, leaving the concentration of dissolved barium in sea-water as the most likely variable causing these barium peaks. Taking the accumulation rate of biogenic barium and the paleoproductivity, as reconstructed on the basis of organic carbon accumulation, it was modelled how the concentration of dissolved barium in the Pacific Ocean has changed in the course of the last glacial and through the Holocene. This model shows that the barium concentrations in the Pacific during the last glacial (90 nmol/kg) were lower than today (110 nmol/kg). The highest dissolved barium concentrations were calculated for two short-term peaks in the Early Holocene (140 nmol/kg) and in the Middle Holocene (180 nmol/kg). This is in good agreement with Ba/Ca ratios in planktic foraminifera, as published in the literature. The Holocene shoaling of the Pacific carbonate compensation depth caused an increased flux of previously carbonate-bound barium from the sediment to the deep ocean waters, leading to the observed broad maximum of dissolved barium in the Pacific during the Holocene. Superimposed short-term changes in the concentration of dissolved barium probably reflect changes in the influx of Ba-enriched waters exported from the North Atlantic as the production of North Atlantic Deep Water resumed after the end of the Last Glacial Maximum (LGM) and after a short interruption during the Younger Dryas.

5.1. Introduction

The regions of high biological productivity in the world's ocean are thought to play an important part in the transfer of carbon from the atmosphere to the sediment through the activity of the 'biological pump' (Berger *et al.*, 1989). To quantify past biological productivity various paleoproductivity indicators have been devised (see e.g. Berger *et al.*, 1989; Elderfield, 1990). One of them is biogenic barite in marine sediments, which has been suggested to be a potential proxy of paleoproductivity (Goldberg and Arrhenius, 1958; Schmitz, 1987). Its main advantage over other proxies, such as organic carbon, is its high degree of preservation in the sediment (30 to 60% preservation). However, the biogeochemical framework of biogenic barite and how it is related to export productivity are not yet well enough understood. Major problems arise from the remaining uncertainty about the terrigenous contribution towards the measured barium signal (Dymond *et al.*, 1992; Klump *et al.*, subm. 1999; Nürnberg *et al.*, 1997), and how water depth, bulk sedimentation rate and changes in the dissolved barium content of the water masses of the oceans influence the accumulation rate of biogenic barite (Dymond *et al.*, 1992).

Particularly puzzling are the anomalously high biogenic barium concentrations found in sediments deposited just prior to glacial Terminations I, II, and IV in the Atlantic (Harris *et al.*, 1996; Kasten, 1996; Thomson *et al.*, subm. 1998) and following Termination I in the Pacific (Schwarz *et al.*, 1996; this paper). Although sometimes associated with productivity peaks, the biogenic barium peaks are too high to be explained by increased productivity. In cores from oxic sedimentary environments a close association of biogenic barium with other productivity indicators makes a diagenetic redistribution of barium unlikely. Increased Ba/Ca ratios measured in benthic foraminifera were found to be contemporaneous with the biogenic barium peaks in the sediment, and are interpreted to. record increased concentrations of dissolved barium in intermediate and deep waters of the Pacific Ocean (Lea and Boyle, 1990), which could have resulted in an increased flux of biogenic barite to the sediment (Dymond *et al.*, 1992).

To assess the suitability of biogenic barium as a paleoproductivity indicator, we investigated whether the anomalously high biogenic barium peaks found around Termination I can be ex-

plained by changes in concentrations of dissolved barium in intermediate and deep waters. To achieve this, the barium contents of two gravity cores (GIK 17748-2 and GeoB 3375-1) from the Chilean continental slope were used to calculate the accumulation rate of biogenic barium. Preservation corrected biogenic barium flux rates (Dymond *et al.*, 1992) were then compared with the export productivity calculated from the organic carbon accumulation rate. The changes in the concentration of dissolved barium in deep waters of the Southeast Pacific during the past 30,000 years were reconstructed by using the relationship between dissolved barium in sea water, and the flux rates of organic carbon and of biogenic barium (Dymond *et al.*, 1992). The resulting changes can be explained by variations in ocean chemistry and ocean circulation. This shows that under certain conditions biogenic barium might be a good paleo-productivity indicator.

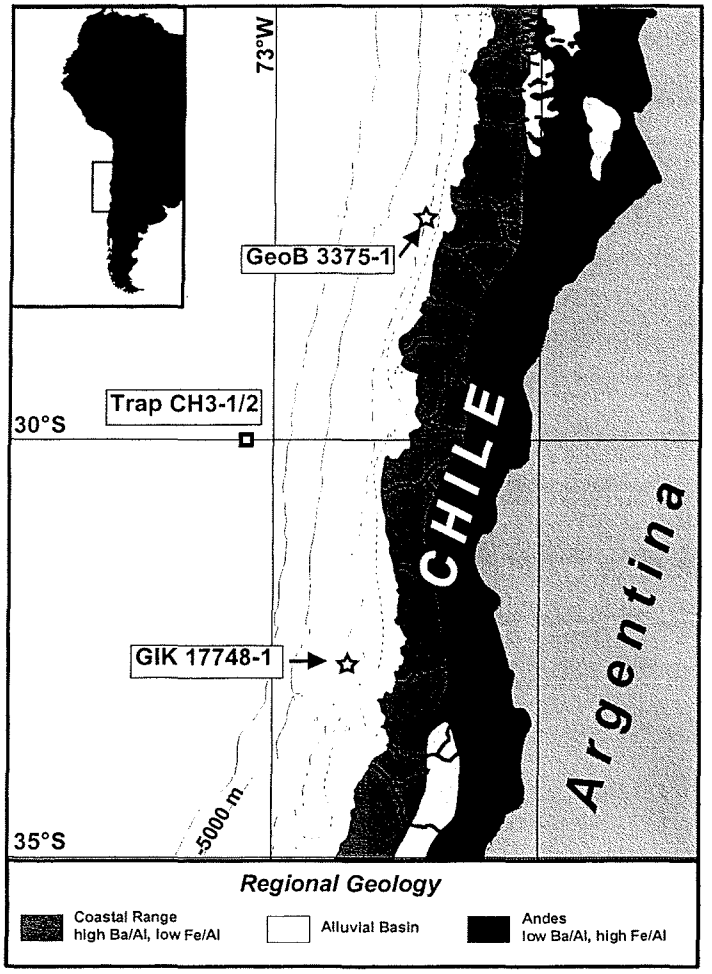

Figure 5.1: Locations of gravity cores GIK 17748-2 and GeoB 3375-1 and sediment traps CH3-1 and CH3-2 (square), and a schematic representation of the Chilean hinterland geology.

5.2. Materials and methods

Gravity core GIK 17748-2 (32°45.0'S; 72°02.0'W; water depth 2545 m; core length 383 cm, Geological Institute, University of Kiel) was retrieved during cruise SO-90 with the German R/V SONNE (Stoffers and Cruise Participants, 1992) from the Valparaiso Basin. Gravity core GeoB 3375-1 (27°28.0'S; 71°15.1'W; water depth 1948 m; core length 489 cm, Dept. of Geosciences, University of Bremen) was retrieved from the Chilean continental slope during cruise SO-102, also with the German R/V SONNE (Hebbeln *et al.*, 1995). The locations of cores GIK 17748-2 and GeoB 3375-1 are marked on Fig. 5.1.

Both core sites lie within the regional deep water mass, the Pacific Deep Water. In addition, sediment trap samples were collected during the period 22 July 1993 to 18 January 1994 during 20 sampling intervals of 9 days each by traps CH3-1 (2300 m) and CH3-2 (3700 m) at 30°01.1'S, 73°11.0'W (Fig. 5.1). Further detail regarding the sediment traps may be found in Hebbeln *et al.* (in press 1998).

For chemical analysis of the Fe, Al and Ba contents, the freeze-dried and homogenised samples were subjected to total acid digestion. The sample material was weighed directly into Teflon pressure vessels. The digestion was performed using HNO_3, $HClO_4$, and HF in a PDS-6 pressure system at 180°C over eight hours. Subsequently, the acid was evaporated close to dryness, and the residue was dissolved in HNO_3 and again digested over eight hours in a PDS-6 pressure system. Finally, the solution was decanted into a pre-cleaned glass flask and filled to 100 ml with deionised water and then filled into pre-cleaned polyethylene bottles for cold storage. The concentrations of Ba, Al, and Fe were measured by inductively coupled plasma atomic emission spectrometry (ICP-AES). The relative error on repeat measurements is 4% for Ba, 2.5% for Al, and 2.1% for Fe. The accuracy was determined by repeated analysis (n = 22) of control standards (USGS Analyzed Marine Mud MAG-1).

The age models for the cores GIK 17748-2 and GeoB 3375-1 are based on AMS-^{14}C dates, oxygen isotope stratigraphy and orbital tuning of sedimentological parameters (Fig. 5.2). Only the record of the last 12,900 years of Core GIK 17748-2 have been used, as the older sections are strongly affected by resedimentation processes (Lamy *et al.*, 1999; Marchant, 1997). All ages are given in calendar years. The details on the age model of GIK 17748-2 can be found in Lamy *et al.* (1999), the age model of core GeoB 3375-1 is described in Lamy *et al.* (1998a).

5.3. Results

The amount of biogenic barium in the sediment can be derived from normative calculations by subtracting the estimated terrigenous barium from the measured total barium content (Dymond *et al.*, 1992). For the Chilean margin Klump *et al.* (subm. 1999) established a

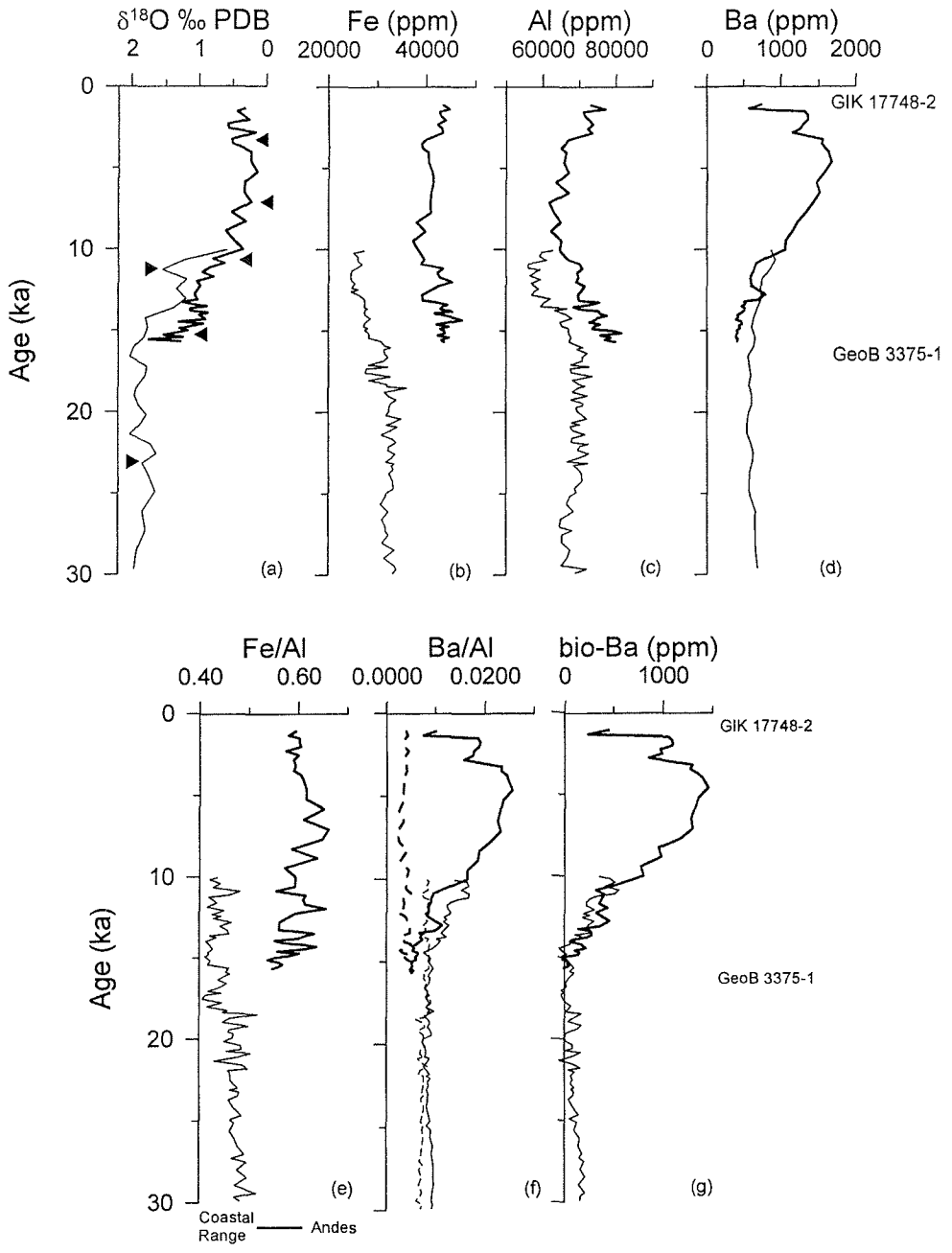

Figure 5.2: Time-series records for gravity cores GIK 17748-2 and GeoB 3375-1(the shaded fields mark the stratigraphical range of the record of Core GIK 17748-2): (a) stable oxygen isotope data measured on N. pachyderma (dex.) (GIK 17748-2) and N. pachderma (sin.) (GeoB 3375-1), the triangles indicate the AMS ^{14}C-age control points (see (Lamy et al., 1998a) and (Lamy et al., 1999) for details), (b) iron contents, (c) aluminium contents, (d) barium contents (e) Fe/Al ratio, (f) Ba/Al ratio, the stippled line marks the reconstructed terrigenous Ba/Al ratio, and (g) content of biogenic barium. The bar at the bottom of Fig. 5.2e shows whether the sedimentary material on the continental slope was derived mainly from the Coastal Range or from the Andes.

provenance dependent relationship between the bulk Fe/Al ratio and the terrigenous Ba/Al ratio in marine sediments, thus allowing to quantify the biogenic barium content from analysing Fe, Al, and Ba. Following this approach, the Fe contents (GIK 17748-2: 37,300 to 47,300 ppm, GeoB 3375-1: 24,500 to 35,900 ppm, Fig. 5.2b), the Al contents (GIK 17748-2: 61,800 to 81,400 ppm, GeoB 3375-1: 56,000 to 73,500 ppm, Fig. 5.2c), and the Ba contents (GIK 17748-2: 390 to 1680 ppm, GeoB 3375-1: 542 to 924 ppm, Fig. 5.2d) have been used to calculate the respective Fe/Al ratios (GIK 17748-2: 0,54 to 0,66, GeoB 3375-1: 0,41 to 0,52, Fig. 5.2e) and Ba/Al ratios (GIK 17748-2: 0,0050 to 0,0255, GeoB 3375-1: 0,0074 to 0,0168, Fig. 5.2f). The difference in the Fe/Al and Ba/Al ratios in the two cores are due to differences in the geochemistry of the main source areas, which are the Andes with high Fe/Al and low Ba/Al ratios for core GIK 17748-2 and the Coastal Range with low Fe/Al and high Ba/Al ratios for core GeoB 3375-1 (Klump *et al.*, subm. 1999) (Fig. 5.1). Varying contributions from these two source areas, induced by climatic changes, and hence variations in weathering and transport, have resulted in changing Fe/Al and terrigenous Ba/Al ratios through time. Based on the established relationship between the Fe/Al and the terrigenous Ba/Al ratios, the biogenic barium content can be determined from the difference between the measured Ba/Al ratio in the sediments and the reconstructed terrigenous Ba/Al ratio (dashed line in Fig. 5.2e; GIK 17748-2: 0 to 1455 ppm, GeoB 3375-1: 0 to 546 ppm, Fig. 5.2g). Besides the extremely high biogenic barium contents in the Holocene, there are no extreme values, but a rather systematic variation between the maximum and minimum values. The data of Klump *et al.* (subm. 1999) show that in the given framework of Chilean hinterland geochemistry changes of sediment provenance cannot account for the increased barium flux during the Holocene. The C_{org}/Ba_{bio} ratio of the sediment trap material was calculated for each trap from the sum of C_{org} and Ba_{bio} contents of all twenty sampling cups (Klump, unpublished data). The biogenic barium component was derived from normative calculations using a terrigenous Ba/Al ratio of 0.0060 (Klump *et al.*, subm. 1999). The resulting C_{org}/Ba_{bio} ratios are 62 for trap CH3-1 and 51 for trap CH3-2.

The complete set of data can be found in the 'Pangaea' database (URL http://www.pangaea.de/Projects/GeoB/JKlump).

5.4. Discussion

5.4.1. Biogenic barium as a proxy of biological productivity in the ocean

Goldberg and Arrhenius (1958) were the first to point out a possible link between high productivity in the surface waters and the accumulation of barium in the sediments below. Dehairs *et al.* (1980) identified biogenic barite ($BaSO_4$) to be the carrier of this signal. Until today the exact mechanism of formation of biogenic barite remains unclear. The proposed models follow two different lines of thought. Some authors interpret the barium enrichment in decaying organic matter to be caused by biotic processes, i.e. organisms enriching barium in their skeletons, like acantharians (Bernstein *et al.*, 1992; Bernstein *et al.*, 1998), xenophyphores (Gooday and Nott, 1982), and filamentous blue-green algae (Gayral and Fresnel, 1979). Other authors interpret the formation of biogenic barite as an abiotic process. In their model the sulphate of decaying proteins in organic aggregates, such as faecal pellets, and dissolved barium in sea-water combine and precipitate to form at first amorphous aggregates of barium sulphate within oxic microenvironments. The barium sulphate aggregates then recrystallise to barite and grow further on their way through the water column (Dehairs *et al.*, 1980; Gingele and Dahmke, 1994; Stroobants *et al.*, 1991).

The effect of water depth on the biogenic barium flux is indicated by sediment trap data from various parts of the world ocean (Dymond *et al.*, 1992) as well as from our study area (this paper), which show a decrease of the C_{org}/Ba ratio in the particle flux with water depth (Fig. 5.3b). The linear increase of biogenic barium contents with water depth, found in surface sediments from the Chilean continental slope (Klump *et al.*, subm. 1999) shows that the decreasing C_{org}/Ba ratio reflects increasing barium contents rather than continuing organic matter degradation. These results also show that biogenic barium is found mainly in sediments from water depths greater than 1000 m, both along the Namibian (von Breymann *et al.*, 1992) and Chilean margins (Klump *et al.*, subm. 1999), which indicates that the crystallisation of marine barite happens mainly below the oxygen minimum zone. The linear increase of biogenic barium with water depth below the oxygen minimum zone makes it unlikely that biogenic barite should be formed primarily by organisms in surface waters. It also rules out a significant role of benthic organisms in the production of biogenic barite. Together these observations support the model of an abiotic process in the formation of marine barite. In this

case the concentration of dissolved barium in sea water may influence the formation of biogenic barite (Dymond *et al.*, 1992; Martin and Lea, 1998). However, without organic matter from export productivity marine barite will not be formed. Therefore, the barium in marine barite related to paleoproductivity will be referred to as 'biogenic barium', regardless of the details of the formation process.

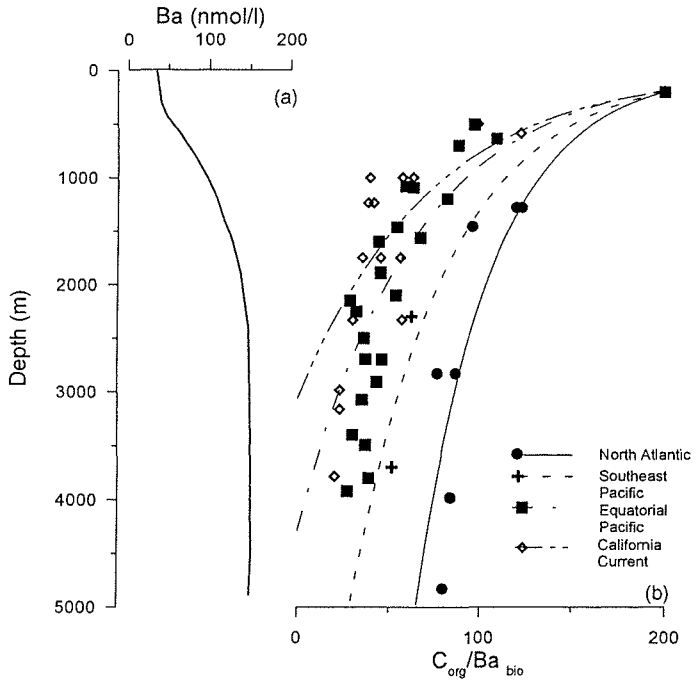

Figure 5.3: (a) Depth profile of dissolved barium in the equatorial Pacific (GEOSECS, 1987), Sta. 204). The concentration of dissolved barium follows a typical nutrient profile with low concentrations near the surface, increasing with depth. (b) C_{org}/Ba ratios of particulate matter in sediment traps. The C_{org}/Ba ratios decrease with depth. The decrease of the C_{org}/Ba ratio from the Atlantic to the North Pacific follows the increasing concentration of nutrients (and barium) along the flow path of the deep water masses. The trap data for the North Atlantic, the California current and the Equatorial Pacific are taken from (Dymond et al., 1992). The exponential fits have been forced through a Corg/Ba value of 200 at a water depth of 200 m (Dymond et al., 1992).

The concentration of dissolved barium in the oceans follows a typical nutrient profile with greater barium contents in deep water (Chan *et al.*, 1977; Chan *et al.*, 1976) (Fig. 5.3a) and increasingly higher barium contents along the path of bottom water flow from the North Atlantic into the Southern Ocean and then further into the South Pacific and North Pacific (Chan *et al.*, 1977; Chan *et al.*, 1976; GEOSECS, 1987). Sediment trap data published by Dymond *et al.* (1992) and in this paper show that today the decrease of the C_{org}/Ba ratio in settling particles with water depth is greater in the Pacific than in the Atlantic (Fig. 5.3b). Therefore, the barium uptake through the decay processes inside organic aggregates may be dependent on the barium content of the water through which the decomposing biogenic debris settles (Dymond *et al.*, 1992; Martin and Lea, 1998).

5.4.2. Changes in the concentration of barium in sea-water

To assess past changes in the concentration of barium in sea-water we use an indirect approach. Dymond *et al.* (1992) developed an algorithm (equation 5.1) which links the flux of biogenic barium and the concentration of dissolved barium in sea-water to (paleo) export productivity:

$$P_{new} = \left(\frac{F_{Ba} \cdot 0.171 \cdot Ba^{2.218} \cdot z^{0.476-0.00478 \cdot Ba}}{2056} \right)^{1.504} \qquad (5.1)$$

where P_{new} is the export productivity (gC m^{-2} a^{-1}), F_{Ba} is the flux of biogenic barium (μg cm^{-2} a^{-1}), which is the accumulation rate of biogenic barium corrected for the preservation effect depending on the sedimentation rate (see Dymond *et al.*, 1992) (Fig. 5.4c), *Ba* is the concentration of barium in sea-water (nmol/kg), and *z* is the water depth (m).

This formula can be used to assess variations in the concentration of dissolved Ba, assuming the paleoproductivity and the biogenic barium flux rate are known. Following the formula of Müller and Suess (1979) the paleoproductivity record of the two cores studied has been determined for the last 117,000 years (Klump *et al.*, in prep. 1999a). For the period considered here the paleoproductivity was highest at around 30,000 cal. yrs. B.P. and during the Early and Middle Holocene and lowest during the LGM and the Late Holocene (Fig. 5.4a)

Using the formula of Eppley and Peterson (1979) (equation 5.2) the paleoproductivity (*P*) taken from Klump *et al.* (in prep. 1999a) can be converted to paleo export productivity (P_{new}):

$$P_{new} = \frac{P^2}{400} \qquad (5.2)$$

Assuming the export productivity P_{new} (Fig. 5.4a), derived from the reconstructed primary production (Klump *et al.*, in prep. 1999a), the biogenic barium flux (Fig. 5.4b), and the water depth are know, equation (5.1) can be solved for the concentration of barium in sea-water. However, as the outcome of this operation the term *Ba* is found both as a base and as an

exponent. This is a transcendental equation which can only be solved by iteration. The equation was solved using a commercial software package (*Mathematica* ™).

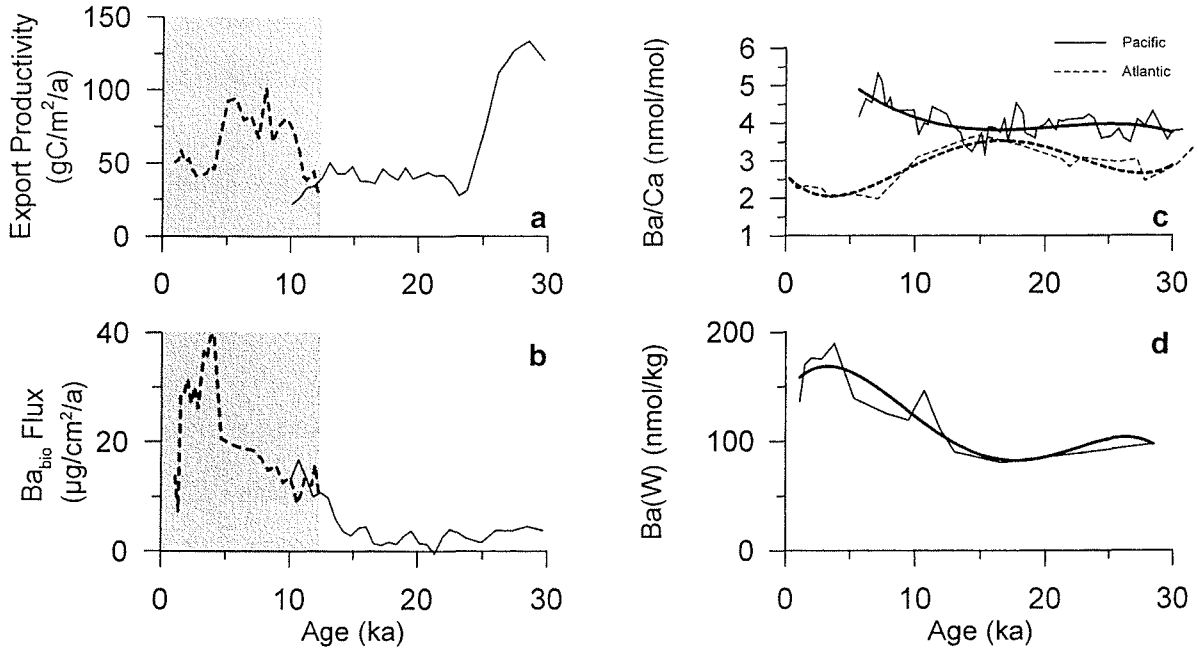

Figure 5.4: Reconstructed time series data for gravity cores GIK 17748-2 and GeoB 3375-1 (the shaded fields mark the stratigraphical range of the record of Core GIK 17748-2): (a) Export productivity calculated according to (Eppley and Peterson, 1979) from primary productivity (Klump et al., in prep. 1999a), (b) Biogenic barium flux rate calculated according to Dymond et al. (1992), (c) Ba/Ca ratio measured in benthic forams from the equatorial Pacific and Atlantic (Lea and Boyle, 1990), and (d) Changes in the concentration of dissolved barium in sea-water in the Southeast Pacific derived from geochemical modelling. Bold lines in (c) and (d) are 4^{th} degree polynomial fits to the data points.

The results of solving equation 5.1 for barium in sea-water show that the concentration of dissolved barium in the Southeast Pacific was around 90 nmol/kg at around 30,000 cal. yrs. B.P. and then decreased to 85 nmol/kg during the LGM (Fig. 5.4d). The dissolved barium concentration increased sharply after the end of the LGM to the end of the Younger Dryas to 140 nmol/kg. Then it decreased slightly to 130 nmol/kg around 9,000 cal. yrs. B.P. The highest dissolved barium concentrations were calculated for the Middle Holocene, around 5,000 cal. yrs. B.P. (180 nmol/kg), after which they decreased to 130 nmol/kg at the core top, which is close to the present-day value of 110 nmol/kg (GEOSECS, 1987).

Paleoceanographic modelling (Lea and Boyle, 1990; Rutsch, 1996) and Ba/Ca ratios in benthic foraminifera (Lea and Boyle, 1990) have shown that the concentration of barium in

sea-water has changed through time. In accordance with the data presented in Fig. 5.4d, benthic Ba/Ca ratios showed that the concentration of barium in sea-water increased in the Pacific after the LGM, while it decreased in the Northwest Atlantic (Lea and Boyle, 1990) (Fig. 5.4c).

5.4.3. Effects of changes in ocean chemistry and global ocean circulation

The changes in the concentration of dissolved barium in sea-water of the Southeast Pacific, as shown by our geochemical model, occur on two different time scales: short-term peaks of dissolved barium are found superimposed on a broad increase of dissolved barium from the end of the LGM to the Middle Holocene, followed by a decrease of dissolved barium concentrations during the Late Holocene (Fig. 5.4d). While the short duration and timing of the superimposed barium peaks right after the end of the LGM and after the Younger Dryas points towards changes in the global ocean circulation, the underlying broad barium maximum found throughout the Holocene cannot be explained by similar circulation changes.

Recent data from measurements on benthic flux chambers by McManus *et al.* (1999) on sediments from the equatorial Pacific and from the Californian margin showed that there is a constant ratio of barium over alkalinity in the remineralisation flux from the sediment to the deep ocean. Since biogenic marine carbonate is the major source of alkalinity in the ocean, these results show that the biogeochemical cycle of barium and the carbonate system are linked (McManus *et al.*, 1999). Although the amount of barium that may be accommodated in the crystal lattice of calcite or aragonite is rather small (max. 200 ppm; Church, 1970), the large amounts of biogenic carbonate raining to the ocean-floor can transfer significant amounts of barium from the surface ocean to greater depths. This could explain the nutrient-like distribution of barium in the ocean, as surface waters would become depleted of barium by its incorporation into biogenic carbonate, and its release to the deeper waters by carbonate dissolution, thereby increasing the barium concentrations of deep and intermediate waters. Here, in deep and intermediate waters, dissolved barium becomes available to be combined with sulphate ions in aggregates of decaying organic matter, precipitating as barium sulphate and crystallising to biogenic barite.

Due to the coupled Ba/alkalinity remineralisation flux, changes in the carbonate system, which occur on Milankovitch time-scales (Archer, 1991a; Farrell and Prell, 1989), would profoundly affect the biogeochemical cycle of barium in the ocean. Deepening of the carbonate compensation depth (CCD) in the Pacific at the onset of the last glacial increased the amount of preserved biogenic carbonate, decreasing the carbonate dissolution driven flux of barium from the sediment to the deep waters of the Pacific. Shoaling of the CCD during the Holocene greatly increased the flux of barium from the sediment by additionally dissolving carbonate from shallower depths. This model would explain the broad maximum of dissolved barium found in the Holocene sediments from the Chilean continental slope (Fig. 5.4d). The continuous decrease until today is in accordance with the results of McManus *et al.* (1999), who showed that in the equatorial Pacific the system has not yet returned to equilibrium conditions.

Short-term peaks in the flux of biogenic barite to the sediment, which are probably due to increased concentrations of dissolved barium in the deep waters, are found at, or immediately prior to, glacial terminations in the subtropical and equatorial Atlantic (Kasten, 1996; Matthewson *et al.*, 1995; Thomson *et al.*, subm. 1998), whereas in the Pacific barium peaks were found right after the end of the LGM and Younger Dryas (Fig. 5.4e).

A possible explanation for these barium peaks observed in the Atlantic and the Pacific may be changes of the global ocean 'conveyor belt' which facilitates the exchange of water between the oceans (Broecker, 1998; Gordon, 1986), and in changes of the concentration of dissolved barium in North Atlantic Deep Water (NADW) (Martin and Lea, 1998). The slowdown of the North Atlantic thermohaline circulation lead to an increase of nutrient levels and also of dissolved barium in the deep North Atlantic (Lea and Boyle, 1990; Martin and Lea, 1998) probably resulting in the observed barium peaks in Atlantic sediments. With the resumption of NADW export from the North Atlantic after the LGM NADW with unusually high barium concentrations enters the Southern Ocean. The water masses being exported from the Southern Ocean to the Pacific then had high concentrations of barium (Fig. 5.4c). During the Younger Dryas the production of NADW decreased again and less water with high barium concentrations entered the Southern Ocean. The resumption of NADW production after the Younger Dryas again brought water masses with elevated barium concentrations into the Pacific, producing the barium peak found after the Younger Dryas (Fig. 5.4d).

5.5. Conclusions

Geochemical analysis of particulate material from sediment traps and from surface sediments show evidence in support of an abiotic process governing the flux of biogenic barium to the sediment. The flux rate of biogenic barium depends on export productivity, water depth, and on the concentration of dissolved barium in the water column, whereas the input of terrigenous barium depends on the geochemistry of the sediment source rock and sums up to the total barium flux. The combined record of two cores from the Chilean continental slope shows that the flux of biogenic barium to continental slope sediments found in the Holocene section of the record is by far too high to be explained by increased productivity or increased input of terrigenous barium. This points to changes in the chemistry of the water masses of the Southeast Pacific.

The results of modelling the concentration of dissolved barium in sea-water from export productivity and from the flux rate of biogenic barium showed that barium concentrations in the Southeast Pacific were lower during the last glacial than they are today. After reaching minimum concentrations during the LGM, the concentration of barium in the Pacific increased throughout the Early and Middle Holocene. Superimposed on this general increase are short-term peaks following the end of the LGM, and the end of the Younger Dryas. Through the Late Holocene barium concentrations declined, but were still higher than glacial values.

Shoaling of the Pacific CCD during the Holocene lead to an increased flux of alkalinity from the sediment into the deep waters of the Pacific. Because of the constant ratio of Ba:alkalinity found in the remineralisation flux from the sediment this indicates an increased flux of previously carbonate-bound barium from the sediment into the deep waters of the Pacific during the Holocene.

The superimposed short-term changes in the concentration of dissolved barium in the Pacific were caused by changes in the rate of production of North Atlantic Deep Water (NADW). During times of low NADW production during the LGM and the Younger Dryas water with low barium concentrations entered the Pacific from the Southern Ocean. With the onset of increased NADW production waters with high barium concentration were exported from the

North Atlantic through the Southern Ocean into the Pacific. This model agrees well with the Ba/Ca ratios in benthic foraminifera from the equatorial Pacific and with the results of biogeochemical ocean models.

The concentration of dissolved barium in Pacific deep and intermediate waters was markedly higher during the Holocene than during the last glacial period. This was caused mainly by carbonate dissolution but also by increased barium supply from Atlantic waters. Through these processes, more barium was available to be used in the formation of biogenic barium in the water column off northern and central Chile. The resulting biogenic barium flux signal increased out of proportion of the mid-Holocene productivity maximum. These changes in the biogeochmical cycle of barium in the ocean have to be kept in mind when assessing the suitability of barium as a paleoproductivity proxy. Knowing the concentration of dissolved barium in intermediate and deep waters, which can be derived from Ba/Ca measurements on benthic foraminifera, and knowing the content of the terrigenous background barium in the sediment, which can be determined from stream sediment and surface sediment analyses, biogenic barium in deep sea sediments has a great potential as a paleoproductivity indicator.

Acknowledgements — The authors would like to thank S. Kasten, R. Schneider, J. Bijma, and A. Sanyal for the constructive discussions. Financial support was provided by the German Bundesministerium für Bildung und Forschung through funding the project *CHIPAL* (03G0102A).

Chapter 6 - Conclusions

Starting from the original objective of this project to reconstruct the Late Quaternary paleoproductivity in the southern Peru-Chile Current, **Chapter 1** provided the background information used to tackle this problem. Due to the uncertainties associated with biogenic barium as a paleoproductivity proxy a number of questions arose. The answers to these questions were discussed in the manuscripts which make up this thesis and the conclusions will be summarised in this chapter.

6.1 Reconstructing paleoproductivity from biogenic barium

Even though the association of barium in the sediment with regions of high biological productivity in the ocean has been known for some time (Dehairs *et al.*, 1980; Goldberg and Arrhenius, 1958; Schmitz, 1987), quantifying paleoproductivity from biogenic barium turned out to be more difficult than expected. Following the suggestion to measure biogenic barite, the carrier phase of the productivity signal, directly (Dehairs *et al.*, 1980; Dymond *et al.*, 1992) it was tested whether this method could be applied to our samples from the Chilean continental slope. However, the terrigenous input diluted the biogenic barite signal to such an extent that biogenic barite could not be detected quantitatively. Therefore, the biogenic barium component had to be derived from normative calculations (Dehairs *et al.*, 1980; Dymond, 1981; Dymond *et al.*, 1984; Leinen and Pisias, 1984). Since detrital aluminosilicates are the major carrier of terrigenous barium, the measured total barium signal has to be corrected for the terrigenous barium input. To be able to do so an accurate knowledge of the terrigenous Ba/Al ratio is required. With no other data available, most authors used the 'average' crustal Ba/Al ratio proposed by Dymond *et al.* (1992), and only few studies report a regional estimates of this ratio from marine sediments (Dean *et al.*, 1997; Nürnberg *et al.*, 1997). However, if the terrigenous component exceeds 50 wt% an inaccurate estimate of the terrigenous Ba/Al ratio will introduce a significant error in any normative calculation of the biogenic Ba fraction (Dymond *et al.*, 1992). **Chapter 3** reports the regional terrigenous Ba/Al ratios that were measured in stream sediments of the rivers Rio Bio-Bio (35°S) and Rio

Aconcagua (27°S). Also in **Chapter 3**, a method is shown to estimate the terrigenous Ba/Al ratio from exponential regression of the Ba/Al ratios measured in surface sediments from continental slope transects. Based on the biogenic barium contents in surface sediment samples it could be shown that the amount of biogenic barium in the sediment increases linearly with depth (**Chapter 3**). Linear regression of biogenic barium content in sediment surface samples from continental slope transects plotted against depth show x-axis intercepts at a depth approximating the base of the oxygen minimum zone along the Chilean margin. These two characteristics, the linear increase with depth and the depth of zero biogenic barium, strongly favour models of an abiotic formation of biogenic barite inside aggregates of decaying organic matter (cf. section 1.5).

Having derived the actual regional Ba/Al ratio of the terrigenous material the question has to be asked whether this ratio varies with changes of sediment provenance. The bimodal distribution of geochemical characteristics of the sediments on the Chilean continental slope can be used to devise a simple two-component mixing model, in which the Andes and the Coastal Range constitute the two end-members. The contribution of these two sources depends on the regional precipitation patterns that control erosion and transport on the continent. Changes of sediment provenance, as indicated by changes in the Fe/Al ratio of the bulk sediment, did result in changes of the terrigenous Ba/Al ratio. These paleo-ratios could be derived from the geochemical model in **Chapter 3**. Using the bulk Fe/Al ratio of the sediment as indicator of sediment provenance, and using illite crystallinity as an indicator of the weathering regime in the Coastal Range, the spatial and time-scale of Late Quaternary climate change in Chile could be reconstructed (**Chapter 2**). It turned out that the most important factor, governing all climate dependent processes along the Chilean margin, is the position of the Southern Westerlies, which determines the regional wind field (i.e. upwelling) and precipitation (i.e. erosion).

Even though the biogeochemical framework of the barium flux to the sediments of the Chilean continental slope is now much better understood than before the anomalous barium peaks found in the Holocene section of all three cores used in this study need to be explained. As discussed in **Chapter 5**, these barium peaks are too high to be caused by increased productivity, when compared to the paleoproductivities given by organic carbon and biogenic carbonate (**Chapter 4**). They are also not of diagenetic origin, and cannot be explained by

changes in sediment provenance to a source rock with higher Ba/Al ratios (**Chapter 3**). Lea and Boyle (1990) showed that Ba/Ca ratios in benthic foraminifera from the equatorial Pacific increased since the end of the LGM. This is highly indicative of an increasing concentration of dissolved barium in the deep waters of the Pacific. Since the flux rate of biogenic barium to the sediment is also a function of the concentration of dissolved barium in sea water (Dymond *et al.*, 1992), the observed high flux rates of biogenic barium to the sediment, in excess of what would be expected to be the result of the mid-Holocene productivity maximum, can be explained by increased concentrations of barium dissolved in sea water.

So far two pools of barium, that are thought to govern the flux of biogenic barium to the sediment in the ocean, have been discussed in the literature: particulate biogenic barite, and dissolved barium in sea water. Recent work by McManus *et al.* (1999) pointed towards a third pool of barium that, until now, had been disregarded as being of minor importance: barium bound in biogenic carbonate. Measurements in benthic lander flux chambers, done on sediments of the equatorial Pacific and of the Californian margin, showed that in the flux from the sediment to the deep water the barium/alkalinity ratio is fixed. Since carbonate dissolution is the source of 95% of alkalinity in the ocean they concluded that the there must be a link between the biogeochemical cycle of barium and the marine carbonate system. Even though the amount of barium that can be incorporated into the crystal lattice of calcite or aragonite is fairly small (max. 200 ppm, Church, 1970), the great amounts of biogenic carbonate produced in the ocean provide a substantial sink for barium. The results in **Chapter 5** show that the increase of dissolved barium in the Pacific is coeval with the Holocene shoaling of the CCD. The increased carbonate dissolution in the Pacific during the Holocene tapped this enormous reservoir and released great amounts of previously carbonate-bound barium into the deep waters of the Pacific, providing enough dissolved barium to greatly increase the flux rate of biogenic barite to the sediment.

Superimposed on this broad increase of the concentration of dissolved barium in sea water are short-term peaks. These follow onto the end of the LGM and after the end of the Younger Dryas. Paleoceanographic modelling (Lea and Boyle, 1990; Rutsch, 1996) showed that changes in the global thermohaline circulation can result in changes of the barium concentration in the ocean. It is currently understood that the formation of North Atlantic Deep-Water (NADW) was substantially reduced during the last glacial and maybe even

ceased during the LGM and during the Younger Dryas (Broecker, 1998). This lead to the formation of barium-enriched deep-water masses in the North Atlantic (Martin and Lea, 1998) which were flushed into the Southern Ocean and then exported to the Pacific when NADW production resumed after the end of the LGM and after the Younger Dryas cold-reversal. The short pulses of water with elevated barium concentrations entering Pacific resulted in short-term increases of the biogenic barium flux.

The results presented in this thesis show that biogenic barite may serve as a paleoproductivity proxy if the following background information is available:

(1) The regional terrigenous Ba/Al ratio has to be known to be able to calculate the biogenic contribution of barium to the measured total barium content of the sediment (**Chapter 3**). This ratio can be influenced by Late Quaternary climate change (**Chapters 2 and 3**).
(2) The concentration of dissolved barium in the water column has to be derived either from Ba/Ca ratios of benthic foraminifera (**Chapter 5**).
(3) The exact relationship of biogenic barium flux to export productivity, water depth, and dissolved barium in sea water has to be established in future work.

6.2. Late Quaternary productivity variations in the Peru-Chile Current

The accumulation rate of biogenic barium can be compared with the results given by the accumulation rates of organic carbon and of biogenic carbonate to assess its suitability as a proxy of paleoproductivity (Fig. 6.1). The combination of three independent paleoproductivity proxies shows that in this case the paleoproductivity can be reliably calculated from organic carbon using the formula of Müller and Suess (1979). Biogenic carbonate could be used to assess the relative contribution of carbonate-shell secreting organisms to the total productivity. This information helps to gauge variations in the size and productivity of the local upwelling cell through time. The results from biogenic barite accumulation in general agree with the results of the paleoproductivity calculations on the basis of organic carbon. However, biogenic barite could only be used as a quantitative proxy of paleoproductivity after investigating its biogeochemical framework in the Peru-Chile Current.

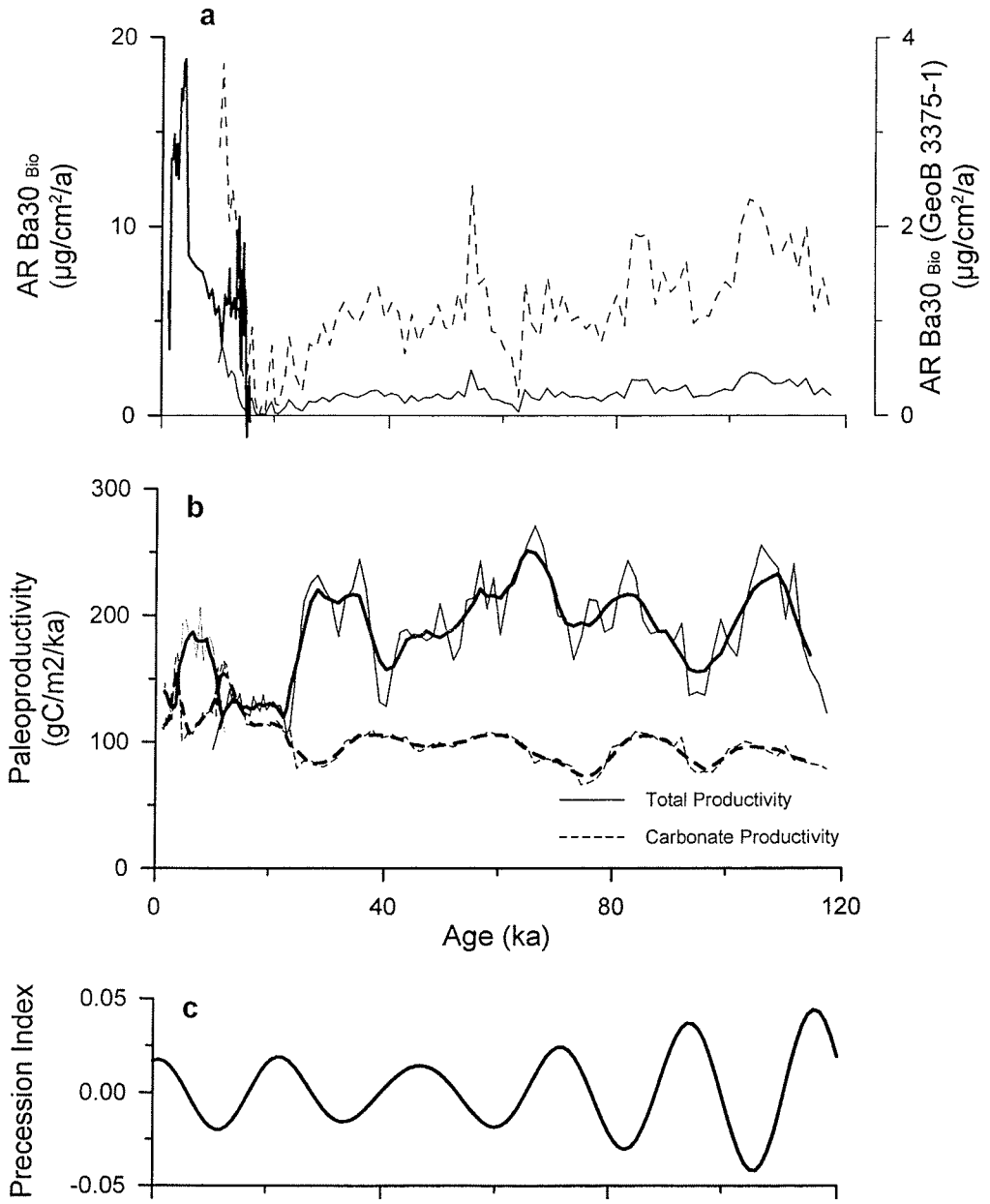

Figure 6.1. Comparison of the Late Quaternary accumulation rates of (a) biogenic barium with (b) paleoproductivities reconstructed from organic carbon and biogenic carbonate. Productivity maxima are found during precession minima (c). Carbonate-based productivities are highest during periods of low total productivity. Shown are the combined records of GIK 17748-2 and GeoB 3375-1 (see Chapter 5). To give a better resolution of the accumulation rate of biogenic barium in core GeoB 3375-1, the record is superimposed as a dashed line on Figure 6.1a. The precession index in Figure 6.1c is after Berger (1978).

While organic carbon accumulation reflects the total productivity, biogenic carbonate accumulation is only representative of the productivity of carbonate-shell secreting organisms. Since upwelling cells remain fixed in their positions over time, but vary in their spatial extent and always show the same phytoplankton zonation from a diatom-dominated centre to the coccolithophorid-dominated filament zone (Abbott *et al.*, 1997; Armstrong *et al.*, 1987; Blasco *et al.*, 1980; Richert, 1975), the changes in the relative contribution of carbonate-shell secreting organisms to the total productivity can be used to gauge the spatial extent of the upwelling cell at the position of the sediment core (Mortyn and Thunell, 1997). In **Chapter 4** organic carbon and biogenic carbonate were used as independent proxies of paleoproductivity. The changes in the relative contribution of carbonate-shell secreting organisms to the total productivity indicate how the biozones of the upwelling cell shifted across the sampled core position as the upwelling cell expanded and contracted with changes in upwelling intensity.

The results from three gravity cores from the Chilean continental slope (GeoB 3302-1 at 33°S, GeoB 3375-1 at 27.5°S, and GIK 17748-2 at 33°S) showed that the paleoproductivity in the Peru-Chile Current during the last glacial shows regional variability on the scale of individual upwelling cells. In general, the paleoproductivity in the southern Peru-Chile Current during the last glacial followed the precessional cycle with productivity maxima during precession minima. The lowest paleoproductivities were found during the Last Glacial Maximum. The productivity increased during the early Holocene. Off central Chile it reached another maximum during the middle Holocene. The productivity variations follow the changes in the regional atmospheric circulation pattern, which is mainly determined by the position of the Southern Westerlies (**Chapters 2 and 4**).

6.3. Future research

Working with biogenic barium showed that it may serve as a paleoproductivity proxy. However, the biogeochemistry of barium in the ocean is still not well enough understood. Further work with material from sediment traps and surface sediments from the Southeast Pacific and from other ocean basins is needed to better understand the behaviour of barium in the ocean. In particular, this future data must be used to unravel the relationship between

export productivity, water depth, and the concentration of dissolved barium in sea-water. To improve calculations which use the accumulation rate of biogenic barite, efforts have to be made to derive exact mass accumulation rates for the surface samples and sediment cores, e.g. by using $^{230}Th_{ex}$ corrections or other suitable dating techniques. Recently ash layers have been identified in cores from the Chilean continental slope. These could be analysed and dated to serve as stratigraphic marker horizons.

More Ba/Ca ratios in both benthic and planktic foraminifera have to be measured to gain a better understanding of how dissolved barium in sea water influences biogenic barite accumulation rates and how the paleochemistry of barium in the ocean has changed in the recent geological past. It will be of particular importance to gain further information on how changes in the marine carbonate system and how changes in the marine carbonate system affected the biogeochemical cycle of barium in the ocean.

It could be shown that any paleoproductivity information gained from sediment samples is only representative of the upwelling cell at the core location. More sediment cores from the Chilean continental margin have to be investigated and additional ones need to be retrieved in future expeditions to allow us to map the development of the paleoproductivity in the entire upwelling system and its regional divisions. Any future expedition should also include an 'on-shore leg' to collect stream sediments, both from near the estuary and from further upstream beyond the Coastal Range, to obtain more information about the hinterland geochemistry and how it is sampled by rivers.

A foreseeable complication in regions of the East Pacific Rise, and possibly in some locations on the South American continental margin, will be barite precipitated from white smokers and cold seeps, respectively. This hydrothermal barite may possibly be distinguishable from biogenic barite by differences in the isotopic composition of its barium and sulphur components.

As postulated by Paytan *et al.* (1993), biogenic barite could be used to measure the isotopic composition of strontium in the paleo-ocean, which holds information about climate, tectonics, weathering and hydrothermal activity at ocean ridges .

7. References

Abbott, M. B., Seltzer, G. O., and Wolfe, A. (1997). Holocene lake-level fluctuations in the Bolivian Andes. *EOS, Transactions, AGU*, **78,** F 43.

Aravena, R., Suzuki, O., and Pollastri, A. (1989). Coastal fog and its relation to groundwater in the IV region of northern Chile. *Chemical Geology*, **79,** 83-91.

Archer, D. E. (1991a). Equatorial Pacific calcite preservation cycles: Production or dissolution? *Paleoceanography*, **6,** 561-571.

Archer, D. E. (1991b). Modelling the calcite lysocline. *Journal of Geophysical Research*, **96,** 17,037-17,050.

Armstrong, D. A., Mitchell-Innes, B. A., Verheye-Dua, F., Waldron, H., and Hutchings, L. (1987). Physical and biological features across an upwelling front in the southern Benguela. *South African Journal of Marine Sciences*, **5,** 171-190.

Bard, E. (1988). Correction of accelerator mass spectrometry ^{14}C ages measured in planktonic foraminifera: Paleoceanographic implications. *Paleoceanography*, **3,** 635-645.

Bard, E., Hamelin, B., R.G., F., and Zindler, A. (1990). Calibration of the ^{14}C timescale over the past 30,000 years using mass spectrometric U-Th ages from Barbados corals. *Nature*, **345,** 405-410.

Barnola, J. M., Raynaud, D., Korotkevich, Y. S., and Lorius, C. (1987). Vostok ice core provides 160,000-year record of atmospheric CO_2. *Nature*, **329,** 408-414.

Ben Othman, D., Luck, J.-M., and Tournoud, M.-G. (1997). Geochemistry and water dynamics: application to short time-scale flood phenomena in a small Mediterranean catchment. I. Alkalis, alkali-earths and Sr isotopes. *Chemical Geology*, **140,** 9-28.

Berger, A. L. (1978). Long-term variations of caloric insolation resulting from the Earth's orbital elements. *Quaternary Research*, **9,** 139-167.

Berger, W. H., Smetacek, V. S., and Wefer, G. (1989). Ocean productivity and paleoproductivity - an overview. *In* "Productivity of the Ocean: Present and Past." (W. H. Berger, V. S. Smetacek, and G. Wefer, Eds.), pp. 1-34. Dahlem Workshop Reports. Wiley-Interscience Publ., Chichester.

Bernstein, R. E., Byrne, R. H., Betzer, P. R., and Greco, A. M. (1992). Morphologies and transformations of celestine in seawater: The role of acantharians in strontium and barium geochemistry. *Geochimica et Cosmochimica Acta*, **56,** 3273-3279.

Bernstein, R. E., Byrne, R. H., and Schijf, J. (1998). Acantharians: a missing link in the oceanic biogeochemistry of barium. *Deep-Sea Research I*, **45,** 491-505.

Bertram, M. A., and Cowen, J. P. (1997). Morphological and compositional evidence for biotic precipitation of marine barite. *Journal of Marine Research*, **55,** 577-593.

Blasco, D., Estrada, M., and Jones, B. (1980). Relationship between the phytoplankton distribution and composition and the hydrography in the northwest African upwelling region near Cabo Corbeiro. *Deep-Sea Research*, **27,** 799-821.

Bond, G., Broecker, W. S., Johnsen, S., McManus, J. F., Labeyrie, L., Jouzel, J., and Bonani, G. (1993). Correlations between climate records from North Atlantic sediments and Greenland ice. *Nature*, **365,** 143-147.

Bonn, W. J., Gingele, F. X., Grobe, H., Mackensen, A., and Fütterer, D. K. (1998). Paleoproductivity at the Antarctic continental margin: opal and barium records for the last 400 ka. *Palaeogeography, Palaeoclimatology, Palaeoecology*, **139,** 195-211.

Broecker, W. S. (1994). Massive iceberg discharge as triggers for global climate change. *Nature*, **372,** 421-424.

Broecker, W. S. (1998). Paleocean circulation during the last deglaciation: A bipolar seesaw? *Paleoceanography*, **13,** 119-121.

Broecker, W. S., and Henderson, G. M. (1998). The sequence of events surrounding Termination II and their implications for the cause of Glacial-Interglacial CO_2 changes. *Paleoceanography*, **13,** 352-364.

Brummer, G. J. A., and van Eijden, A. J. M. (1992). "Blue-ocean" paleoproductivity estimates from pelagic carbonate mass accumulation rates. *Marine Micropaleontology*, **19,** 99-117.

Chamley, H. (1989). "Clay sedimentology." Springer, Berlin.

Chan, L. H., Drummond, D., Edmond, J. M., and Grant, B. (1977). On the barium data from the Atlantic GEOSECS Expedition. *Deep-Sea Research*, **24,** 613-649.

Chan, L. H., Edmond, J. M., Stallard, R. F., Broecker, W. S., Chung, Y. C., Weiss, R. F., and Ku, T. L. (1976). Radium and barium at GEOSECS stations in the Atlantic and Pacific. *Earth and Planetary Science Letters*, **32,** 258-267.

Church, T. M. (1970). "Marine Barite." Unpublished PhD Thesis thesis, University of California.

Clapperton, C. (1993). "Quaternary geology and geomorphology of South America." Elsevier Science Publishers, Amsterdam, The Netherlands.

Clapperton, C. M., Sugden, D. E., Kaufman, D. S., and McCulloch, R. D. (1995). The last glaciation in Central Magellan Strait, southernmost Chile. *Quaternary Research*, **44,** 133-148.

Dansgaard, W., Johnsen, S. J., Clausen, H. B., Dahl-Jansen, D., Gundestrup, N. S., Hammer, C. U., Hvindberg, C. S., Steffensen, J. P., Sveinbjørnsdottir, A. E., Jouzel, J., and Bond, G. (1993). Evidence for general instability of past climate from a 250-kyr ice-core record. *Nature*, **364,** 218-220.

Dean, W. E., Gardner, J. V., and Piper, D. Z. (1997). Inorganic geochemical indicators of glacial-interglacial changes in productivity and anoxia on the Californian continental margin. *Geochimica et Cosmochimica Acta*, **61,** 4507-4518.

Dehairs, F., Chesselet, R., and Jedwab, J. (1980). Discrete suspended particles of barite and the barium cycle in the open ocean. *Earth and Planetary Science Letters*, **49,** 528-550.

Delmas, R. J., Ascencio, J.-M., and Legrand, M. (1980). Polar ice evidence that atmospheric CO_2 20,000 yr BP was 50% of present. *Nature*, **284,** 155-157.

Dymond, J. (1981). Geochemistry of the Nazca Plate surface sediments: An evaluation of hydrothermal, biogenic, detrital, and hydrogenous sources. *In* "Nazca Plate: Crustal Formation and Andean Convergence." (L. D. Kulm, J. Dymond, E. J. Dasch, and D. M. Hussong, Eds.), pp. 133-174. Mem. Geol. Soc. Am. Geol. Soc. Am.

Dymond, J., Lyle, M., Finney, B., Piper, D. Z., Murphy, K., Conard, R., and Pisias, N. G. (1984). Ferromanganese nodules from MANOP Site H, S, and R - Control of mineralogical and chemical composition by multiple accretionary processes. *Geochimica et Cosmochimica Acta*, **48,** 931-949.

Dymond, J., Suess, E., and Lyle, M. (1992). Barium in deep-sea sediment: A geochemical proxy for paleoproductivity. *Paleoceanography*, **7,** 163-181.

Elderfield, H. (1990). Tracers of ocean paleoproductivity and paleochemistry: An introduction. *Paleoceanography*, **5,** 711-717.

Eppley, R. W., and Peterson, B. J. (1979). Particulate organic matter flux and planktonic new production in the deep ocean. *Nature*, **282,** 677-680.

Farrell, J. W., and Prell, W. L. (1989). Climatic change and $CaCO_3$ preservation: an 800,000 year bathymetric reconstruction from the central equatorial Pacific Ocean. *Paleoceanography*, **4,** 447-466.

François, R., Honjo, S., Manganini, S. J., and Ravizza, G. E. (1995). Biogenic barium fluxes to the deep sea: Implications for paleoproductivity reconstruction. *Global Biogeochemical Cycles*, **9,** 289-303.

Gayral, P., and Fresnel, J. (1979). *Exanthemachrysis gayraliae* Lepailleur (Prymnesiophyceae, Pavlovales): ultrastructure et discussion taxonomique. *Protistologica*, **XV,** 271-282.

Genthon, C., Barnola, J. M., Raynaud, D., Lorius, C., Jouzel, J., Barkov, N. I., Korotkevich, Y. S., and Kotlyakov, V. M. (1987). Vostok ice-core: climatic response to CO_2 and orbital forcing changes over the last climatical cycle. *Nature*, **329,** 414-418.

GEOSECS. (1987). "Atlantic, Pacific, and Indian Ocean Expeditions." National Science Foundation, Washington, D.C.

Gingele, F. X., and Dahmke, A. (1994). Discrete barite particles and barite as tracers of paleoproductivity in South Atlantic sediments. *Paleoceanography*, **9,** 151-168.

Goldberg, E. D., and Arrhenius, G. O. S. (1958). Chemistry of Pacific pelagic sediments. *Geochimica et Cosmochimica Acta*, **13,** 153-212.

Gooday, A. J., and Nott, J. A. (1982). Intracellular barite crystals in two Xenophyphores, *Aschemonella ramuliformis* and *Galatheaminna* sp. (Protozoa: Rhizopoda) with comments on the taxonomy of *A. ramuliformis*. *Journal of the Marine Biology Association U.K.*, **62,** 595-605.

Gordon, A. L. (1986). Interocean exchange of thermocline water. *Journal of Geophysical Research*, **91,** 5037-5046.

Grootes, P. M., Stuiver, M., White, J. W. C., Johnsen, S. J., and Jouzel, J. (1993). Comparison of oxygen isotope records from the GISP2 and GRIP Greenland ice cores. *Nature*, **366,** 552-554.

Grosjean, M., Núñez, L., Cartajena, I., and Messerli, B. (1997). Mid-Holocene climate and culture change in the Atacama Desert, Northern Chile. *Quaternary Research*, **48,** 239-246.

Harris, P. G., Zhao, M., Rosell-Mele, A., Tiedemann, R., Sarnthein, M., and Maxwell, J. R. (1996). Chlorin accumulation rate as a proxy for Quaternary marine productivity. *Nature*, **383,** 63-65.

Hebbeln, D., Marchant, M., and Freudenthal, T. (in prep. 1998). Surface sediment distribution along the Chilean continental slope: Sedimentary, planktic foraminifera and stable isotope data.

Hebbeln, D., Marchant, M., and Wefer, G. (in press 1998). Seasonal variations of the particle flux in the Peru-Chile Current at 30°S under "normal" and under El Niño conditions. *Deep-Sea Research I.*

Hebbeln, D., Wefer, G., and Cruise Participants. (1995). Cruise Report of R/V SONNE Cruise 102, Valparaiso - Valparaiso, 9.5.-28.6.95, pp. 126. Fachbereich Geowissenschaften, Bremen.

Herguera, J. C., and Berger, W. H. (1991). Paleoproductivity from benthic foraminifera abundance: Glacial to post glacial change in the west-equatorial Pacific. *Geology*, **19,** 1173-1176.

Heusser, C. J. (1984). Late Quaternary climates of Chile. *In* "Late Cainozoic Climates of the Southern Hemisphere." (J. C. Vogel, Ed.), pp. 59-83. Balkema, Rotterdam.

Heusser, C. J. (1989). Southern westerlies during the Last Glacial Maximum. *Quaternary Research*, **31,** 423-425.

Heusser, C. J. (1990). Ice age vegetation and climate of subtropical Chile. *Palaeogeography, Palaeoclimatology, Palaeoecology*, **80,** 107-127.

Heusser, C. J., Lowell, T. V., Heusser, L. E., Hauser, A., Andersen, B. G., and Denton, G. H. (1996). Full-glacial-late-glacial paleoclimate of the Southern Andes: evidence from pollen, beetle and glacial records. *Journal of Quaternary Science*, **11,** 173-184.

Hulton, N., Sugden, D. E., Payne, A., and Clapperton, C. M. (1994). Glacier modelling and the climate of Patagonia during the Last Glacial Maximum. *Quaternary Research*, **42,** 1-19.

Imbrie, J., Hays, J. D., Martinson, D. G., McIntyre, A., Mix, A. C., Morley, J. J., Pisias, N. G., Prell, W. L., and Shackleton, N. J. (1984). The orbital theory of Pleistocene climate: Support from a revised chronology of the marine $\delta^{18}O$ record. *In* "Milankovitch and Climate (Part 1)." (A. L. Berger, J. Imbrie, J. D. Hays, G. Kukla, and J. Satzmann, Eds.), pp. 269-305. Reidel, Hingham, MA.

Johnson, D. R., Fonseca, T., and Sievers, H. (1980). Upwelling in the Humboldt Coastal Current near Valparaiso, Chile. *Journal of Marine Research*, **38,** 1-16.

Jordan, T. E., Isacks, B. L., Allmendinger, R. W., Brewer, J. A., Ramos, V. A., and Ando, C. J. (1983). Andean tectonics related to geometry of subducted Nazca plate. *Geological Society of America Bulletin*, **94,** 341-361.

Jung, M., Ilmberger, J., Mangini, A., and Emeis, K. C. (1997). Why some Mediterranean sapropels survived burn-down (and others did not). *Marine Geology*, **141,** 51-60.

Kasten, S. (1996). Early diagenetic metal enrichments in marine sediments as documents of nonsteady-state depositional conditions. Fachbereich Geowissenschaften, Universität Bremen, Bremen.

Klump, J., Hebbeln, D., and Wefer, G. (in prep. 1999a). Late Quaternary paleoproductivity variations in the Peru-Chile Current off northern and central Chile. *Marine Geology.*

Klump, J., Hebbeln, D., and Wefer, G. (subm. 1999). The impact of sediment provenance on barium-based productivity estimates. *Paleoceanography.*

Klump, J., Lamy, F., Hebbeln, D., and Wefer, G. (in prep. 1999b). Late Quaternary rapid climate change in northern Chile. *Geology.*

Lamy, F., Hebbeln, D., and Wefer, G. (1998a). Late Quaternary precessional cycles of terrigenous sediment input off the Norte Chico (27.5°S) and paleoclimatic implications. *Palaeogeography, Palaeoclimatology, Palaeoecology*, **141,** 233-251.

Lamy, F., Hebbeln, D., and Wefer, G. (1998b). Terrigenous sediment supply along the Chilean continental slope: Modern latitudinal trends of texture and composition. *Geologische Rundschau*, **87,** 477-494.

Lamy, F., Hebbeln, D., and Wefer, G. (1999). High resolution marine record of climatic change in mid-latitude Chile during the last 28 ka based on terrigenous sediment parameters. *Quaternary Research*, **51,** 83-93.

Le Maitre, R. W. (1976). The chemical variability of some common igneous rocks. *Journal of Petrology*, **17,** 589-637.

Lea, D. W. (1993). Constraints on the alkalinity and circulation of glacial Circumpolar Deep Water from benthic foraminiferal barium. *Global Biogeochemical Cycles*, **7,** 695-710.

Lea, D. W., and Boyle, E. A. (1990). Foraminiferal reconstruction of barium distributions in water masses of the glacial oceans. *Paleoceanography*, **5,** 719-742.

Leinen, M., and Pisias, N. G. (1984). An objective technique for determining end-member compositions and for partitioning sediments according to their sources. *Geochimica et Cosmochimica Acta*, **48,** 47-62.

Lowell, T. V., Heusser, C. J., Andersen, B. G., Moreno, P. I., Hauser, A., Heusser, L. E., Schlüchter, C., Marchant, D. R., and Denton, G. H. (1995). Interhemispheric correlation of Late Pleistocene glacial events. *Science*, **269,** 1541-1549.

Lyle, M. (1988). Climatically forced organic carbon burial in the equatorial Atlantic and Pacific Oceans. *Nature*, **335,** 529-532.

Marchant, M. (1997). Rezente und Spätquartäre Sedimentation planktischer Foraminiferen im Peru-Chile Strom. Fachbereich Geowissenschaften, Bremen.

Markgraf, V. (1989). Reply to C.J. Heusser's "Southern Westerlies during the Last Glacial Maximum". *Quaternary Research*, **31,** 426-432.

Martin, P. A., and Lea, D. W. (1998). Comparison of water mass changes in the deep tropical Atlantic derived from Cd/Ca and carbon isotope records: Implications for changing Ba composition of deep Atlantic water masses. *Paleoceanography*, **13,** 572-585.

Martinson, D. G., Pisias, N. G., Hays, J. D., Imbrie, J., Moore, T. C. J., and Shackleton, N. J. (1987). Age Dating and the Orbital Theory of the Ice Ages: Development of a High-Resolution 0 to 300,000-Year Chronostratigraphy. *Quaternary Research*, **27,** 1-29.

Matthewson, A. P., Shimmield, G. B., Kroon, D., and Fallick, A. E. (1995). A 300 kyr high-resolution aridity record of the North African continent. *Paleoceanography*, **10,** 677-692.

McGlone, M. S., Kershaw, A. P., and Markgraf, V. (1992). El Niño/Southern Oscillation climatic variability in Australasian and South American paleoenvironemntal records. *In* "El Niño - Historical and Paleoclimatic Aspects of the Southern Oscillation." (H. F. Díaz, and V. Markgraf, Eds.), pp. 435-462. Cambridge University Press, Cambridge.

McManus, J. F., Berelson, W. M., Hammond, D. E., and Klinkhammer, G. P. (1999). Barium cycling in the North Pacific: Implications for the utility of Ba as a paleoproductivity and paleoalkalinity proxy. *Paleoceanography*, **14,** 53-61.

Miller, A. (1976). The Climate of Chile. *In* "The Climate of Central and South America." (W. Schwerdtfeger, Ed.), pp. 113-145.

Mortyn, P. G., and Thunell, R. C. (1997). Biogenic sedimentation and surface productivity changes in the Southern California Borderlands during the last glacial-interglacial cycle. *Marine Geology*, **138,** 171-192.

Müller, G. (1967). Methods in sedimentary petrology. *In* "Sedimentary Petrology, 3." (W. von Engelhardt, H. Füchtbauer, and G. Müller, Eds.), pp. 283. Schweizerbart'sche Verlagsbuchhandlung, Stuttgart.

Müller, P. J., Schneider, R. R., and Ruhland, G. (1994). Late Quaternary pCO_2 variations in the Angola Current: evidence from organic carbon $\delta^{13}C$ and alkenone temperatures. *In* "Carbon cycling in the glacial ocean: constraints on the oceans role in global change." (R. Zahn, M. A. Kaminski, L. Labeyrie, and T. F. Pedersen, Eds.), pp. 343-366. NATO ASI Series I. Springer, Heidelberg.

Müller, P. J., and Suess, E. (1979). Productivity, sedimentation rate, and sedimentary organic matter in the oceans - I. Organic carbon preservation. *Deep-Sea Research*, **26A,** 1347-1362.

Nadeau, M.-J., Schleicher, M., Grootes, P. M., Erlenkeuser, H., Gottolong, A., Mous, D. J. W., Sarnthein, M., and Willkomm, H. (1997). The Leibniz-Labor AMS facility at the Christian-Albrechts University, Kiel, Germany. *Nuclear Instruments and Methods in Physics Research*, **123,** 22-30.

Nürnberg, C. C., Bohrmann, G., Schlüter, M., and Frank, M. (1997). Barium accumulation in the Atlantic sector of the Southern Ocean: Results from 190,000-year records. *Paleoceanography*, **12,** 594-603.

Orians, K. J., and Bruland, K. W. (1986). The biogeochemistry of aluminum in the Pacific Ocean. *Earth and Planetary Science Letters*, **78,** 397-410.

Paytan, A., Kastner, M., and Chavez, F. P. (1996). Glacial to interglacial fluctuations in productivity in the equatorial Pacific as indicated by marine barite. *Science*, **274,** 1355-1357.

Paytan, A., Kastner, M., Martin, E. E., Macdougal, J. D., and Herbert, T. D. (1993). Marine barite as a monitor of seawater strontium isotope composition. *Nature*, **366,** 445-449.

Peirce, J. W., Weissel, J. K., and Cruise_Participants. (1989). Proceedings of the ODP, Initial Report. Ocean Drilling Program, College Station, TX.

Petschick, R., Kuhn, G., and Gingele, F. X. (1996). Clay mineral distribution in surface sediments of the South Atlantic: sources, transport and relation to oceanography. *Marine Geology*, **130,** 203-229.

Pickard, G. L., and Emery, W. J. (1990). "Descriptive Physical Oceanography." Pergamon Press, Oxford.

Richert, P. (1975). "Die räumliche Verteilung und zeitliche Entwicklung des Phytoplanktons mit besonderer Berücksichtigung der Diatomeen im NW afrikanischen Auftriebsgebiet." Unpublished PhD thesis, Universität Kiel.

Rühlemann, C., Frank, M., Hale, W., Mangini, A., Mulitza, S., Müller, P. J., and Wefer, G. (1996). Late Quaternary productivity changes in the western equatorial Atlantic: Evidence from ^{230}Th-normalized carbonate and organic carbon accumulation rates. *Marine Geology*, **135,** 127-152.

Rutlland, J., and Fuenzalinda, H. (1991). Synoptic aspects of the central Chile rainfall variability associated with the southern oscillation. *International Journal of Climatology*, **11,** 63-76.

Rutsch, H.-J. (1996). "Modellierung des globalen Barium-Kreislaufs mit Hilfe eines zonal gemittelten Ozeanmodells für thermohaline Zirkulation." Unpublished PhD thesis, Universität Heidelberg.

Sarnthein, M. (1978). Sand deserts during glacial maximum and climatic optimum. *Nature*, **272,** 43-46.

Sarnthein, M., Pflaumann, U., Ross, R., Tiedemann, R., and Winn, K. (1992). Transfer functions to reconstruct ocean palaeoproductivity: A comparison. *In* "Upwelling Systems: Evolution Since the Early Miocene." (C. P. Summerhayes, W. L. Prell, and K. C. Emeis, Eds.), pp. 411-427. Geological Society Special Publication. Geological Society, London.

Sarnthein, M., Winn, K., Duplessy, J.-C., and Fontugne, M. R. (1988). Global variations of surface ocean productivity in low and mid latitudes: Influence on CO_2 reservoirs of the deep ocean and atmosphere during the last 21,000 years. *Paleoceanography*, **3,** 361-399.

Schmitz, B. (1987). Barium, equatorial high productivity, and the northward wandering of the Indian continent. *Paleoceanography*, **2,** 63-77.

Schmitz, B., Charisi, S. D., Thompson, E. I., and Speijer, R. P. (1997). Barium, SiO_2 (excess), and P_2O_5 as proxies of biological productivity in the Middle East during the Palaeocene and the latest Palaeocene benthic extinction event. *Terra Nova*, **9,** 95-99.

Scholl, D. W., Christensen, M. N., von Huene, R., and Marlow, M. S. (1970). Peru-Chile Trench sediments and sea-floor spreading. *Geological Society of America Bulletin*, **81,** 1339-1360.

Schwarz, B., Mangini, A., and Segl, M. (1996). Geochemistry of a piston core from Ontong Java Plateau (western equatorial Pacific): Evidence for sediment redistribution and changes in paleoproductivity. *Geologische Rundschau*, **85,** 536-545.

Schweller, W. J., Kulm, L. D., and Prince, R. A. (1981). Tectonics, structure, and sedimentary framework of the Peru-Chile trench. *Geological Society of America Memorandum*, **154,** 323-349.

Shaffer, G., Salinas, S., Pizarro, O., Vega, A., and Hormazabal, S. (1995). Currents in the deep ocean off Chile (30°S). *Deep-Sea Research I*, **42,** 425-436.

Silva, N. (1996). Data Report Preliminar, Datos Químicos, Crucero JGOFS-Chile 9-11. Universidad Catolica de Valparaiso, Valparaiso.

Singer, A. (1984). The paleoclimatic interpretation of clay minerals in sediments - a review. *Earth Science Reviews*, **21,** 251-293.

Stoffers, P., and Cruise Participants. (1992). Cruise Report SONNE 80a - Midplate III Oceanic Volcanism in the South Pacific. Geologisch-Paläontologisches Institut und Museum, Kiel.

Stroobants, N., Dehairs, F., Goeyens, L., Vanderheijden, N., and Van Grieken, R. (1991). Barite formation in the Southern Ocean water column. *Marine Chemistry*, **35,** 411-421.

Strub, P. T., Mesías, J. M., Montecino, V., Rutlland, J., and Salinas, S. (1998). Coastal ocean circulation off western South America. *In* "The Global Coastal Ocean - Regional Studies and Syntheses." (A. R. Robinson, and K. H. Brink, Eds.), pp. 273-313. The Sea - Ideas and Observations in the Study of the Seas. John Wiley & Sons, Inc., New York, NY.

Suess, E. (1980). Particulate organic carbon flux in the oceans - surface productivity and oxygen utilization. *Nature*, **288,** 260-263.

Thomas, A. C., Huang, F., Strub, P. T., and James, C. (1994). Comparison of the seasonal and interannual variability of phytoplankton pigment concentrations in the Peru and California Current systems. *Journal of Geophysical Research*, **99,** 7355-7370.

Thompson, E. I., and Schmitz, B. (1997). Barium and the late Paleocene $\delta^{13}C$ maximum: Evidence of increased marine surface productivity. *Paleoceanography*, **12,** 239-254.

Thomson, J., Nixon, S., Summerhayes, C. P., Rohling, E. J., Schönfeld, J., Zahn, R., Grootes, P. M., Abrantes, F., Gaspar, L., and Vaqueiro, S. (subm. 1998). Enhanced productivity on the Iberian margin during glacial/interglacial transitions revealed by barium and diatoms. *Geological Society London*, 23.

Thornburg, T., and Kulm, L. D. (1987). Sedimentation in the Chile Trench: Petrofacies and provenance. *Journal of Sedimentary Petrology*, **57,** 55-74.

Thornburg, T. M., Kulm, L. D., and Hussong, D. M. (1990). Submarine-fan development in the southern Chile Trench: A dynamic interplay of tectonics and sedimentation. *Geological Society of America Bulletin*, **102,** 1658-1680.

Thunell, R. C., Moore, W. S., Dymond, J., and Pilskaln, C. H. (1994). Elemental and isotopic fluxes in the Southern Californian Bight: A time-series sediment trap study in the San Pedro Basin. *Journal of Geophysical Research*, **99,** 875-889.

van Kreveld, S. A., Knappertsbusch, M., Ottens, J., Ganssen, G. M., and van Hinte, J. E. (1996). Biogenic carbonate and ice-rafted debris (Heinrich Layers) accumulation in deep-sea sediments from a Northeast Atlantic piston core. *Marine Geology*, **131,** 21-46.

Veit, H. (1996). Southern Westerlies during the Holocene deduced from geomorphological and pedological studies in the Norte Chico, Northern Chile (27-33°S). *Paleogeography, Paleoclimatology, Paleoecology*, **123,** 107-119.

Villagrán, C. (1993). Una interpretación climática del registro palinológico del último ciclo glacial-postglacial en Sudamérica. *Bulletin de l'Institut Française d'Ètudes Andines*, **22,** 243-258.

Villagrán, C., and Varela, J. (1990). Palynological evidence for increased aridity on the Central Chilean coast during the Holocene. *Quaternary Research*, **34,** 198-207.

von Breymann, M. T. v., Emeis, K. C., and Suess, E. (1992). Water depth and diagenetic constraints on the use of barium as a paleoproductivity indicator. *In* "Upwelling Systems: Evolution Since the Early Miocene." (C. P. Summerhayes, W. L. Prell, and K. C. Emeis, Eds.), pp. 273-284. Geological Society Special Publication. Geological Society, London.

von Huene, R., Corvalan, J., Korstgard, J., and Cruise Participants. (1995). Fahrtbericht zur Forschungsreise SO 101 - Condor, pp. 171. GEOMAR, Kiel.

Waylen, P. R., and Caviedes, C. N. (1990). Annual and seasonal fluctuations of precipitation and streamflow in the Aconcagua River basin, Chile. *Journal of Hydrology*, **120,** 79-102.

Zeil, W. (1986). "Südamerika." Enke Verlag, Stuttgart.

In dieser Reihe bereits erschienen:

Nr. 1 **Wefer, G., E. Suess und Fahrtteilnehmer**
Bericht über die POLARSTERN-Fahrt ANT IV/2, Rio de Janeiro - Punta Arenas, 6.11. - 1.12.1985.
60 Seiten, Bremen, 1986.

Nr. 2 **Hoffmann, G.**
Holozänstratigraphie und Küstenlinienverlagerung an der andalusischen Mittelmeerküste.
173 Seiten, Bremen, 1988. (vergriffen)

Nr. 3 **Wefer, G. und Fahrtteilnehmer**
Bericht über die METEOR-Fahrt M 6/6, Libreville - Las Palmas, 18.2. - 23.3.1988.
97 Seiten, Bremen, 1988.

Nr. 4 **Wefer, G., G.F. Lutze, T.J. Müller, O. Pfannkuche, W. Schenke, G. Siedler, W. Zenk**
Kurzbericht über die METEOR-Expedition Nr. 6, Hamburg - Hamburg, 28.10.1987 - 19.5.1988.
29 Seiten, Bremen, 1988. (vergriffen)

Nr. 5 **Fischer, G.**
Stabile Kohlenstoff-Isotope in partikulärer organischer Substanz aus dem Südpolarmeer (Atlantischer Sektor). 161 Seiten, Bremen, 1989.

Nr. 6 **Berger, W.H. und G. Wefer**
Partikelfluß und Kohlenstoffkreislauf im Ozean.
Bericht und Kurzfassungen über den Workshop vom 3.-4. Juli 1989 in Bremen.
57 Seiten, Bremen, 1989.

Nr. 7 **Wefer, G. und Fahrtteilnehmer**
Bericht über die METEOR - Fahrt M 9/4, Dakar - Santa Cruz, 19.2. - 16.3.1989.
103 Seiten, Bremen, 1989.

Nr. 8 **Kölling, M.**
Modellierung geochemischer Prozesse im Sickerwasser und Grundwasser.
135 Seiten, Bremen, 1990.

Nr. 9 **Heinze, P.-M.**
Das Auftriebsgeschehen vor Peru im Spätquartär. 204 Seiten, Bremen, 1990. (vergriffen)

Nr. 10 **Willems, H., G. Wefer, M. Rinski, B. Donner, H.-J. Bellmann, L. Eißmann, A. Müller, B.W. Flemming, H.-C. Höfle, J. Merkt, H. Streif, G. Hertweck, H. Kuntze, J. Schwaar, W. Schäfer, M.-G. Schulz, F. Grube, B. Menke**
Beiträge zur Geologie und Paläontologie Norddeutschlands: Exkursionsführer.
202 Seiten, Bremen, 1990.

Nr. 11 **Wefer, G. und Fahrtteilnehmer**
Bericht über die METEOR-Fahrt M 12/1, Kapstadt - Funchal, 13.3.1990 - 14.4.1990.
66 Seiten, Bremen, 1990.

Nr. 12 **Dahmke, A., H.D. Schulz, A. Kölling, F. Kracht, A. Lücke**
Schwermetallspuren und geochemische Gleichgewichte zwischen Porenlösung und Sediment im Wesermündungsgebiet. BMFT-Projekt MFU 0562, Abschlußbericht. 121 Seiten, Bremen, 1991.

Nr. 13 **Rostek, F.**
Physikalische Strukturen von Tiefseesedimenten des Südatlantiks und ihre Erfassung in Echolotregistrierungen. 209 Seiten, Bremen, 1991.

Nr. 14 **Baumann, M.**
Die Ablagerung von Tschernobyl-Radiocäsium in der Norwegischen See und in der Nordsee.
133 Seiten, Bremen, 1991. (vergriffen)

Nr. 15 **Kölling, A.**
Frühdiagenetische Prozesse und Stoff-Flüsse in marinen und ästuarinen Sedimenten.
140 Seiten, Bremen, 1991.

Nr. 16 **SFB 261 (Hrsg.)**
1. Kolloquium des Sonderforschungsbereichs 261 der Universität Bremen (14.Juni 1991):
Der Südatlantik im Spätquartär: Rekonstruktion von Stoffhaushalt und Stromsystemen.
Kurzfassungen der Vorträge und Poster. 66 Seiten, Bremen, 1991.

Nr. 17 **Pätzold, J., T. Bickert, L. Brück, C. Gaedicke, K. Heidland, G. Meinecke, S. Mulitza**
Bericht und erste Ergebnisse über die METEOR-Fahrt M 15/2, Rio de Janeiro - Vitoria,
18.1. - 7.2.1991. 46 Seiten, Bremen, 1993.

Nr. 18 **Wefer, G. und Fahrtteilnehmer**
Bericht und erste Ergebnisse über die METEOR-Fahrt M 16/1, Pointe Noire - Recife,
27.3. - 25.4.1991. 120 Seiten, Bremen, 1991.

Nr. 19 **Schulz, H.D. und Fahrtteilnehmer**
Bericht und erste Ergebnisse über die METEOR-Fahrt M 16/2, Recife - Belem, 28.4. - 20.5.1991.
149 Seiten, Bremen, 1991.